THE EFFECTS OF SAMPLE SIZE, MAGNETIC FIELD,
AND TEMPERATURE ON THE ELECTRICAL RESISTIVITY
AND THERMOPOWER OF ALUMINUM

Thesis for the Degree of Ph. D.
MICHIGAN STATE UNIVERSITY
JOHN B. VAN ZYTVELD
1967

This is to certify that the

thesis entitled
THE EFFECTS OF SAMPLE SIZE,
MAGNETIC FIELD AND TEMPERATURE
ON THE ELECTRICAL RESISTIVITY
AND THERMOPOWER OF ALUMINUM

presented by

John B. Van Zytveld

has been accepted towards fulfillment
of the requirements for

__Ph. D.__ degree in __Physics__

_____
Major professor

Date__8 -30- 67__

O-169

ABSTRACT

THE EFFECTS OF SAMPLE SIZE, MAGNETIC
FIELD, AND TEMPERATURE ON THE
ELECTRICAL RESISTIVITY AND
THERMOPOWER OF ALUMINUM

by John B. Van Zytveld

Transverse magnetoresistance measurements on thin foils reproduce the general effects observed by Försvoll and Holwech:[1] Sondheimer oscillations are observed in samples thinner than 0.004" when the magnetic field is perpendicular to the plane of the foil; a MacDonald-Sarginson peak is observed when the magnetic field is in the plane of the foil. Transverse magnetoresistance measurements on fine wires yield a MacDonald-Sarginson peak for wire diameters less than 0.002", but no Sondheimer oscillations have been observed. Longitudinal magnetoresistance measurements on fine wires show qualitative agreement with the Chambers' theory; longitudinal magnetoresistance measurements on thin foils do not show the peak predicted by Kao: several possible explanations for this disagreement are discussed.

Measurements of the temperature dependence of electrical resistivity in thin foils show a size-dependence consistent with Fuchs' theory. No substantial effect consistent with the theory of Azbel' and Gurzhi was observed.

This we have interpreted to mean that electron-phonon Um-klapp scattering dominates the electrical resistivity of aluminum at low and intermediate temperatures. Measurements of the temperature dependence of electrical resistivity of fine wires show an anomalous enhancement consistent with the Blatt and Satz theory. However, at temperatures above 4.2°K, the magnitude of this effect was too large to reconcile with independent estimates of the contribution of Normal electron-phonon scattering to the electrical resistance of aluminum at these temperatures. We have suggested that the observed behavior at these temperatures may be due to impurity induced deviations from Mattheissen's Rule. The theory of Blatt and Satz is satisfactorily consistant with data obtained below 4.2°K.

We have determined the absolute thermopower of bulk aluminum from 1.5°K to 300°K, finding it to be negative at all temperatures, with a negative phonon-drag peak at about 75°K. The thermopower, above 200°K, fits an AT + B/T law; the phonon-drag component, estimated from this relation, constitutes nearly 50% of the total thermopower at 300°K.

Preliminary measurements of effects of sample size on thermopower reveal changes in the thermopower below 25°K which can be correlated to sample size. High temperature variations were neither sufficiently reproducible, nor of the right form to allow comparison with theory.

Preliminary measurements of the magnetic field dependence of the thermopower of bulk aluminum at ~10°K, show

an apparent change in sign of the thermopower with increasing magnetic field. This is qualitatively consistent with the change in sign of the Hall coefficient of aluminum with increasing magnetic field.

---

[1]K. Försvoll and I. Holwech, Phil. Mag. 9, 435 (1964).

THE EFFECTS OF SAMPLE SIZE, MAGNETIC

FIELD, AND TEMPERATURE ON THE

ELECTRICAL RESISTIVITY AND

THERMOPOWER OF ALUMINUM

By

John B. Van Zytveld

A THESIS

Submitted to
Michigan State University
in partial fulfillment of the requirements
for the degree of

DOCTOR OF PHILOSOPHY

Department of Physics

1967

ACKNOWLEDGMENTS

TABLE OF CONTENTS

LIST OF FIGURES

iv

v

vii

I. INTRODUCTION

It has long been known that the surface of a metallic conductor can scatter electrons.[1-3] Such scattering can become important and may even dominate the electronic transport properties of the metal if at least one dimension of the conductor is made comparable to, or smaller than, the mean free path of an electron in the conductor. The effects of such surface scattering are called "size effects."

The criterion that the length of at least one dimension of a conductor be equal to or less than the electronic mean free path in the conductor can be satisfied in two ways: one can decrease the sample dimension; or one can lengthen the electronic mean free path. We will, in fact, do both. Small samples can be produced by vacuum deposition of very thin films; by rolling the metal into thin foils; or by drawing the metal into fine wires. Only thin films can be produced comparable in thickness to the mean free path of a conduction electron at and above 300°K (100-1000Å). The transport properties of a thin film, however, often reflect the type and nature of the substrate upon which it was formed, and cannot necessarily be trusted to yield parameters characteristic of the bulk metal. To study size effects on "bulk" material one usually studies high-purity foils or fine wires

1

at cryogenic temperatures, where the mean free path of the electron is long. The high purity insures reduced electron-impurity scattering, and the low temperature "freezes out" the phonons.

The measurement of size effects is of interest for two reasons: transport measurements on small metallic samples can yield considerable information, not easily obtained in other ways, about the properties of the bulk metal; size effect measurements can provide a test of basic physical models. For example, measurements of the magnetoresistance of thin foils and fine wires provide an estimate of the Fermi momentum of the bulk metal. Measurements of the effect of sample size on the electrical resistivity yield values for the density of electrons in the metal, and the product of the bulk electrical resistivity and bulk electronic mean free path. The temperature dependence of the resistivity of small samples gives the temperature dependence of the bulk electronic mean free path and (for wires) an insight into the nature of the electron-phonon interaction in the metal. Measurement of the effect of sample size on the thermopower provides information about the energy dependence of the electronic mean free path at the Fermi surface, and the energy dependence of the area of the Fermi surface. In addition, by comparing experimental results with theory, the applicability of such basic theoretical models as the free electron approximation and the isotropic relaxation time assumption (Boltzmann equation) can be tested. We also test the extent to which

different scattering mechanisms can be treated as independent of each other (eg: Matthiessen's Rule[4]).

Aluminum was chosen as a sample material for the following reasons: the Fermi surface of aluminum is a reasonably close approximation to a sphere,[5,6] suggesting that aluminum might behave like a free-electron metal (ie. simple theories may be adequate); the bulk transverse magnetoresistance $\rho(H)$ nearly saturates in aluminum, providing a region in which $\rho(H)$ varies slowly enough with H to allow observation of superimposed size effects; the thermopower of aluminum even in bulk had not yet been measured over the entire range from 4.2°K to 300°K; aluminum is available in high purity, providing the low residual resistivity and, at low temperatures, the long electronic mean free path required for the observation of size effects; and aluminum can be prepared in thin foils and fine wires with relative ease. In the following we will describe measurements, performed on aluminum, of: the effect of sample size on the longitudinal and transverse magnetoresistance of thin foils and fine wires at 4.2°K; the effects of sample size and temperature on the electrical resistivity of thin foils and fine wires from 1.5°K to 50°K; and the bulk thermopower of pure aluminum. In addition, we describe preliminary measurements of the size dependence and magnetic field dependence of the thermopower of aluminum. The specific aims of our present study will be discussed in detail in the appropriate sections.

II. GENERAL BACKGROUND

General Theory of "Size Effects"

An electron impinging on a conductor surface can be scattered in one of two ways, specularly or diffusely. In the case of specular reflection of an electron at a surface, the component of electronic momentum perpendicular to the conductor surface changes only its sign, while the components parallel to the surface remain unchanged. Specular reflection will introduce no size effect into a transport measurement, since the "axial" momentum of the electron remains unchanged. An electron scattered diffusely at a conductor surface loses all memory of its previous momentum. Diffuse surface scattering does introduce size effects in transport measurements, since the surface acts to randomize the electronic momentum.

Surface scattering can be introduced in a consistant way into transport theory by means of properly chosen boundary conditions on solutions of the Boltzmann equation. As an example of how this can be done,[7] we define the electronic distribution function $f(\vec{r},\vec{v},t)$ by the relation $f(\vec{r},\vec{v},t)d\vec{v}\ d\vec{r}\ dt$ = number of electrons in the interval $d\vec{v}\ d\vec{r}\ dt$. Taking the total time derivative of f, we obtain

$$\frac{df}{dt} = \frac{\partial f}{\partial t} + \nabla_{\vec{v}} f \cdot \vec{a} + \nabla_{\vec{r}} f \cdot \vec{v} \qquad (1)$$

where t = time, and $\vec{v}$, $\vec{a}$ and $\vec{r}$ are the electronic velocity, acceleration, and position vectors respectively.

If we assume that, upon removal of a perturbing force, f will relax to its equilibrium value f_o <u>exponentially</u> with time, we may write

$$\frac{df}{dt} = -\frac{f - f_o}{\tau} \qquad (2)$$

where τ is the time constant characteristic of the relaxation mechanism. Since all measurements of interest to us involve a D.C. steady state situation, f will have no explicit time dependence, giving $\frac{\partial f}{\partial t} = 0$. Combining these three equations, we obtain the Boltzmann transport equation

$$\nabla_{\vec{v}} f \cdot \vec{a} + \nabla_{\vec{r}} f \cdot \vec{v} = -\frac{f - f_o}{\tau}. \qquad (3)$$

This equation is the starting point for the analysis of most of our data.

Externally applied forces enter the Boltzmann equation through the electron acceleration $\vec{a}$: for conduction in electric and magnetic fields one has

$$\vec{a} = \frac{\vec{F}}{m} = \frac{e}{m}(\vec{E} + \frac{1}{c}\vec{v} \times \vec{H}). \qquad (4)$$

We recall that f_o, for electrons, is just the Fermi-Dirac distribution function

$$f_o = \frac{1}{e^{(E-\mu)/kT} + 1}. \qquad (5)$$

In a bulk conductor at constant temperature and subject to a D.C. field, the function f obtained by solving

Equation (3) will be independent of position vector $\vec{r}$. f is therefore a constant across the specimen dimensions. However, in a sufficiently small sample, diffuse surface scattering will randomize the electron velocities at the surface, requiring that f take on its equilibrium value f_o at the surface. In this case f, which tends toward its bulk value inside the conductor, will not be independent of position in the conductor, but will vary appreciably across the small conductor dimension. In this way the sample size effects the distribution function f, and through f the transport properties of the metal. Mathematically we introduce diffuse surface scattering into f by requiring that f satisfy

$$f\Big|_{\text{surfaces}} = f_o. \tag{6}$$

All the transport properties of the metal can now be obtained from f. As an example, the electric current density is given by

$$|\vec{J}_e| = \int_{-\infty}^{\infty} e|\vec{v}| f \, d\vec{v}. \tag{7}$$

This $|\vec{J}_e|$ is dependent upon the position vector r, and varies appreciably across the small conductor dimension. One must therefore obtain an average J_e^{ave}, of J_e in coordinate space across the conductor before one can obtain the total electrical conductivity σ:

$$\sigma = J_e^{ave}/E. \tag{8}$$

The earliest size effect calculations dealt only with the change in electrical resistance caused by decrease of sample size. Fuchs[8] solved the Boltzmann equation with the proper boundary conditions to obtain the electrical conductivity of thin foils, and Dingle[9] did the same for fine wires.

Earlier, Nordheim[10] had considered the electrons in a wire to resemble a gas flowing inside a cylindrical tube. The scattering of such electrons at the metal surface produced a size-dependent electrical resistivity of the form:

$$\rho = \rho_\infty(1 + \ell_\infty/d) \qquad (9)$$

where ρ = wire resistivity, ρ_∞ = bulk resistivity, ℓ_∞ = bulk electronic mean free path, d = tube (wire) diameter. This approximate result differs from Dingle's result by less than 5% over the entire range $(0 \le \frac{\ell_\infty}{d} \le \infty)$. This fact, and the relation's simplicity, make it a handy first approximation for comparing experiment to theory. We will treat calculations relating to other size effects in conjunction with the relevant experimental data.

Sample Preparation

Hard-drawn aluminum wires of nominal bulk purity 99.999% were obtained from the Atomergic Chemetals Corporation of Garden City, New York. Spectrographic analysis of the bulk ingot performed by the Atomergic Chemetals Corporation revealed the following impurities (concentrations in ppm):

TABLE 1

Ca	.1	Mg	.08	Si	.05

Spectrographic analysis of the 0.016 inch diameter wire was performed at the Battelle Memorial Institute, Columbus, Ohio. This analysis, obtained from the sample after it had been converted to an oxide, showed the presence of the following impurities (concentrations in ppm):

TABLE 2

Mn	0.25	Bi	0.6	Ti	1.0
Fe	5.0	Ca	15.0	Ni	2.5
Mg	2.0	Cu	2.0	Cd	0.5
Cr	2.5	Zn	4.0	Be	0.9

It should be noted that some impurities were probably introduced into the samples when they were converted into oxides, implying that the latter analysis is likely to exaggerate the impurity content.

The diameters of the wires obtained from the Atomergic Chemetals Corporation were nominally: .032", .016", .008", .004", .002". We prepared wires with diameters smaller than 0.002" by drawing the aluminum through new diamond dies ranging in diameter from 0.0018" to 0.0005". These dies were supplied by the Balloffet-Vianney Wire Die Corporation of Guttenberg, New Jersey. The wires were drawn through the dies

at a rate of about six inches per minute, using distilled water as the only lubricant. The wires were wiped with reagent grade methanol twice before and twice after each draw. Microscopic examination revealed no irregularities in either the surface or dimensions of these wires.

Cold rolled aluminum foils were obtained from the Cominco Corporation of Mount Vernon, New York. The bulk metal, nominally 99.999$^+$% aluminum, was given an additional twenty zone refining passes before being rolled into foils. The approximate thicknesses of these foils were 0.080", 0.040", 0.008", 0.004", 0.002", 0.001", 0.0005". We prepared foils ranging in thickness from 0.00015" to 0.0003" by placing 0.0005" foils between two 0.002" aluminum foils, and rolling this sandwich to the desired thickness.

The samples used in all resistivity measurements were annealed in air at about 450°C for periods of time ranging from 1/2 hour to 24 hours.

Samples used in thermopower measurements were annealed in vacuum ($\sim$10^{-4} Torr) at about 450°C for about 1 hour.

III. EFFECTS OF SAMPLE SIZE AND MAGNETIC

FIELD ON RESISTIVITY

Theory

MacDonald and Sarginson[11] were the first to con-
sider theoretically effects of sample size on the magneto-
resistance of thin samples. Using the Boltzmann equation
and assuming diffuse surface scattering they obtained a
size dependent magnetoresistivity, $\rho_s(H)$, for thin foils in
a magnetic field $\vec{H}$. They assumed H transverse to the cur-
rent density $\vec{J}$ and in the plane of the foil. Their results,
simplified by their assumption of a uniform Hall field
across the foil thickness t, predicted a maximum in $\rho_s(H)$
which was related to the magnitude of H and to the foil thick-
ness t. This can be understood qualitatively by considering
the circular trajectories of free electrons in a magnetic
field. The cyclotron radius r_c, or the radius of curvature
of the electron trajectory, is related to H by

$$r_c = \frac{mv_f c}{eH} = \frac{p_f c}{eH} \tag{10}$$

where m, v_f and e are the mass, velocity (ie. Fermi velocity),
and charge, respectively, of the electron. At small H, r_c
is large and the resistivity is enhanced due to deflection
by H of the current carrying, axially directed, electrons
into the foil surface, where diffuse scattering is assumed
to take place. At sufficiently large H, the cyclotron radius
r_c becomes much smaller than the foil thickness, electrons are

actually deflected away from the surface, and the resistivity of the foil approaches the resistivity of the bulk material at the same magnetic field; surface scattering is no longer of importance. Taken together these two limiting cases imply a maximum in ρ_s approximately at $r_c = t$.

Ditlefsen and Löthe[12] have recently improved on the MacDonald-Sarginson argument by solving the problem without the assumption of a uniform Hall field. Also using the Boltzmann equation approach, they found that the peak in $\rho_s(H)$ shifted to higher H for a given t, and a sharp break appeared in $\rho(H)$ at $2r_c = t$. This is the point at which ρ_s reaches the bulk value. Their results show that both the break and the peak in ρ_s should occur at constant values of $\frac{t}{r_c} \sim Ht$. Since the theoretically predicted t/r_c and the experimentally determined Ht are related by the Fermi momentum, the experimental positions of the break and the peak should provide a measure of the Fermi momentum.

Sondheimer[13] solved the Boltzmann transport equation for a thin foil with $\vec{H}$ transverse to $\vec{J}$ and perpendicular to the surface of the foil. For diffuse scattering, he found that ρ_s should oscillate in the magnetic field with period $\beta \equiv \frac{t}{r_c} \simeq 6$. As in the case with $\vec{H}$ in the plane of the foil, the positions of the oscillatory maxima and minima as a function of Ht provide a measure of the Fermi momentum.

The problem of a cylindrical wire in a transverse magnetic field has not as yet been solved, due in the main to calculational difficulties arising from the cylindrical

geometry and the non-uniform Hall field. We would expect the general features to be similar to those for the foil, but with certain modifications. ρ_S is likely to consist of a superposition of the MacDonald-Sarginson peak and the Sondheimer oscillations, but without a sharp break at $2r_c = d$, where d = wire diameter. The absence of this break is anticipated because the wire "thickness" is not constant but varies continuously from zero to d.

The problem of longitudinal magnetoresistance in thin foils has been attacked by Kao[14] and by Koenigsberg.[15] They find a narrow maximum in ρ_S approximately at constant $\sqrt{\ell_\infty t}$. Chambers,[16] considering the problem of longitudinal magnetoresistance in fine wires, has predicted a monotonic decrease of ρ_S to $\rho_\infty(H = \infty)$ assymptotically with the increasing H, where ρ_∞ = the resistivity of the bulk material. The rate of decrease of ρ_S to $\rho_\infty(H = \infty)$ also depends upon ℓ_∞. Azbel[17] presents some semi-quantitative predictions of the behavior of ρ_S in fine wires and thin foils for all orientations of H: longitudinal, transverse, and inclined. All of these calculations of the effects of sample size on longitudinal magnetoresistance are based on kinetic arguments concerning the helical trajectories of the electrons in the parallel $\vec{E}$ and $\vec{H}$ fields. All approaches but that of Chambers also assume totally diffuse surface scattering.

The above theories deal only with the size dependent portion of the magnetoresistance. In practice, the magnetoresistivity obtained in a given measurement is a complicated

superposition of bulk and size dependent magnetoresistivities. We now apply ourselves to the problem of separating $\rho_S(H)$ and $\rho_\infty(H)$.

Kohler[18] has shown that, providing a relaxation time τ, independent of magnetic field, can be defined, the magnetoresistivity $\rho(H)$ of a metal should satisfy the "Kohler Relation":

$$\frac{\Delta\rho}{\rho_o} \equiv \frac{\rho(H) - \rho_o}{\rho_o} = f(H/\rho_o) \tag{11}$$

where $\rho(H)$ and ρ_o are the resistivities with magnetic field H and zero respectively. Justi[19] has shown experimentally that if this relation is expressed in terms of the "reduced resistivity" $\rho_{red} \equiv \rho_o(T)/\rho_o(\Theta_D)$:

$$\frac{\Delta\rho(H,T)}{\rho_o(T)} = f(H/\rho_{red}), \tag{12}$$

it is uneffected by large changes in H, temperature T, and residual resistivity ρ_r. Θ_D is the Debye temperature of the metal lattice. For each metal, two functions f are defined, $f_{||}$ for $\vec{H}||\vec{J}$ and $f_\perp$ for $\vec{H}_\perp\vec{J}$.

Since ℓ, (where ℓ denotes the actual electronic mean free path) and hence $\tau(v_f = \ell/\tau)$, are both size and magnetic field dependent in small samples, we may expect to see deviations from Kohler's Rule in our measurements on small samples. Olsen[20] suggested that this situation be handled in the following way. Since the argument H/ρ_o of the function f varies as $\tau \times \omega_c$, where ω_c = electron cyclotron frequency, and since this τ must be independent of H for the Kohler

Relation to hold, we can correct the Relation at each (d,H) by using the correct $\tau(d,H)$. To introduce this τ, we substitute the size dependent magnetoresistivity $\rho_s(H)$ for the zero-field resistivity in Kohler's Relation obtaining:

$$\frac{\rho(H) - \rho_s(H)}{\rho_s(H)} = f(H/\rho_s(H)), \tag{13}$$

where $\rho(H)$ is the total resistivity of the thin sample in magnetic field H, and f remains the bulk function. Experimentally one obtains f from the measured magnetoresistance of a bulk sample and Equation (11). (Equation (12) must be used if measurements are taken over a range of temperatures.) Equation (13) then yields $\rho_s(H)$ which can be compared directly to the theories of size effects. One should note that because f is defined experimentally, $\rho_s(H)$ must be obtained by numerical methods.

Review of Previous Experiments and Purpose of the Present Study

MacDonald and Sarginson[11] were the first to demonstrate experimentally the effect of sample size on the magnetoresistance of a metallic conductor. Working with fine sodium wires, they noted a maximum in $\rho(H)$ with $\vec{H} \perp \vec{J}$. No quantitative attempt was made to compare experiment to theory--the theory for $\vec{H} \perp \vec{J}$ had been worked out only for samples of rectangular cross section. Olsen[20] working with fine indium wires noted size dependent deviations of the transverse

magnetoresistance from Kohler's Rule, but made no attempt to compare this with the existing MacDonald-Sarginson theory (for foils). Blatt et al.[21] recently extended Olsen's work on indium to thinner wires and higher magnetic fields. Babiskin and Siebenmann[22] were the first to note resistivity oscillations in transverse magnetic fields in small conductors. Working with sodium wires, they were able to correlate the experimentally observed oscillations with those predicted by Sondheimer[13] for thin foils. These oscillations have also been noted in thin plates of cadmium single crystals (Zebouni et al.[23]), and in polycrystalline aluminum foils (Försvoll and Holwech[24]). Försvoll and Holwech used Olsen's[20] suggestion to compare their oscillations to the theory of Sondheimer, obtaining an estimate for the Fermi momentum of aluminum. The single maximum noted by Försvoll and Holwech for $\vec{H}\perp\vec{J}$ and $\vec{H}||$ (plane of the foil) has been shown[12] to be consistent with a MacDonald-Sarginson peak, as the theory was formulated by Ditlefsen and Lothe.[12]

Chambers[16] measured the effect of sample size on the longitudinal magnetoresistance of a single sodium wire at several temperatures. Comparison of his results with the accompanying theory showed fairly large discrepancies between the experimental values and the theoretical predictions. Olsen,[20] measuring the magnetoresistance of thin indium wires for $\vec{H}||\vec{J}$, also found fairly large differences between his results and Chambers' theory. Olsen used the Kohler function to obtain his size dependent

resistivity. Measurements of longitudinal magnetoresistance in small single crystals have been performed (cf. Steel,[25] Aleksandrov,[26]) but no attempts have been made to correlate these quantitatively with theory. Chopra[27] has recently measured the longitudinal magnetoresistance of thin _films_ of gold, silver, indium, and aluminum, comparing the results to the numerical theory of Kao by assuming the sample resistivity to be the sum of the size dependent resistivity $\rho_s(H)$ and the bulk resistivity $\rho_\infty(H)$.

The purposes of the present study were as follows: to check the results of Försvoll and Holwech[24] for thin foils of aluminum and to extend their measurements to higher magnetic fields; to obtain estimates of physical quantities (p_f, ρ_∞, ℓ_∞) for our foils for comparison of subsequent experiments with theory; to carefully and systematically compare our transverse magnetoresistivity for fine wires, using Olsen's suggestion, to the theories of Sondheimer[13] and Ditlefsen and Lothe.[12] We hoped to definitely identify a MacDonald-Sarginson peak in fine wires, and to study the size dependence of the Sondheimer oscillations for fine wires if such oscillations were observed.

We undertook studies of the effect of size on the longitudinal magnetoresistivity of fine wires to study this effect in wires smaller by a factor of three than any previously used and smaller by a factor of 20 than Aleksandrov's[26] Al wires. We could also attain magnetic fields twice those of previous studies on polycrystalline wires. With this

additional capacity, we hoped by using Olsen's suggestion, to be able to compare our results to Chambers' theory over a much wider range of size and magnetic field.

Until the recent work of Chopra,[27] no attempt had been made to compare the longitudinal magnetoresistivity of thin foils (or films) to the theory of Kao[14] for any metal. Since the analysis employed by Chopra assumed Kao's theory, rather than attempted to verify it, and since his experiments did not extend over a range of film thicknesses, we felt it worthwhile to extend our measurements into this area as well, hoping for a direct test of the theory.

Description of the Apparatus

A four-probe D.C. potentiometric method was employed in measuring magnetoresistance. The D.C. current was supplied by a series-parallel combination of four large storage batteries. This current was controlled by a variable resistance network and monitored by means of the potential drop across a standard resistor. This potential drop, and hence the current, was measured on a K-3 potentiometer to an accuracy of better than one part in 10^4. A Leeds and Northrup D.C. Null Detector was used with this potentiometer. The potential drop across the specimen was measured on a Minneapolis-Honeywell Rubicon-Instruments six-dial potentiometer whose most sensitive dial graduation was 0.01 microvolts. A

photocell galvanometer amplifier and an optical galvano-
meter were used with the six-dial potentiometer as a null
detector. Slowly varying thermally induced voltages in
the potential leads to the samples were eliminated by re-
versing the current to the samples and averaging the for-
ward and reverse measurements of the voltage. The inputs
to the K-3 were reversed by a heavy, double pole-double
throw knife switch; the inputs to the six-dial were crossed
at an oxygen-free copper terminal block, making it possible
to reverse the input terminals by using the internal,
shielded, two-source selector switch on the six-dial.

The magnetic field was supplied by a Harvey-Wells
iron core electromagnet capable of producing fields of 21
Kilogauss across a three-inch pole gap with six-inch pole
faces. This magnetic field, uniform across the four-inch
sample length to better than 0.5%, was measured with a
Rawson-Lush rotating-coil gaussmeter to an accuracy of
about 0.5%.

In certain orientations of the samples (notably for
the foils in the Sondheimer Position), misalignment of the
potential contacts sometimes introduced substantial Hall
voltages. These were removed by reversing the current to
the electromagnet and averaging readings at corresponding
field strengths.

For the measurements, the samples were placed in a
helium bath in a glass double dewar. Temperatures as low
as 1.2°K were obtained by reducing the pressure above the
helium bath. The 1958 Helium Temperature Scale was used to

convert bath pressure to absolute temperature. The bath pressure was regulated by pumping through a small length of soft collapsible tubing, the outer pressure on this tubing being provided by a pressure reservoir set at the desired bath pressure. This arrangement permitted regulation of the bath temperature to about 0.01°K over periods of about 15 minutes. The bath pressures were measured on mercury and oil manometers, permitting determination of bath temperatures to 0.01°K.

Transverse Magnetoresistance of Fine Wires

Three sets of current and potential contacts were placed around a one-inch diameter insulating rod. This rod, made of glass impregnated plastic, had a linear thermal expansion coefficient at room temperature similar to that of aluminum.

The sample wires were annealed at 450°C in air in high purity alumina boats and then immobilized in these boats by means of a glycerine-soap melt which gelled at room temperature. This melt was formed by heating together, by weight, 75% glycerine and 25% non-detergent soap. All magnetoresistance samples had to be immobilized to prevent deformation by the Lorentz force in the magnetic field. The wire and boat were then placed in a groove in the plastic rod and sealed with more glycerine-soap gel. The potential contacts for the larger (0.002" to 0.008" diameter) wires were formed by pressing the wires between to very flat brass

bars. The surfaces of the bars pressing the samples were flat to better than 0.001". This arrangement provided an effective sample length equal to the distance between the inside faces of the contacts. For the smaller wires (less than 0.002" diameter) different contacts were used: a grooved plexiglass holder pressed a 0.016" diameter gold wire, which served as the potential contact, onto the sample wire. This permitted the length of the sample wire to be measured as the distance between the gold wires. No difference in magnetoresistance was noted when these different potential contacts were used on the same size sample wire. The current contacts, small brass plates pressed onto the samples, were placed about 3/8" away from the potential contacts to avoid end effects. The lengths of the thicker samples were about four inches; the finer samples were about 1.25" long.

Transverse Magnetoresistance of Thin Foils

Three sets of potential and current contacts were placed on three sides of a glass impregnated plastic rod of square cross-section. The potential contacts (0.008" diameter gold wires) and the current contacts were similar to those described for the wires.

The samples were annealed as above on a bar of high purity alumina which in turn was placed in a groove in the plastic rod. The entire sample was immobilized with glycerine-soap gel. The samples were about 0.2" wide and 4" long

(the effective length being the distance between the potential contacts).

Longitudinal Magnetoresistance

The experimental arrangement was essentially the same for both the wires and foils. The samples were positioned across the end of a one-inch diameter plexiglass rod. This permitted us to use the Harvey Wells iron core electromagnet for the longitudinal magnetoresistance measurements and still retain an effective sample length of about 0.75". The current and potential contacts were 0.008" diameter gold wire pressed onto the specimens by small plexiglass plates. Pressure was applied to the plexiglass by spring loaded feet. The samples were immobilized as before. Alignment of the specimens parallel to the magnetic field was limited by wrinkles in the foils and bows in the wires. The current and magnetic field directions, however, were probably effectively aligned to better than 5°.

Results and Discussion

Transverse Magnetoresistance

We have measured the resistivity of aluminum wires and foils in transverse magnetic fields ranging from zero to 20 Kilogauss. Figure 1 shows the Kohler plot of a typical 16 mil diameter wire. The low field resistivity has very nearly an H^2 dependence and the resistivity has nearly saturated

at 20 Kilogauss. For comparison, the theoretical curve of Sondheimer and Wilson[28] has been fitted to the data in the low and high field regions. The theoretical curve is derived on the basis of a two-overlapping-band model, each band containing charge carriers of effective mass m_i, relaxation time τ_i, and density n_i. The resulting relation for the bulk-transverse magnetoresistance is

$$\frac{\rho - \rho_o}{\rho_o} = \frac{AH^2}{1 + BH^2} \qquad (14)$$

where ρ and ρ_o are the resistivities in magnetic field H and zero respectively, and A and B are constants containing m_i, τ_i, and n_i. The experimental low field dependence, an average over several samples of different diameters, actually lies between $H^{1.92}$ and $H^{2.05}$. In high field, however, no one has yet observed complete saturation even though Lüthi[29] has measured the magnetoresistance in magnetic fields up to 220 Kilogauss. Borovik[30] has suggested that perhaps this is merely an extended region between two different quadratic regions. The discrepancy between the experimental points and the theoretical curve in the region of the knee may be a "real metal" effect. Olsen[20] suggested that this effect, which he noted in indium, could possibly be due to the fact that there are not just two unique effective masses, relaxation times, and electronic densities, corresponding to the two bands, but a limited continuum of them. The variations seen at low field are due to experimental

error in the low resistivity range. The experimental points define a Kohler Function f from the Kohler Relation (Equation 11) which will be used with Olsen's suggestion to obtain the size effect magnetoresistivity.

Figure 2 shows the resistivity plotted as a function of magnetic field strength H for thin foils of aluminum with $\vec{H}$ perpendicular to the plane of the foil (Sondheimer position). The Sondheimer oscillations are visible in foils four mil and less in thickness. It should be noted that both the amplitude and the period in H increase with decreasing foil thickness. The small variations seen in the data for the .040" foil are due to experimental error introduced by the small resistance of the sample. Figure 3 shows the resistivity of the same foils in magnetic field $\vec{H}$ with $\vec{H}$ in the plane of the foil and $\vec{H} \perp \vec{J}$ (MacDonald-Sarginson position). The MacDonald-Sarginson peak is seen increasing in amplitude and moving to higher H with decreasing t. Figure 4 shows the resistivity of fine wires of aluminum in transverse $\vec{H}$ as a function of H. The general features are not as striking as those for the foils, but a maximum can be seen in the resistivity moving to higher H with decreasing diameter d as in the above case for foils in the MacDonald-Sarginson position. We will show that this peak seen in the wires has the properties of a MacDonald-Sarginson peak.

High field deviations from Kohler's Rule for the wires are clearly seen in the Kohler Plots of these data (Figure 5). The deviations at low H appear to be random, not being

correlated to sample size. The deviations at high field, however, are real, the maxima in $\rho(H)$ appearing for diameters less than one mil. Jüsti[19] has shown that changes in residual resistivity should not effect the Kohler Plots of a given metal provided measurements are taken at a single temperature. The high field deviations are therefore not likely to be due to impurities in the fine wires.

We now use Olsen's suggestion to obtain the size effect resistivity for the thin aluminum wires. We use the Kohler function f defined by the data shown in Figure 1 in conjunction with Equation (11) to obtain $\rho_s(H)$ from Equation (13). No significant changes in the ρ_s occur when the slightly different functions f obtained by Lüthi[29] and by Försvoll and Holwech[24] are used in the analysis.

ρ_s versus H is plotted in Figure 6. With the size dependent portion of the resistivity ρ_s separated from the bulk magnetoresistivity, we see the maximum in ρ_s occurs in wires of diameter as large as four mil. This peak was obscured in the previous plot since it occurred at H below saturation, where the bulk resistivity is still varying quite rapidly with H.

In order to make a comparison to theory, it is necessary to determine whether the scattering which occurs at the conductor surface is diffuse or specular. If the scattering is totally diffuse, we may compare our data directly to the theories of Sondheimer[13] and of Ditlefsen and Lothe.[12] We cannot, however, if substantial specular scattering occurs.

We see (Figures 7 and 8) that our data can be made to fit reasonably well to the theoretical curves of Dingle and Fuchs for totally diffuse scattering, provided we choose an appropriate $\rho_\infty \ell_\infty$, where ρ_∞ and ℓ_∞ are the bulk resistivity and bulk electronic mean free path respectively. Anomalous skin effect experiments also seem to indicate total diffuse scattering [31,32] in aluminum.

However, as Wyder[33] has pointed out, data that is consistent with the $\varepsilon = 0$ (diffuse) curve for one choice of $\rho_\infty \ell_\infty$ can just as well fit the $\varepsilon = 1/2$ (half specular) curve for a different $\rho_\infty \ell_\infty$. In addition, Chopra,[27] following a suggestion of Parrot,[34] has shown, at least in films, that some specular scattering can occur for sufficiently small electron-surface scattering angles. This seems to be borne out to some extent by our data, since for the smaller wires the experimental points actually tend to fall below the theoretical curve. One would expect the points to lie progressively higher above the curve with decreasing wire size if impurities were introduced into the wires in their preparation and the surface scattered diffusely. Partial specular scattering would tend to lower the points, perhaps enough to over-ride the increase due to enhanced impurity scattering. Even so, the deviations from the curve characteristic of totally diffuse scattering are small.

Since nothing in our data indicates substantial specular scattering, we shall assume totally diffuse scattering in our analysis. However, we should recognize that this assumption has not been unambiguously demonstrated.

On this assumption of total diffuse scattering, we find our best values of $\rho_\infty \ell_\infty$ to be about 11.3×10^{-12} Ω - cm^2 and 11.5×10^{-12} Ω - cm^2 for the wires and foils respectively. These agree well with the values given by Montariol and Reich,[35] but are higher than the value 8×10^{-12} Ω - cm^2 given by Försvoll and Holwech.[36] One should note, however, (cf. Figure 7) that the experimental fit to the $\varepsilon = 0$ curve is relatively insensitive to fairly large changes (as large as a factor of two) in the product $\rho_\infty \ell_\infty$. Using Sommerfeld's[37] formula

$$\rho_\infty \ell_\infty = \left(\frac{3}{8\pi}\right)^{1/3} \frac{h}{e^2 n^{2/3}},$$

where h = Plank's constant, n = number of electrons per unit volume and $\rho_\infty \ell_\infty = 11.5 \times 10^{-12}$ Ω - cm^2 we obtain the estimate $n_a \simeq .63$ for the number of conduction electrons per atom in aluminum.

To obtain an experimental value of the Fermi momentum necessary for comparison of our fine wire data to theory, we obtain $\rho_s(H)$ for our foils in the Sondheimer position using Olsen's suggestion. These data for the 2 mil and 4 mil samples are shown in Figure 9. The Sondheimer oscillations appear to be superimposed on a $\rho(H)$ varying linearly with H. This is due probably to the incomplete removal of the Hall field in the measurements. An error of 5% in measurement of the Hall field and its subsequent removal would account for the field dependence of the 2 mil foil, and an inclusion of less than 1% of the Hall field would give the dependence shown

for the 4 mil sample. The positions of the maxima and mini-
ma in ρ_s are used to calculate the Fermi momentum p_f in the
following way. Sondheimer's theory predicts that the extrema
occur at constant values of $\beta \equiv t/r_c$; the first maximum occurs
at β_1, the first minimum at β_2, etc. Recalling that we have
$\rho(H)$ experimentally, we use the relation

$$r_c(cm) = \frac{p_f(gm\ cm/sec)}{(1.59 \times 10^{-20})H(gauss)} \tag{15}$$

to compare our positions to those predicted by Sondheimer.
To do this, we plot (see Figure 10) our experimental values
of Ht against the theoretical β for corresponding extrema;
the slope of the straight line gives $p_f = 1.22 \times 10^{-19}$ gm cm/sec.
This line however, does not pass through the origin, and hence
makes no physical sense (Equation (15) has no term independent
of r_c and H). The best fit that also intersects the origin
yields $p_f = 1.35 \times 10^{-19}$ gm cm/sec. This value agrees well
with that of Försvoll and Holwech[24] obtained in the same way.

We use this value of p_f in comparing our thin wire
data to the MacDonald-Sarginson theory as formulated by
Ditlefsen and Lothe.[12] The theory predicts a single maxi-
mum in ρ_s occurring at a constant value of Hd, fixed by the
value chosen for p_f. In Figure 11 we show $\rho_s/\rho_\infty(H = 0)$ versus
Hd for our fine wires compared to the theoretical curve for
$d/\ell_\infty = .19$ assuming $p_f = 1.35 \times 10^{-19}$ gm cm/sec. The peak is
well aligned with the experimental maxima. The less rapid
decrease of the experimental data for Hd greater than
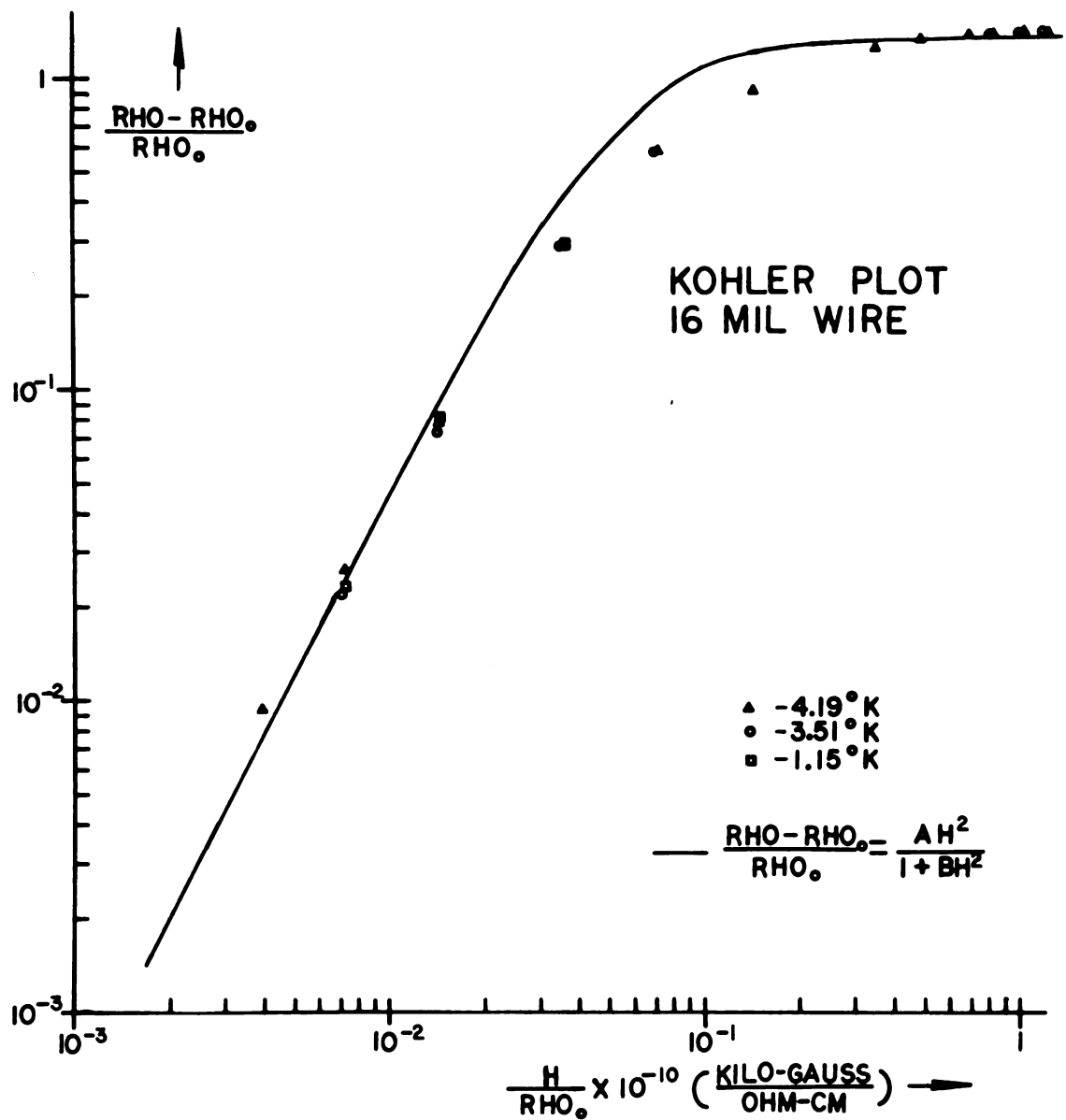
Figure 1. Kohler Plot of the electrical resistivity of a 16 mil diameter aluminum wire in a transverse magnetic field
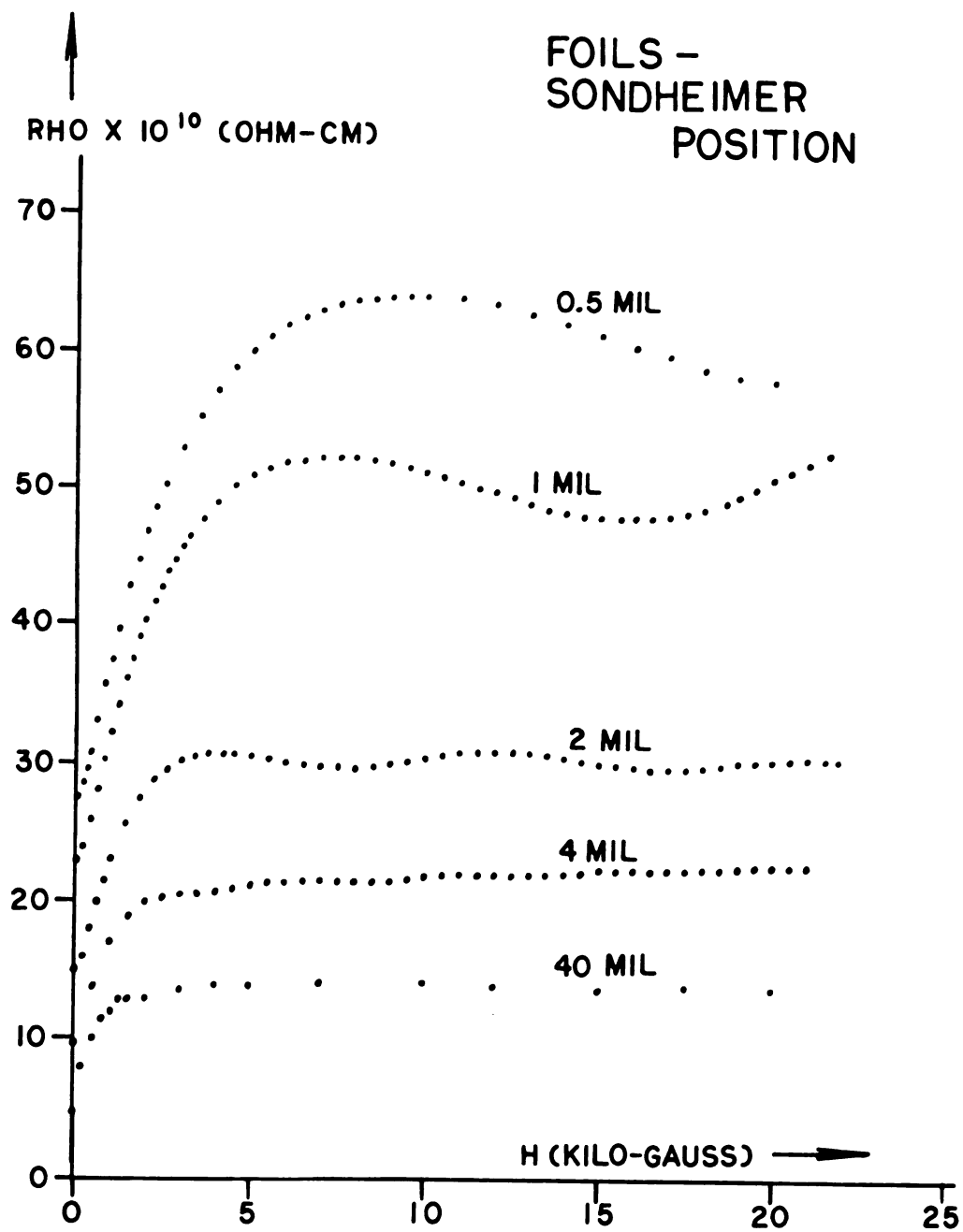
Figure 2. The electrical resistivity of thin aluminum foils in a transverse magnetic field directed perpendicular to the plane of the foils
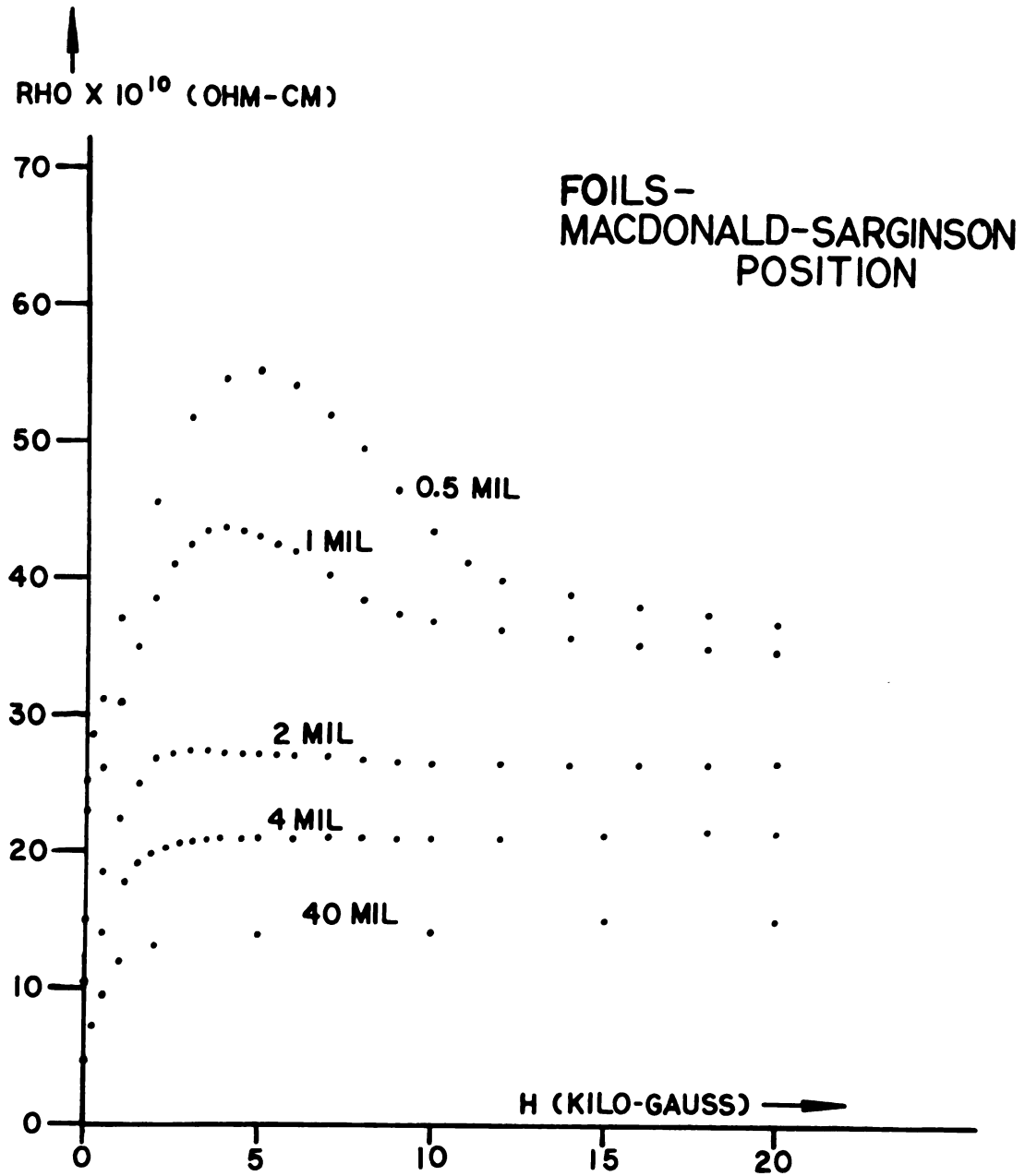
Figure 3.   The electrical resistivity of thin aluminum foils in
a transverse magnetic field directed in the plane of the foils
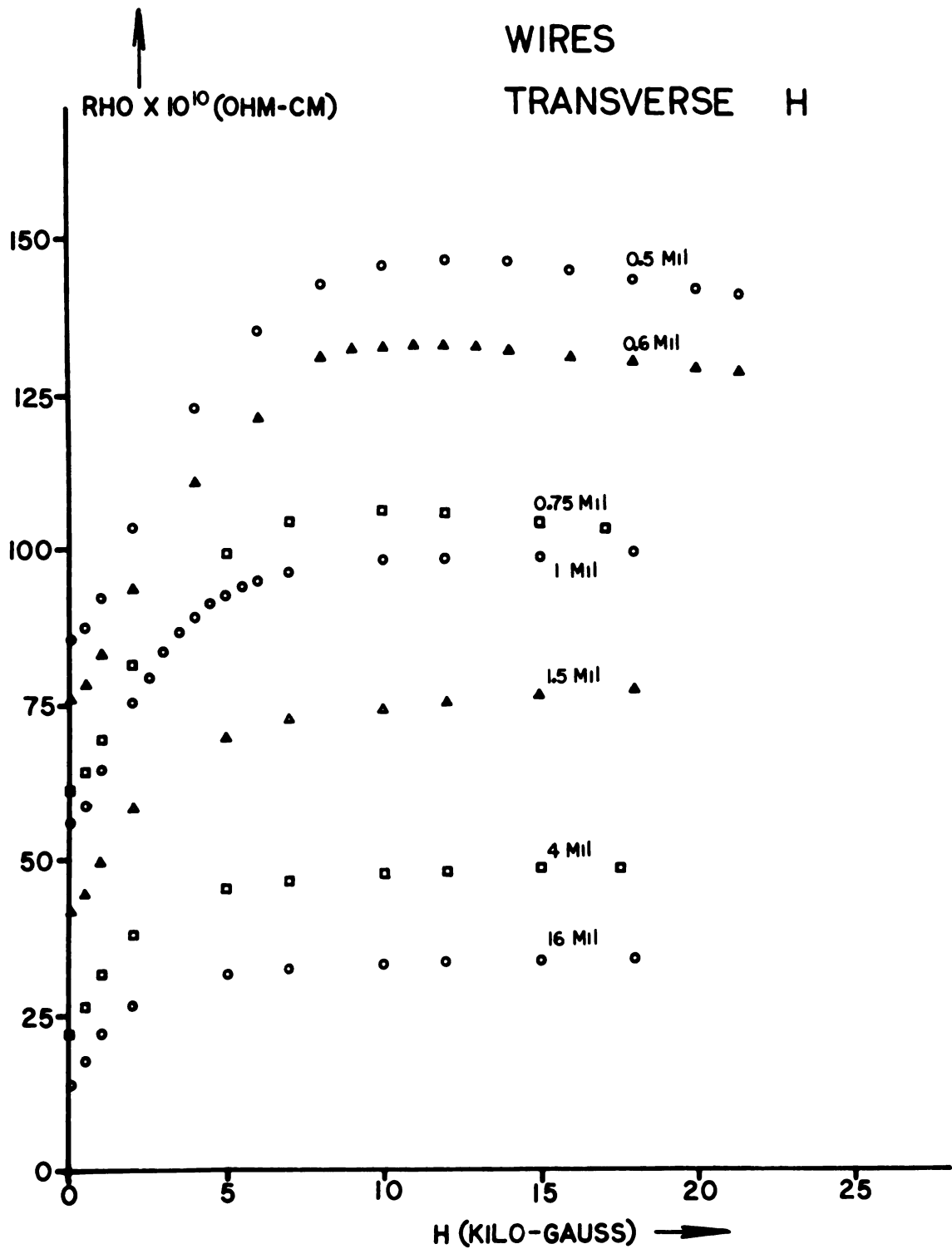
Figure 4. The electrical resistivity of fine aluminum wires in a transverse magnetic field
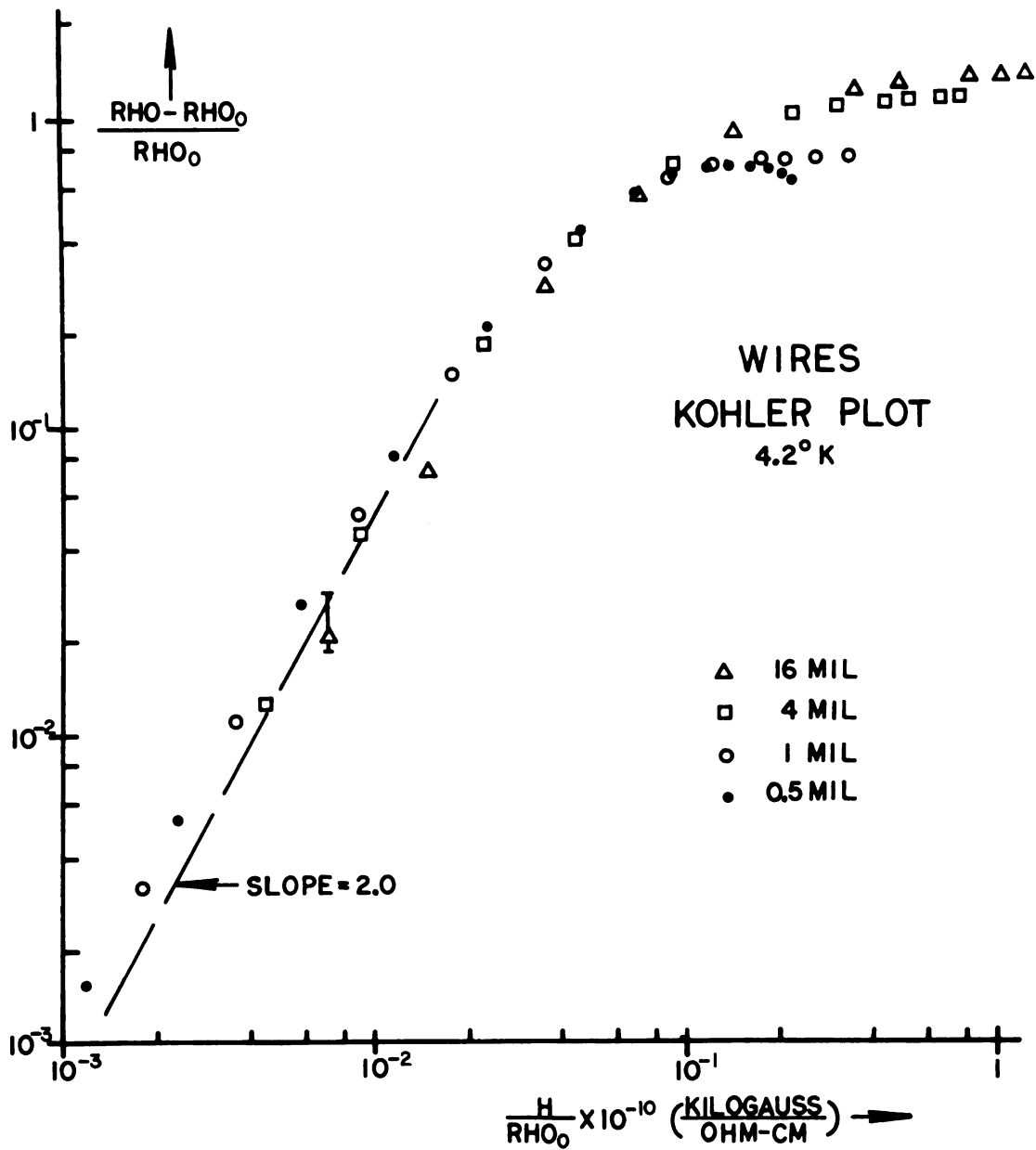
Figure 5.   Kohler Plot of some of the data from Figure 4
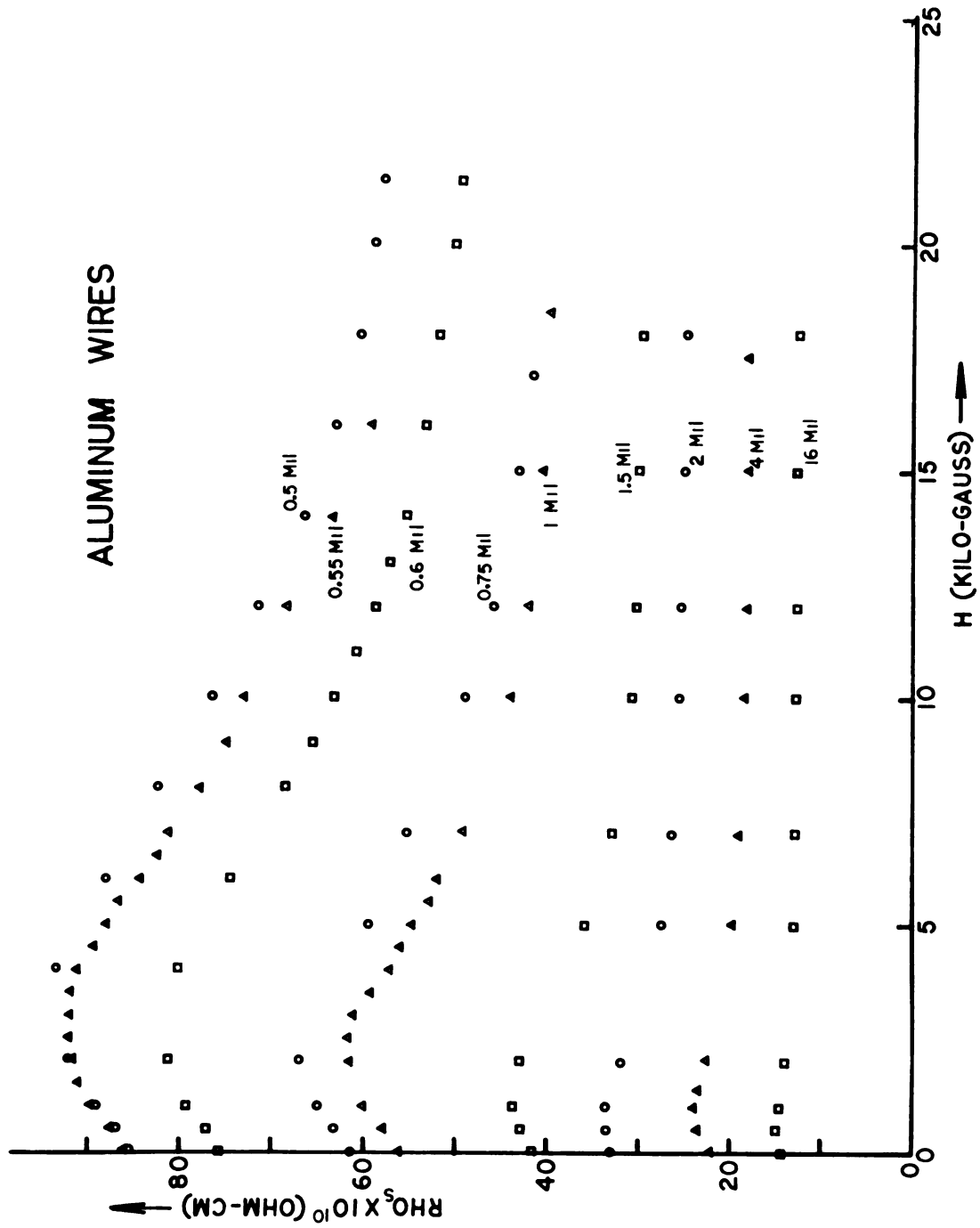
Figure 6. The size-dependent magnetoresistivity of aluminum wires in a transverse magnetic field
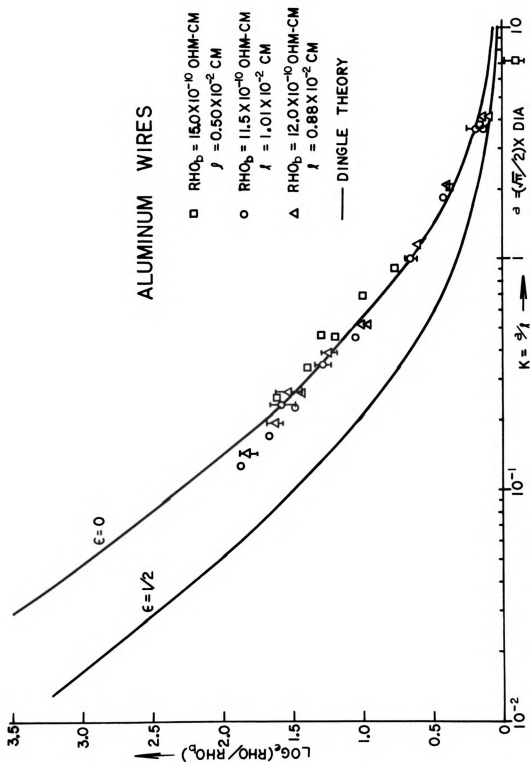
Figure 7. Comparison of the size-dependence of the electrical resistivity of aluminum wires at 4.2°K with Dingle's prediction

ALUMINUM FOILS

o   RHO$_b$ =4.00X10^{-10} OHM-CM

l =3.73X10^{-2} CM

—— DINGLE THEORY

K = t/l

LOG$_e$(RHO/RHO$_b$)
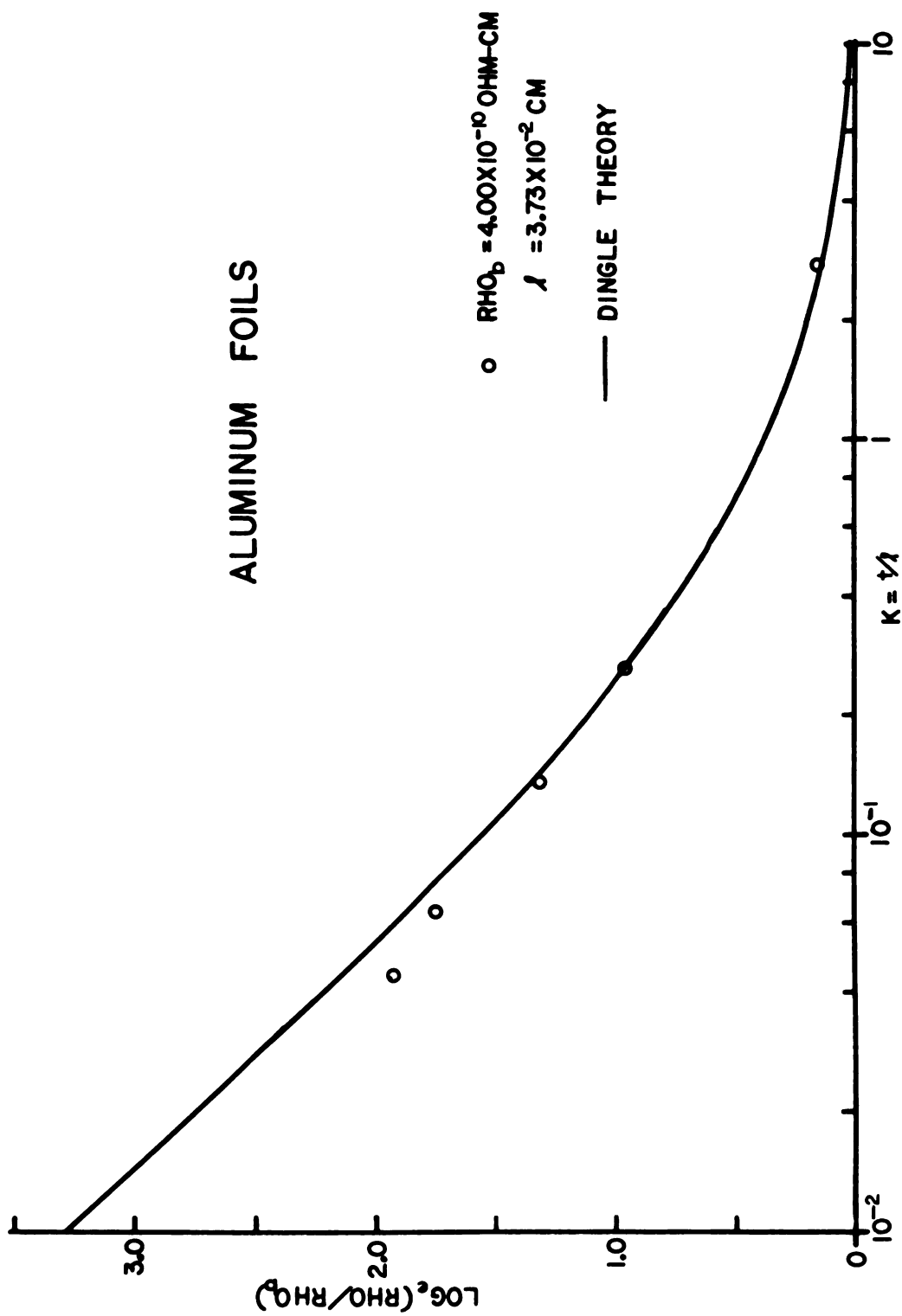
Figure 8. Comparison of the size-dependence of the electrical
resistivity of aluminum foils at 4.2°K with Dingle's numerical
formulation of Fuch's theory
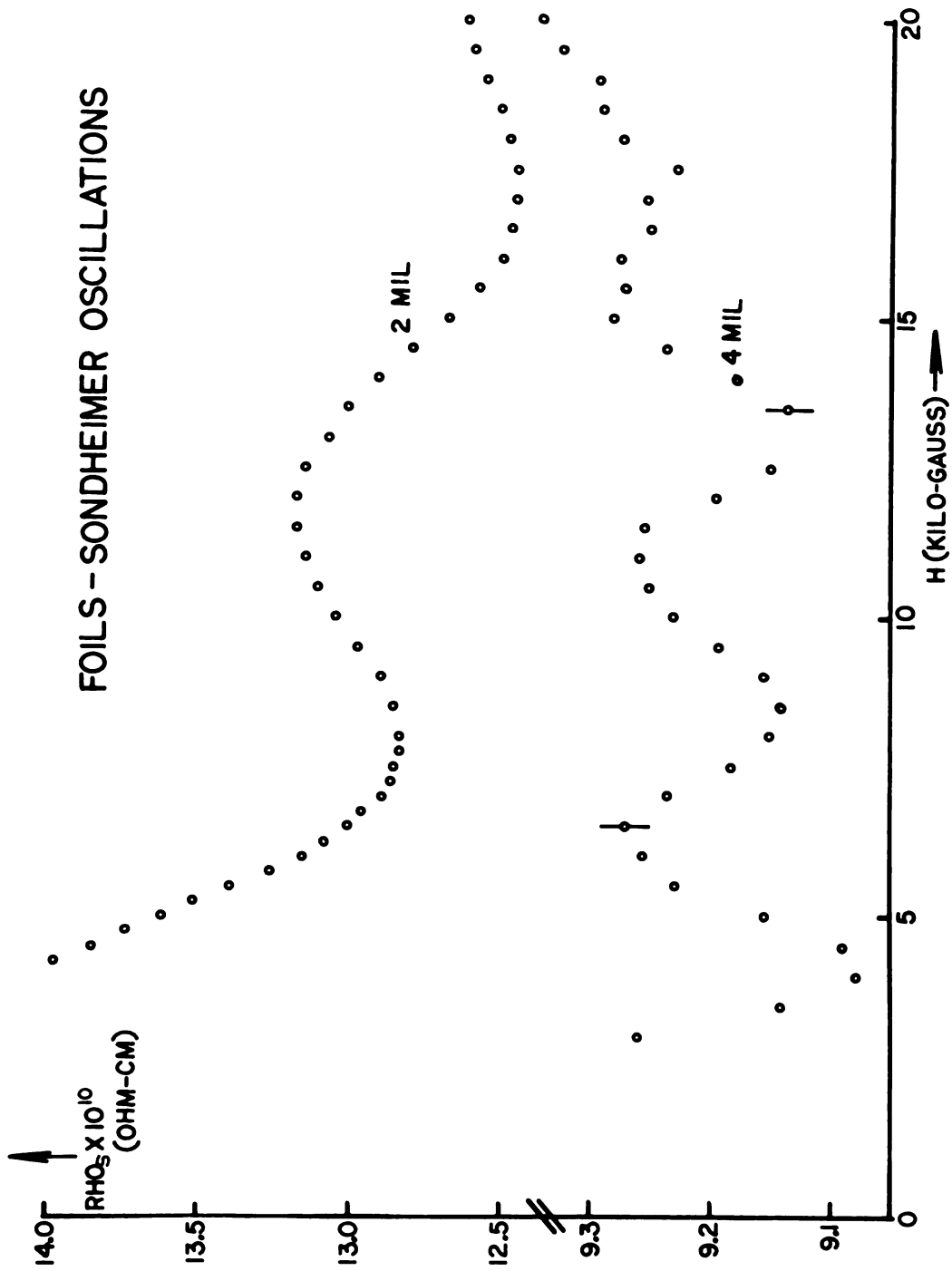
Figure 9. Sondheimer oscillations in the size-dependent
magnetoresistivity of thin foils in a transverse magnetic field
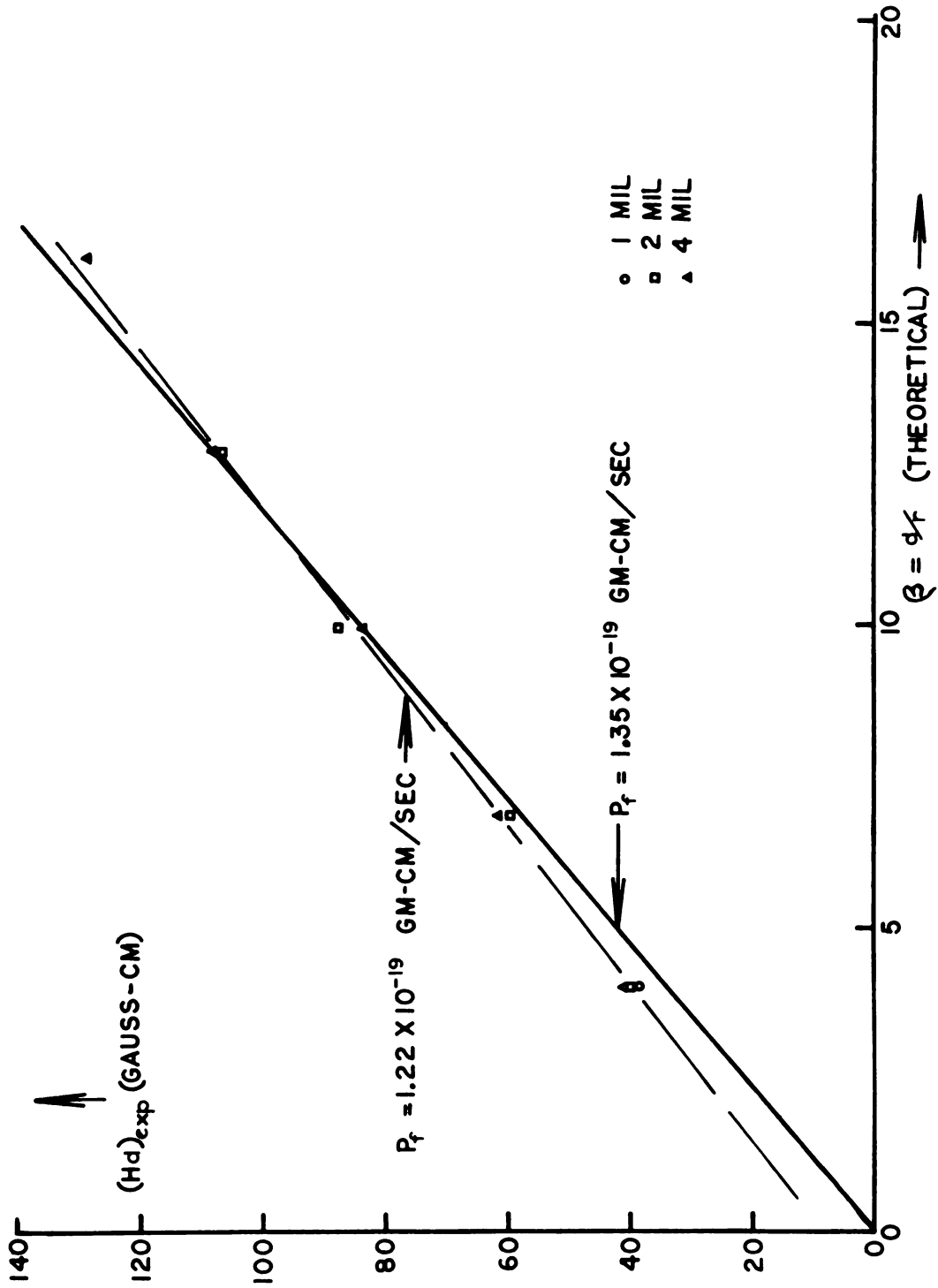
Figure 10. Determination of the effective Fermi momentum of aluminum from analysis of Sondheimer oscillation data
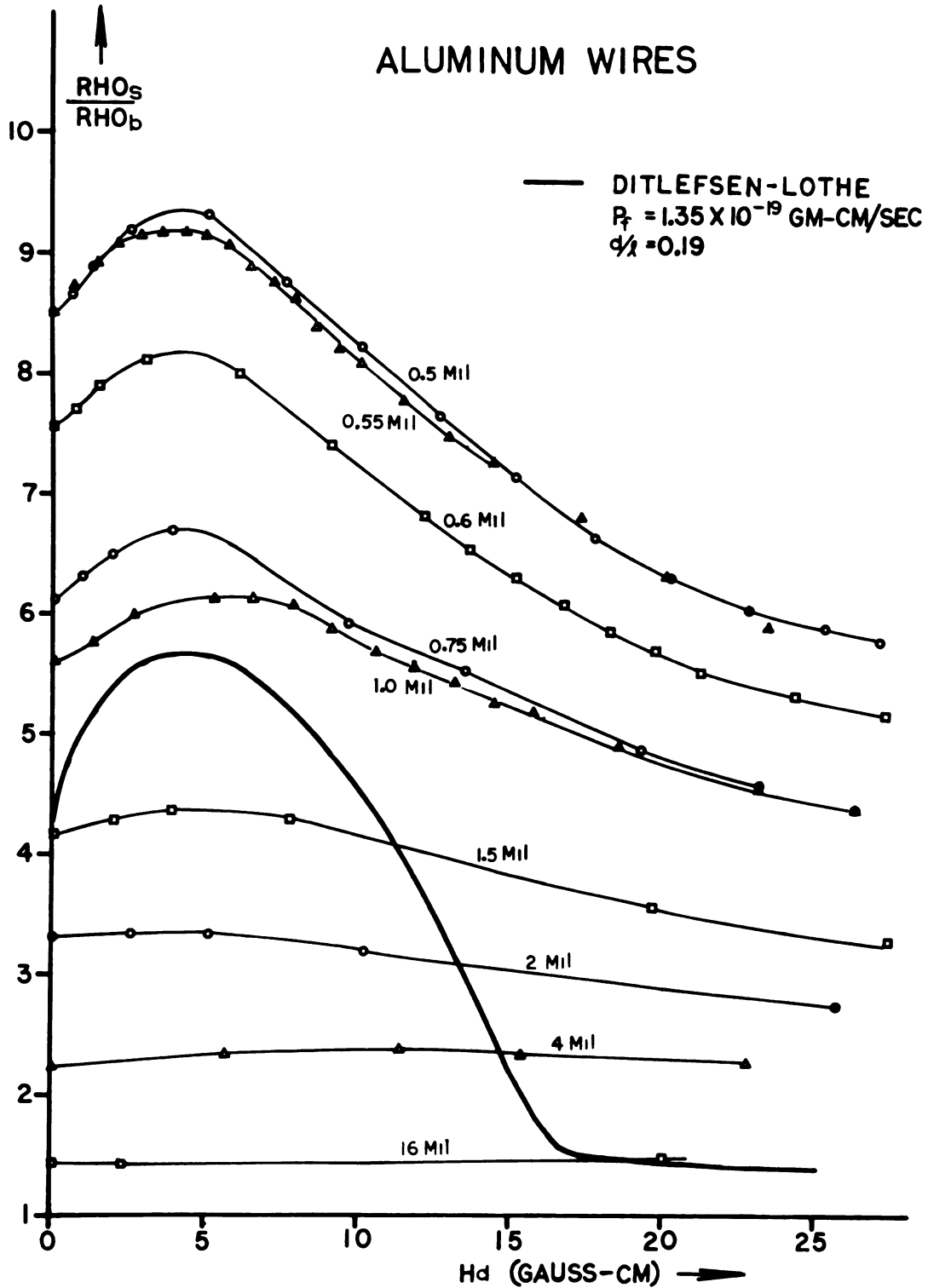
Figure 11. The size-dependent magnetoresistivity produced in aluminum wires by a transverse magnetic field, compared to the predicted size-dependent magnetoresistivity in a thin foil in the MacDonald-Sarginson position

~ 8 gauss-cm can be due to at least two causes: the introduction of progressively more impurity into the thinner wires results in an increase of ρ_∞ for these wires and since $\rho_s \rightarrow \rho_\infty$ as $H \rightarrow \infty$, the curves of $\rho_s/\rho_\infty(0)$ would remain abnormally high; the break in the theoretical curve at Hd $\simeq$ 17 gauss-cm occurs when the thickness t = $2r_c$, and since the "thickness" of a wire is continuous between zero and d, this break would never be seen and the reduction in $\rho_s/\rho_\infty(H = 0)$ would be more gradual.

This is the first systematic study of transverse magnetoresistance in fine wires of any material to demonstrate, using the ρ_s versus Hd analysis, that a MacDonald-Sarginson peak does indeed occur. The agreement in the peak position between theory and experiment is such that this method could be used to estimate p_f for fine wires better than 10%. It should be noted, however, that we find no evidence of Sondheimer oscillations in our wire data.

Longitudinal Magnetoresistance

We have measured the longitudinal magnetoresistance of thin foils and fine wires of aluminum in magnetic fields up to 20 Kilogauss. $\rho(H)$ for the thin foils and fine wires is shown in Figures 12 and 13. The maximum seen in $\rho(H)$ for the thin foils appears superficially to have the correct field and size dependence predicted by Azbel'[17] and by Kao.[14] This peak is not a size-effect peak, however, as we shall show by isolating the size dependent resistivity $\rho_s(H)$. A broad maximum in $\rho(H)$ also occurs for wires with

diameter less than .75 mil. It should be noted that the high field

bulk magnetoresistivity in longitudinal H is about half that

observed for transverse H, in general agreement with observa-

tions on other materials (cf. [20]), ie.:

$$\left. \frac{\rho(H=20KG) - \rho(H=0)}{\rho(H=0)} \right|_{||\vec{H}} \simeq \frac{1}{2} \left. \frac{\rho(H=20KG) - \rho(H=0)}{\rho(H=0)} \right|_{\perp\vec{H}} \tag{16}$$

The data are again presented as Kohler Plots (Figures 14 and

15). The best fit to the low field region of the 16 mil diam-

eter wires gives $\rho \sim H^{1.70}$. Clear high field deviations from

Kohler's Rule are noted in both wires and foils. The experi-

mental error is quite large over the entire range of H for

the 4 mil foil and at low H for the 2 mil and 4 mil foils.

The data for the 16 mil diameter wire will be used to define

a new f "longitudinal" for purposes of obtaining $\rho_s(H)$, using

Olsen's suggestion as before. This f agrees quite well with

the function obtained by Lüthi.[29] The $\rho_s(H)$ so obtained

are shown in Figures 16 and 17 with the corresponding theo-

retical curves of Kao[14] and Chambers.[16] In the foils we

see that the peak has disappeared and we have a monotonic de-

crease of $\rho_s(H)$ with H showing a small shoulder in the thin-

nest foils. The peak seen in $\rho(H)$ is due to the combination

of the rapid increase in $\rho_\infty(H)$ at low H, with the decrease in

$\rho_s(H)$ for H above saturation. The peak results from superpo-

sition of these two oppositely direct, monatonic effects.

The comparison of the experimental data with the theoretical

curve of Kao is not very satisfying. Taking $\ell_\infty = 3.73 \times 10^{-2}$ cm

from our best fit to the Dingle curve at zero field, and

p_f = 1.35 × 10^{-19}gm cm/sec as determined by transverse magnetoresistance data, we obtain the theoretical curve labeled by ℓ_∞ in Figure 16. Not only does the low field peak not appear, but ρ_s(H) decreases much more slowly than the theoretical curve. ℓ_∞ must be changed by a factor of four to give any reasonable high field agreement. This discrepancy may be due to several things: since $\rho_s \rightarrow \rho_\infty$ as H→∞ in the case of $\vec{H}||\vec{J}$ (where $\vec{J}$ is the electric current density) as for $\vec{H}\perp\vec{J}$, increased impurity in the thinner foils would tend to raise ρ_s at high H; imperfect alignment of $\vec{H}$ with $\vec{J}$ would introduce some transverse magnetoresistance which, being larger in high fields by a factor of two, would also tend to keep ρ_s abnormally high; Azbel'[17] predicts that improper alignment of $\vec{H}$ with $\vec{J}$ will introduce a small minimum at low field--this could possibly wash out the low field maximum; if the increase of small-angle surface scattering with increasing magnetic field does indeed result in enhanced specular scattering, as suggested by Chopra, the ρ_s(H) should fall more rapidly to ρ_∞(H), perhaps eliminating the low field peak.

The comparison of the wire data to theory is somewhat better, but still not good (cf. Figure 17). The value ℓ_∞ = 10^{-2}cm obtained from the best fit to Dingle's curve gives qualitative agreement with theory for the 2 mil diameter wire. Adjustment of p_f by an order of magnitude can give a similar fit for the smallest wire, but we choose to consider p_f fixed from our transverse measurements. Olsen[20] had similar difficulty in fitting theory to experiment over a range of wire

diameters, working with indium. The criticisms of the thin foil results are also applicable to the results on the fine wires.

While our results are not too promising, the work we present on the thin foils is to our knowledge, the first systematic attempt to study the size dependence of longitudinal magnetoresistance in thin foils of any material. It should be noted that aluminum is ideal for studying the transverse magnetoresistance size effects because $\rho_\infty(H)$ nearly "saturates" for high H, where the size effects occur, and because the residual resistivity does not affect the features of the size effect phenomena in transverse field. This is not true, however, for longitudinal magnetoresistance. In this case, even for fine wires and thin foils, the size effect features occur at H below saturation, where $\rho_\infty(H)$ is a rapidly varying function of H. Variations in residual resistance due to the rolling of the foils and drawing of the wires, imply variations in ℓ_∞, and will effect the general features of $\rho_s(H)$. Drawn wires and rolled foils of aluminum are not then ideal materials to use in testing the theories of longitudinal magnetoresistance.
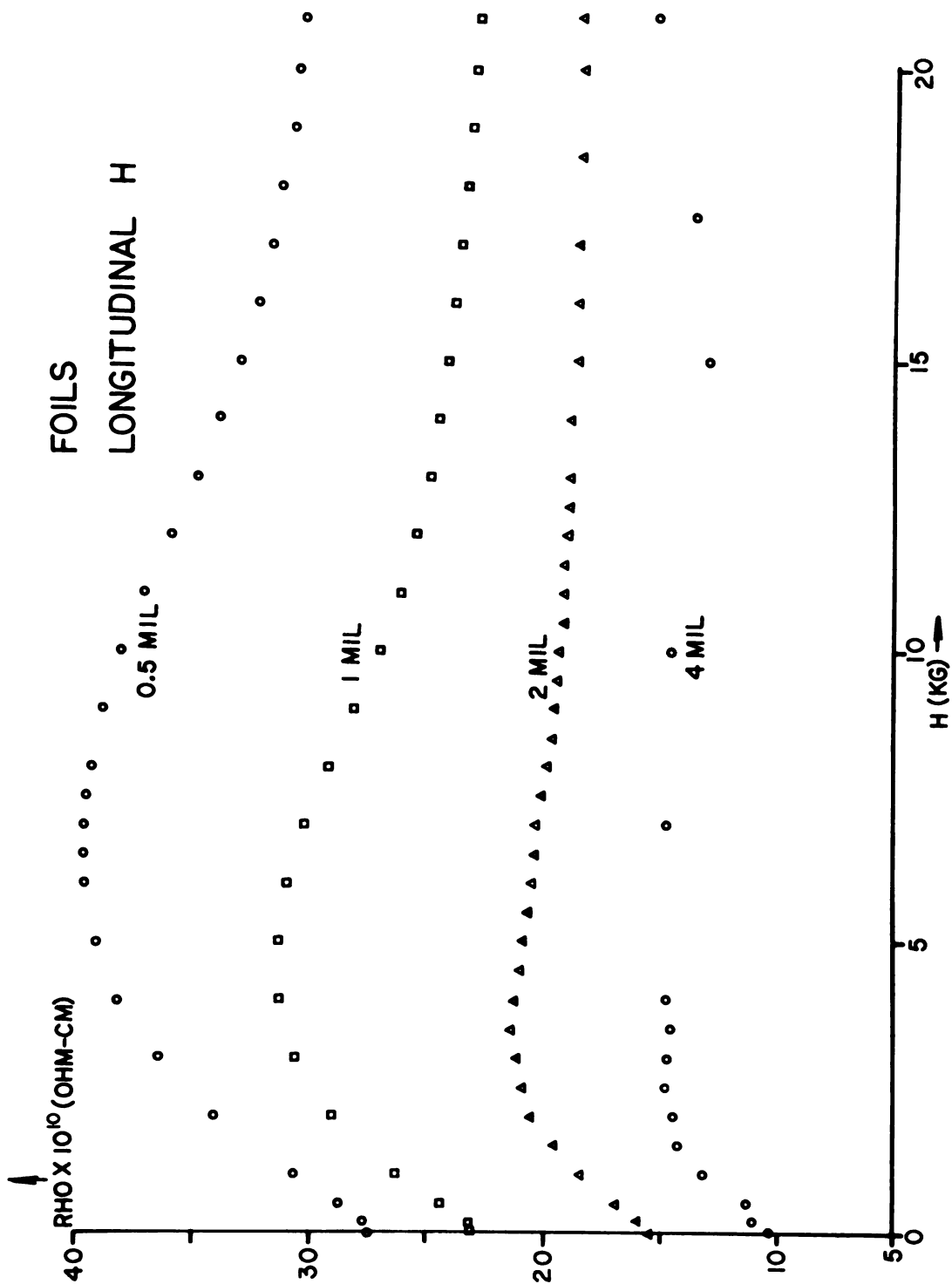
Figure 12. The electrical resistivity of thin aluminum foils in a longitudinal magnetic field
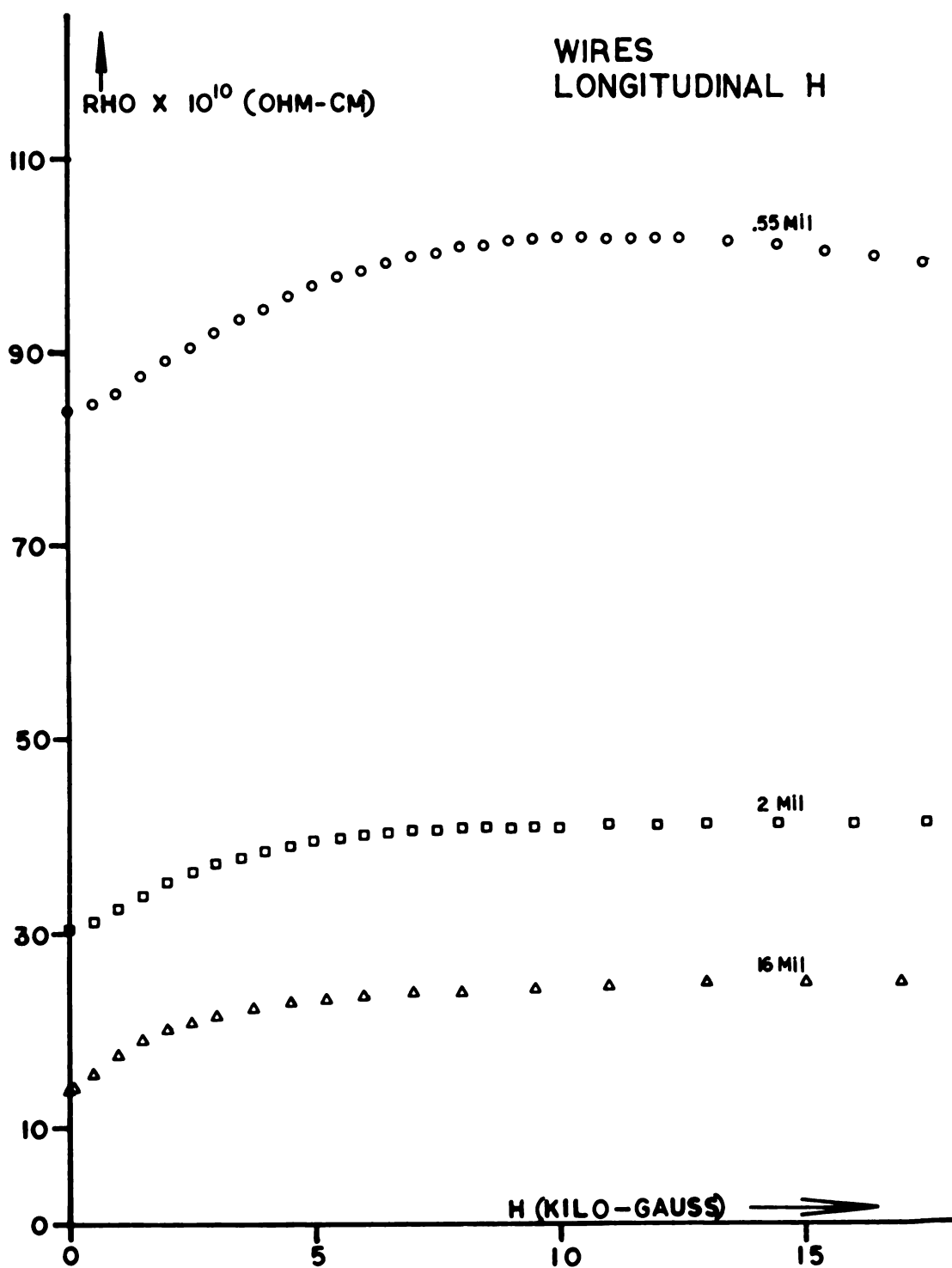
Figure 13. The electrical resistivity of fine aluminum wires
in a longitudinal magnetic field
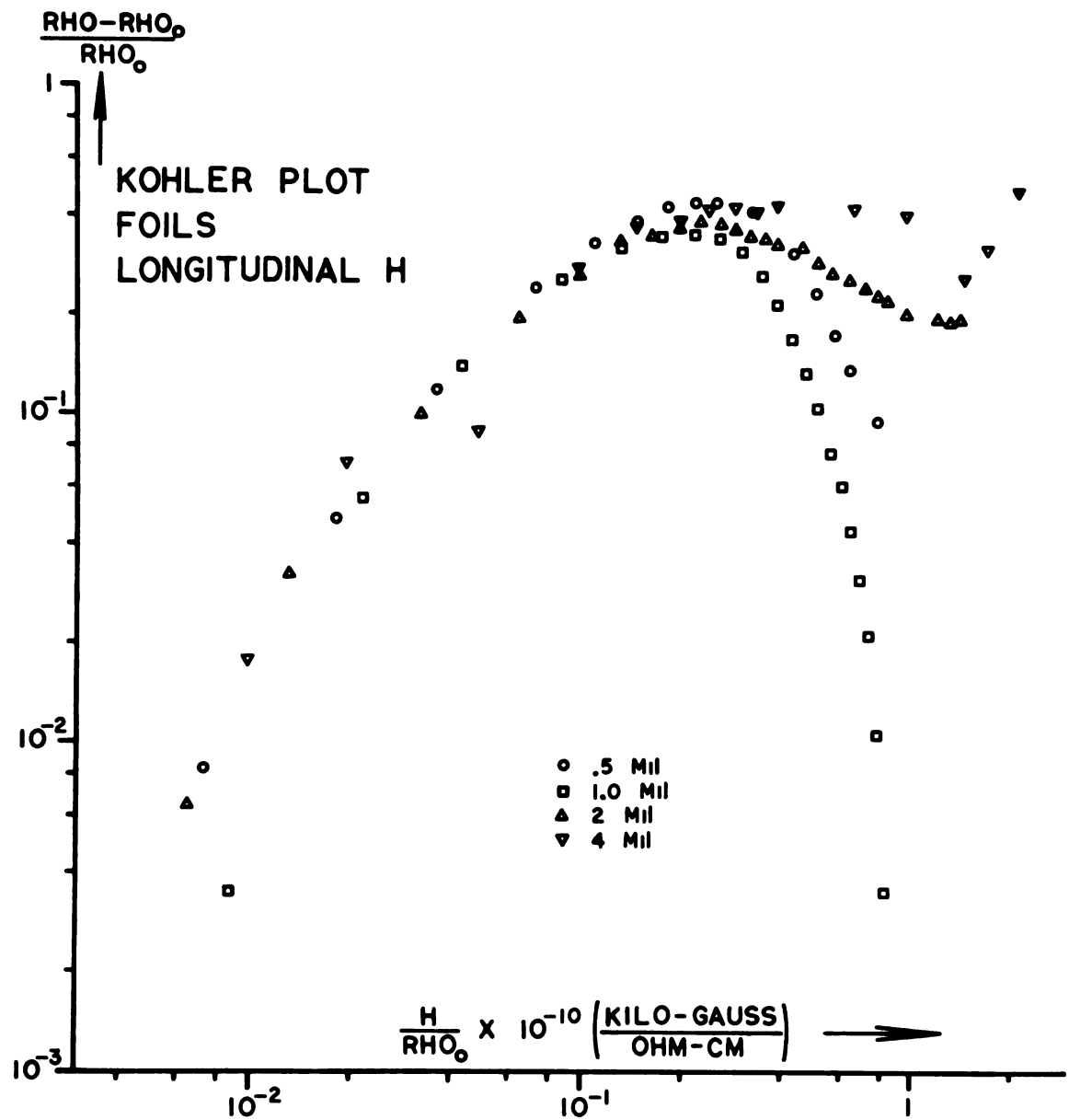
Figure 14. Kohler Plot of the data from Figure 12
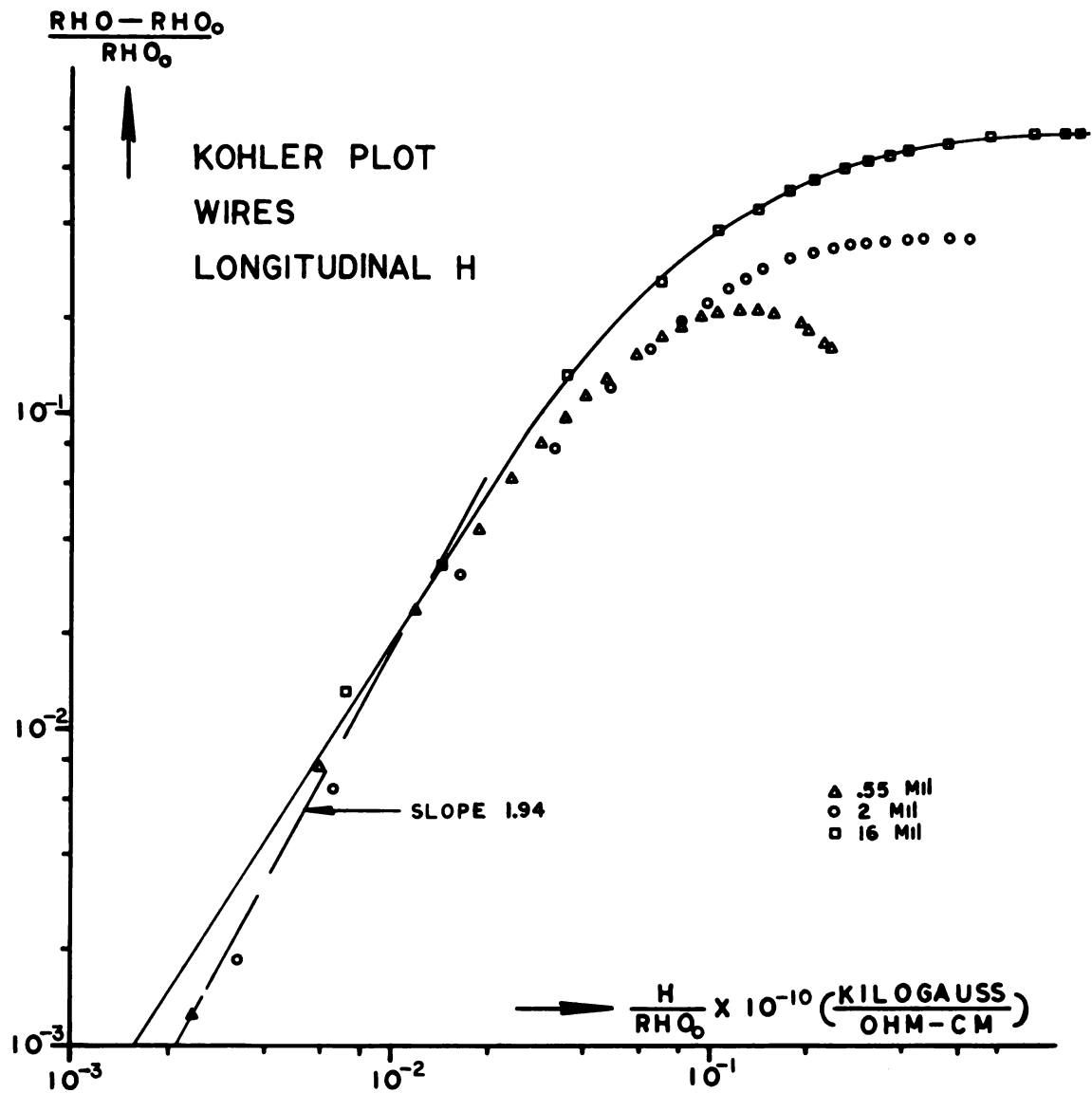
Figure 15. Kohler Plot of the data from Figure 13
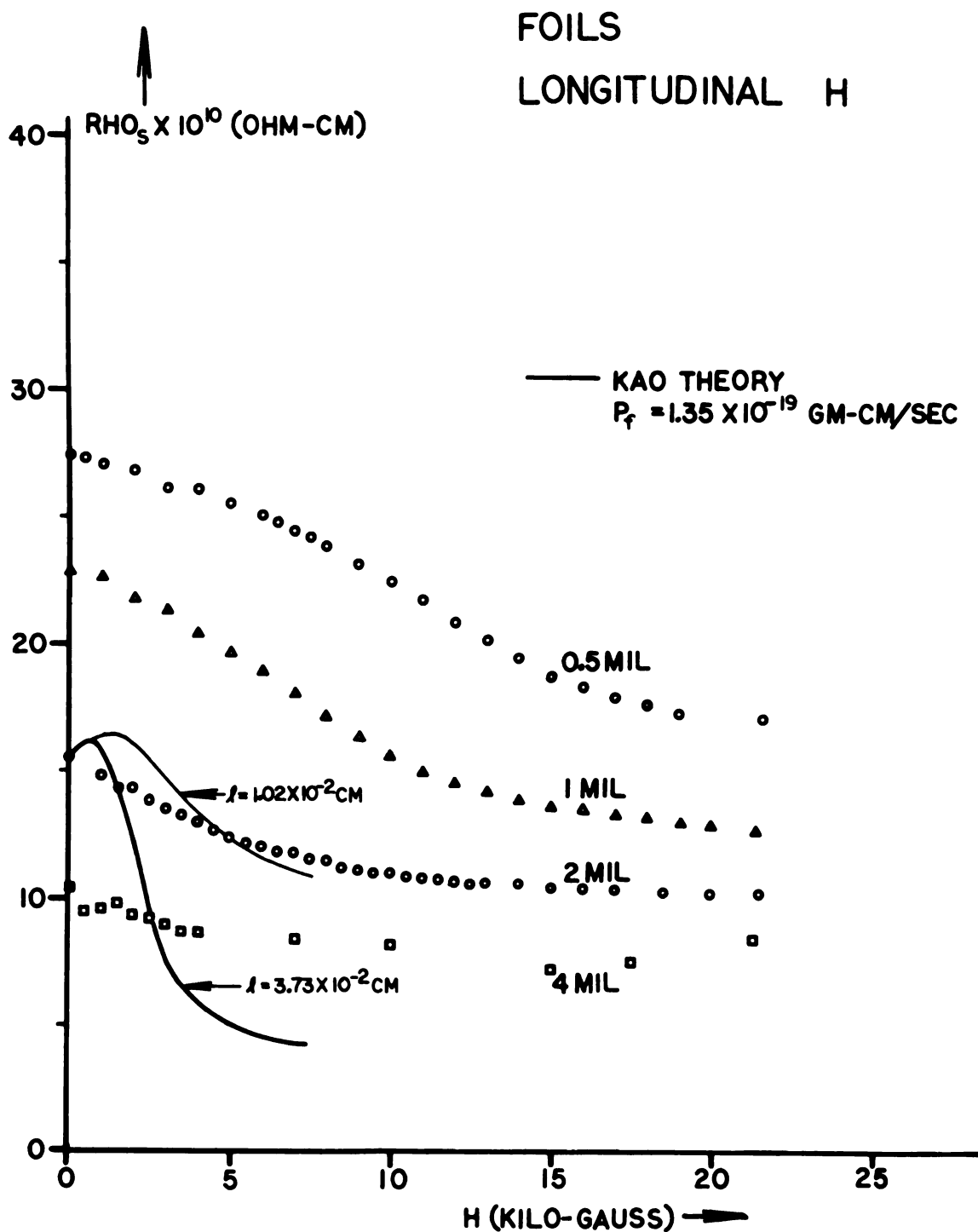
Figure 16. The size-dependent magnetoresistivity produced in aluminum foils by a longitudinal magnetic field, compared to Kao's prediction
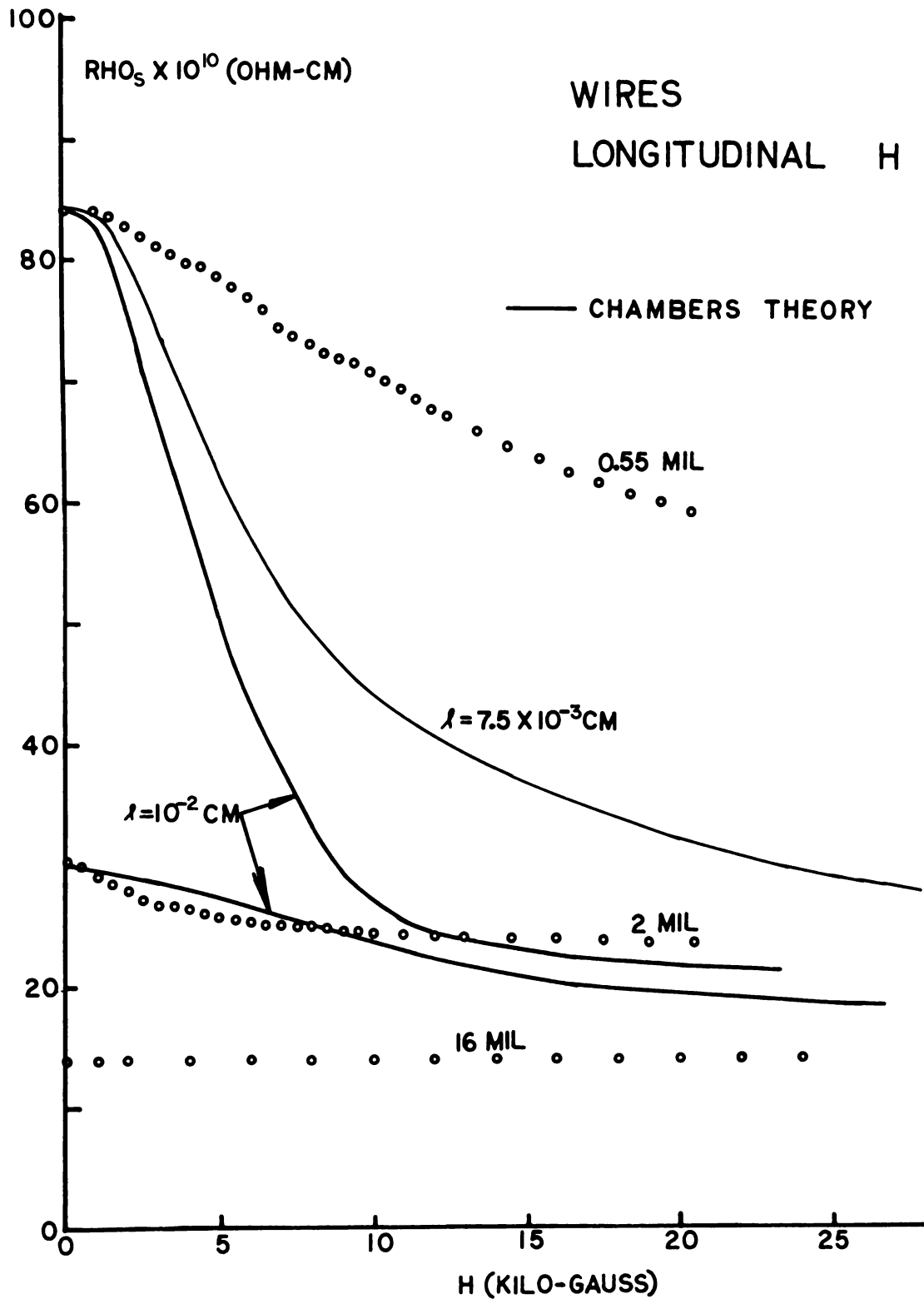
Figure 17. The size-dependent magnetoresistivity produced in aluminum wires by a longitudinal magnetic field, compared to Chambers' prediction

IV.   EFFECTS OF SAMPLE SIZE AND TEMPERATURE
ON ELECTRICAL RESISTIVITY

Theory

We will now look at some theories which yield an effect of sample size on the temperature dependence of the electrical resistivity in thin foils or fine wires. We first examine the size effect theories of Fuchs[8] (for foils) and Dingle[9] and Nordheim[10] (for wires) for possible size-temperature dependent effects.

Looking first at the Nordheim relation

$$\rho/\rho_\infty = 1 + \ell_\infty/d, \tag{9}$$

where ρ_∞ and ℓ_∞ are the total bulk electronic resistivity and total bulk electronic mean free path, we see that it can be rearranged into the form

$$(\rho - \rho_\infty) = (\rho_\infty \ell_\infty)/d, \tag{17}$$

implying that $\rho(d)$ has a dependence on temperature different from $\rho_\infty(T)$ only if $\rho_\infty \ell_\infty = \rho_\infty \ell_\infty (T)$. We therefore estimate the temperature dependence of $\rho_\infty \ell_\infty$.

If one solves the Boltzmann equation for free electrons subject to a D.C. electric field and having a single relaxation process (characterized by relaxation time τ), one obtains

$$1/\rho_\infty \equiv \sigma_\infty = \frac{ne^2\tau}{m} \tag{18}$$

where ρ_∞ is the bulk electrical resistivity, σ_∞ is the bulk electrical conductivity, and n, e and m are the electronic density, charge and mass respectively. If we further set $v_f = \ell_\infty/\tau$ where v_f = Fermi velocity and ℓ_∞ = bulk electronic mean free path, we find

$$\rho_\infty \ell_\infty = \frac{m}{e^2} \left(\frac{v_f}{n} \right) \tag{19}$$

Thus $\rho_\infty \ell_\infty$ has the temperature dependence of v_f/n.

Insofar as the assumptions used above can be applied to aluminum, we can estimate the temperature dependence of (n_f/n), and hence of $\rho_\infty \ell_\infty$, in the following way. We assume the temperature dependence of n to be due only to lattice thermal expansion, and find for aluminum

$$n \simeq n_o e^{-1\times10^{-4} T(^\circ K)} \tag{20}$$

where n_o is the electronic density at T = 0°K. Subject to the assumption that kT<< $E_f(T = 0) \equiv E_f(0)$ and $E_f = mv_f^2/2$, we find that

$$\frac{v_f}{n_o} \simeq \frac{3\pi^2 \hbar^3}{2m^2 E_f(0)} \left[1 - \frac{\pi^2}{24} \left(\frac{kT}{E_f(0)} \right)^2 \right] \tag{21}$$

where $\hbar$ is defined as $h/2\pi$. We then have

$$v_f/n \simeq \frac{3\pi^2 \hbar^3}{2m^2 E_f(0)} \left[1 - \frac{\pi^2}{24} \left(\frac{kT}{E_f(0)} \right)^2 \right] e^{1\times10^{-4} T(^\circ K)}. \tag{22}$$

For aluminum $E_f(0) \simeq 15$ ev, and, assuming T = 40°K, the correction to v_f/n will be about one part in 10^3. We see, then,

that subject to the assumptions we have made, $\rho_\infty \ell_\infty$ should be effectively temperature independent. We will show below that our experimental data is consistent with this prediction.

Returning to the Nordheim relation, we conclude that ρ and ρ_∞ will have the same temperature dependence, since $\rho_\infty \ell_\infty \neq \rho_\infty \ell_\infty(T)$. The Nordheim relation predicts no size-temperature dependent effect.

In the limit of <u>very fine</u> wires $(\frac{\ell_\infty}{d} \gg 1)$ the Nordheim relation becomes

$$\frac{\rho}{\rho_\infty} \simeq \frac{\ell_\infty}{d}$$

or

$$\rho \simeq (\rho_\infty \ell_\infty)/d \tag{23}$$

implying that ρ becomes temperature independent for $\rho_\infty \ell_\infty$ independent of T.

If we look, however, at Dingle's result in the limit of <u>thick wires</u>

$$\frac{\rho_\infty}{\rho} \equiv \frac{\sigma}{\sigma_\infty} = 1 - \frac{3}{4}\left(\frac{\ell_\infty}{d}\right) + \frac{3}{8}\left(\frac{\ell_\infty}{d}\right)^3 + \cdots \tag{24}$$

we obtain

$$(\rho - \rho_\infty) = \frac{3}{4}(\rho_\infty \ell_\infty)/d + \rho_\infty \times (\text{terms nonlinear in } \ell_\infty) \tag{25}$$

Thus the assumption $\rho_\infty \ell_\infty$ = constant does <u>not</u> imply that $(\rho - \rho_\infty)$ is temperature independent. On the contrary, we have a "built in" temperature dependence in the terms enclosed in the parentheses.

Likewise if we look at Dingle's result in the limit of <u>very fine wires</u> ($\frac{\ell_\infty}{d} \gg 1$)

$$\frac{\rho_\infty}{\rho} \equiv \frac{\sigma}{\sigma_\infty} = \frac{d}{\ell_\infty} - \frac{3}{8}\left(\frac{d}{\ell_\infty}\right)^2 \left[\ell n\left(\frac{\ell_\infty}{d}\right) + 1.059\right] - \frac{2}{15}\left(\frac{d}{\ell_\infty}\right)^3$$

(26)

we find

$$\rho \simeq (\rho_\infty \ell_\infty)/d + \rho_\infty \times \text{(terms nonlinear in } \ell_\infty) \quad (27)$$

ie., ρ is no longer temperature independent since the terms in the parenthesis introduce a temperature dependence through ℓ_∞. If one looks at this additional effect numerically over the entire range of $\frac{d}{\ell_\infty}$, one finds that the function $(\rho - \rho_\infty)$ has a maximum at $d/\ell_\infty \simeq .5$. This is the point of maximum deviation between the Dingle and Nordheim theories.

The comments we have made about the size dependent resistivity for thin wires according to Dingle's theory can also be applied to Fuch's theory for thin foils: a temperature-dependent size effect is also built into Fuch's theory if we assume $\rho_\infty \ell_\infty$ = constant.

We now look at various scattering processes which contribute to electrical resistivity and the degree to which they might produce a temperature dependence of electrical resistance which is dependent on sample size.

We first consider in detail a mechanism proposed by Olsen[20] to explain an experimentally observed effect of sample size on the temperature dependence of electrical resistivity in indium. This is the mechanism we wish to study

experimentally. We then discuss other ways by which size-temperature dependent effects on electrical resistivity can arise, both for completeness, and because we will need to use one or more of them to explain our data. In this discussion we will assume that the Boltzmann equation, using either one or two independent scattering times, is adequate to describe the physical situation. Strictly speaking, the Boltzmann equation, even with a generalized relaxation time, is only valid at very low temperatures or above the Debye temperature of the metal. However, since our data seems to show nothing obviously inconsistent with solutions of the Boltzmann equation in the τ approximation, and since we have no adequate alternative approach for analysis of our data, we shall usually assume the validity of the single τ approximation at all temperatures.

The electrical resistivity of a typical bulk metal is dominated by three scattering processes: electron-electron scattering, electron-impurity scattering, and electron-phonon scattering. The first two processes involve predominantly large angle scattering, scattering which produces a large change in the momentum of the scattered electron. Electron-phonon scattering is of two types: Normal electron-phonon scattering, which may be small angle; and electron-phonon Umklapp scattering, which is always large angle. The two electron-phonon scattering processes differ in the following way: Normal scattering requires that the total crystal momentum of the incoming electron-phonon pair be transmitted

undiminished to the outgoing electron-phonon pair, implying that the change in electronic momentum cannot exceed the momentum of the scattering phonon; Umklapp scattering requires that some of the momentum of the electron-phonon pair be transferred to the crystal lattice: a reciprocal lattice vector appears in the momentum conservation equation.

We now show how Normal electron-phonon scattering at low temperatures can enhance the temperature dependence of the electrical resistivity of small wires over the temperature dependence for bulk material. Mott and Jones[38] show, for Normal electron-phonon scattering in the approximation of free electrons and a Debye phonon spectrum, that the maximum angle θ_m through which an electron can be scattered by a phonon is given by

$$\theta_m \simeq 2^{1/3}(T/\Theta_D), \tag{28}$$

where T is the absolute temperature and Θ_D is the Debye temperature of the lattice. This implies that the contribution to the electrical resistivity due to Normal electron-phonon scattering must decrease to zero as T approaches zero. At small, non-zero temperatures this resistivity contribution is small since a large number of small-angle scattering events are necessary to randomize the momentum of a current-carrying electron.

If we now reduce one conductor dimension to a size comparable to the electronic mean free path, and permit the surface thus introduced to scatter electrons diffusely, we see that the most important current-carrying electrons will

be just those which travel very nearly parallel to the con-
ductor axis, since the momenta of the others will be quickly
randomized by collisions with the sample surface. If the
specimen is sufficiently small, an electron traveling along
the conductor axis may, after only a few small-angle phonon
events, be deflected into the conductor surface and be scat-
tered diffusely. This means that electrical resistivity due
to Normal electron-phonon scattering should become important
at lower temperatures in small samples than in large samples.
This is, in effect, the suggestion which Olsen[20] made to
qualitatively explain the enhancement of the temperature-
dependent electrical resistivity which he found in fine indium
wires, and which Andrew[39] noted in fine wires of mercury.

This problem of surface-enhanced low-temperature
electron-phonon scattering has been attacked theoretically
by Blatt and Satz,[40] Lüthi and Wyder[41] and Azbel' and
Gurzhi.[42] All three approaches require that Matthiessen's
Rule be obeyed; that is, that one can define a total relaxa-
tion time $\frac{1}{\tau_{total}}$ which is the sum of the various inverse
partial relaxation times

$$\frac{1}{\tau_{total}} = \frac{1}{\tau_1} + \frac{1}{\tau_2} + - - -.$$

Lüthi and Wyder have used a purely kinetic approach, perform-
ing a Monte-Carlo calculation on the trajectory of a single
conduction electron in a fine wire under the independent ef-
fects of impurity, surface, and small-angle electron-phonon
scattering. Their results show that resistivity enhancement
should occur under these conditions.

Blatt and Satz use the basic model originally assumed by Nordheim--that of an electron gas flowing down a conducting tube--to obtain a solution of the problem for fine wires, which, while admittedly approximate, provides a basis for quantitative comparison with experiment. They assume that the resistivity $\rho_\omega(T)$ of a fine wire can be described by the relation

$$\rho_\omega(T) = [\rho_i(T) + \rho_r] + [\rho_s + \rho_{ps}(r,T)], \qquad (29)$$

where the first bracket contains the bulk, and the second bracket the size-dependent portion of the resistivity. $\rho_i(T)$, ρ_r and ρ_s are the resistivities due to bulk electron-phonon scattering, electron-impurity scattering, and direct electron-surface scattering respectively. They find the resistivity $\rho_{ps}(r,T)$ due to surface enhanced small-angle electron-phonon scattering to be given by the relation:

$$\rho_{ps}(r,T) = (2\pi)^{1/3}(\rho_\infty \ell_\infty)^{2/3}(T/\Theta_D)^{2/3}[\rho_i^N(T)]^{1/3}r^{-2/3}$$

$$(30)$$

where $\rho_\infty \ell_\infty = mv_f/ne^2$, Θ_D is the Debye temperature of the metal lattice, $\rho_i^N(T)$ is the bulk resistivity due to <u>Normal</u> electron-phonon scattering, and r is the wire radius. It should be noted that this equation contains no adjustable parameters. If we further assume that $\rho_i(T)$ can be written as the sum of the Normal and Umklapp contributions

$$\rho_i(T) = \rho_i^N(T) + \rho_i^U(T) \qquad (31)$$

and if we write

$$\rho_i^N(T) = f^N(T)\rho_i(T),\qquad(32)$$

where $f^N(T)$ is the fractional part of $\rho_i(T)$ due to Normal electron-phonon events at temperature T, we have

$$\rho_i^U(T) = (1 - f^N(T))\rho_i(T).\qquad(33)$$

We obtain f^N from Equation (30) by substituting expression (32) for $\rho_i^N(T)$, all other quantities being constants or experimentally determined parameters. This method then gives us a means of obtaining, at least approximately, the fraction of the total resistivity due to normal electron-phonon events, and the actual Umklapp resistivity as a function of temperature.

For the case of thin foils, Azbel' and Gurzhi appeal to the existing theory of the anomalous skin effect. Their resulting formula, correct for bulk metal as well, can be written

$$\frac{1}{\rho} \equiv \sigma \simeq \left(\frac{1}{\rho_\infty \ell_\infty}\right) t \; \ell n(1 + X_0^{-1})$$

where

$$X_0 = t\left(\frac{1}{\ell_{ei}} + \frac{1}{\ell_{ee}} + \frac{1}{\ell_{ep}^\infty}\right) + \frac{t/\ell_{ep}^\infty}{(T/\Theta_D)^2 + (t/\ell_{ei})^2 + (t/\ell_{ep}^\infty)^{2/3}}$$

$$(34)$$

Here $\sigma \equiv 1/\rho$ = the electrical conductivity of the foil

t = the thickness of the foil

ℓ_{ei} = the electron-impurity mean free path

ℓ_{ee} = the electron-electron mean free path

ℓ_{ep}^{∞} = the bulk electron phonon mean free path

T = absolute temperature

Θ_D = Debye temperature

$\rho_{\infty} \ell_{\infty} = mv_f/ne^2$.

They predict that the residual resistivity should be reached in a thin foil, not at $\ell_{ep}^{\infty} \simeq \ell_{ei}$ as in a bulk sample, but at

$$\ell_{ep}^{\infty}(T/\Theta_D)^2 \simeq \ell_{ei},$$

which occurs at a considerably lower temperature.

In practice we still have the problem of determining $\rho_i(T)$, but this will be discussed in conjunction with the appropriate data.

Wyder[33] recently proposed another mechanism involving the interaction between electrons and phonons which could result in a size-dependent enhancement of the temperature dependence of electrical resistivity. Following a suggestion of Pippard,[43] he suggested that reduction of the total electronic-relaxation time by scattering other than electron-phonon scattering (in particular, electron impurity scattering), may result in enhancement of the electron-phonon interaction. Since electron-phonon scattering produces most of the temperature dependence of the electrical resistivity, enhancement of this interaction will increase the electrical resistivity. Because no detailed calculation of the effects

of such enhancement on electrical resistivity have been made,
we will not attempt to investigate this mechanism in detail.

Having discussed the interaction between the speci-
men surface and electrons scattered "normally" by phonons
we now turn to the other scattering mechanisms listed above.
Electron-electron scattering, electron-impurity scattering,
and electron-phonon Umklapp scattering, are all examples
of large angle scattering; each scattering event produces
a substantial change in the direction of motion of the
electron. A nearby surface cannot add much more to the
effect of such scattering, and no enhancement due to speci-
men size (similar to that discussed for Normal electron-
phonon scattering) results. In fact, if these various
large angle scattering processes can be considered to act
independently upon the electrons, we do not expect them to
introduce any size-effect into the temperature dependence
of the electrical resistivity. When scattering indepen-
dently, these processes should retain their bulk charac-
teristics even in small samples. However it is not
necessarily true that these scattering processes must act
independently.

The problem of temperature dependent deviations from
Matthiessen's Rule (independent scattering mechanism) has
drawn some recent attention. Dugdale and Basinski[44] ap-
proach the problem in the following way. They assume that
electrons on two different portions of the Fermi surface can
be considered as effectively forming two independent bands,
each subject to independent electron-phonon and electron-impurity

scattering processes. Since the "bands" are independent the total conductivity σ_{Tot} is the sum of the conductivities from each band

$$\sigma_{Tot} = \sigma^{(1)} + \sigma^{(2)}. \tag{35}$$

The independence of the scattering processes implies that Matthiessen's Rule is valid _in each band_, or

$$\rho^{(1)} = \rho_{ep}^{(1)} + \rho_r^{(1)} \text{ and } \rho^{(2)} = \rho_{ep}^{(2)} + \rho_r^{(2)}. \tag{36}$$

We then have

$$\frac{1}{\rho_{Tot}} = \sigma^{(1)} + \sigma^{(2)} = \frac{1}{\rho_{ep}^{(1)} + \rho_r^{(1)}} + \frac{1}{\rho_{ep}^{(2)} + \rho_r^{(2)}}$$

$$\tag{37}$$

and, except for special cases,

$$\rho_{Tot} \neq \rho_{ep}^{(Tot)} + \rho_r^{(Tot)}. \tag{38}$$

Here Matthiessen's Rule can be violated.

Although Dugdale and Basinski consider only scattering of electrons by impurities, it seems reasonable to assume that a "two band" metal would also show deviations from Matheissen's Rule due to surface scattering, since the surface would be likely to scatter the two types of electrons in a different manner from the way they are scattered by phonons.

Review of Previous Experiments and the
Purpose of the Present Study

Andrew[39] (for fine mercury wires) and Olsen[20] (for fine indium wires) were the first to note an effect of sample size on the temperature dependence of the electrical resistivity. Blatt and Satz[40] (B & S) have shown that the effects seen by Andrew and Olsen in the temperature range 1°K-4.2°K can be correlated to surface enhancement of the resistivity due to small-angle electron-phonon scattering. They have also shown that their (B & S) theory, when applied to the data of Olsen and Andrew, predicts values for f^N which are in reasonable agreement with independent estimates. More recently Wyder[33] repeated Olsen's work on indium and found no temperature-size effect. Blatt, et al.[21] also working with fine indium wires, report an effect comparable in size to that noted by Olsen.

Experiments on single crystals have been performed by Yaqub and Cochran[45] (gallium) and by Aleksandrov[46] (aluminum). Aleksandrov attempted to apply the theory of Blatt and Satz to aluminum at 14°K and at 20°K, the only temperatures (other than 4.2°K) for which he reports measurements. He found f^N to be $\simeq$ .6 - .8 at these temperatures. However, for his thinnest sample at 14°K, $\ell_i^\infty \simeq d$, and at 20.4°K, $\ell_i^\infty < d$. The theory as developed by B & S is limited to the case of $\ell_i^\infty \gg d/2$, which is outside the range of Aleksandrov's measurements.

We began our experiments on thin foils in an attempt to test the predictions of Azbel' and Gurzhi[42] for the

temperature dependence of the electrical resistivity of thin foils. This had not been previously done on thin foils of any material. Just prior to a report of our preliminary findings, made at the Chicago meeting of the American Physical Society, March 1967, Holwech and Jeppesen[47] published a report on a similar study, also on aluminum. They reported no unusual behavior of the electrical resistivity in thin aluminum foils attributable to an Olsen mechanism. We have been able to extend the measurements of Holwech and Jeppesen to foils thinner than theirs by a factor of five. We will compare our results to theirs below.

In view of the disagreement concerning the temperature-size dependent resistivity in indium between Wyder[33] on the one hand and Blatt et al.[21] and Olsen[20] on the other hand, we decided to test the theory of Blatt and Satz on an independent metal, aluminum.

We have also attempted to extend the region of applicability of the B & S theory for fine wires to considerably higher temperatures than has been previously done, in an attempt to obtain a more rigorous test of the theory. This is possible in aluminum since the high Debye temperature ($\Theta_D \simeq 410°K$) implies a slower decrease of ℓ_i^∞ with T than for metals with lower $\Theta_D (\ell_i^\infty \sim (\Theta_D/T)^5$ in the Bloch theory). Thus for our smallest sample $\ell_i^\infty \simeq \frac{d}{2}$ at 35°K and $\ell_i^\infty \simeq 5(\frac{d}{2})$ at 25°K. We should therefore be able to apply the theory safely to about 20°K. This should give us a measure of f^N and $\rho_i^U(T)$

from 2°K to 20°K. It was also hoped that an electron-phonon
relaxation time τ (dependent on sample size and temperature)
could be determined from the resistivity measurements and
compared to that determined from the size dependent portion of
the phonon-drag thermopower.

Description of Apparatus

The sample chamber used for measurements above 4.2°K
is shown in Figure 18. Four specimens (E) were mounted on
the four sides of an aluminum bar (D) of square cross-section.
This bar was attached at one end to a 1/4" thick plexiglass
disc (J) which in turn served as a flange to cover the open-
ing of the aluminum chamber (B). The electrical leads
entered the chamber between (J) and the teflon ring (I). The
plexiglass disc positioned the aluminum bar inside the cham-
ber and thermally insulated the bar from its surroundings.
A heater of manganin wire (C) was wound non-inductively about
this outer chamber, and a copper finger (K) provided a heat
leak from the outer chamber to the helium bath. The current
and potential leads to the specimens, 0.0025" diameter copper wire
were wound several times (H) about the end of the inner rod
and encased in GE7031 varnish to prevent heat loss down the
leads. The specimens were insulated from the aluminum bar
by 0.0005" thick teflon. The current and potential leads were
attached to the specimens in the same way as those used for

measuring transverse magnetoresistance of thin foils. The
temperature in the chamber was measured by means of a ger-
manium resistance thermometer (F) placed in the center of
the aluminum bar and surrounded by Apiezon N grease to pro-
vide good thermal contact with the bar. The leads to this
thermometer were also of 0.0025" diameter copper wire and
were anchored with the leads described above. Helium gas
(G) at atmospheric pressure provided the heat exchange in-
side the can to bring the metal and specimens to equilibrium.
A 0.125" thick styrofoam shield (A) was placed around the
entire outer container to minimize heat loss to the bath and
thermal gradients across the container walls. Desired
equilibrium temperatures were obtained by varying the heater
current to balance the heat loss down the copper finger. The
measuring circuit employed with this apparatus was similar
to that used to measure magnetoresistance. The current was
measured on a Honeywell model 2780 potentiometer with a
Leeds-Northrup D.C. Galvanometer, and the potential drop
across the samples was read on a Honeywell model 2779 poten-
tiometer employing a photocell galvonometer amplifier and
optical galvanometer. The measuring current could be held
stable to one part in 10^4; the potential drop across the
samples could be read to ± 0.01 microvolt. The calibration
for the germanium resistance thermometer, obtained from the
Minneapolis-Honeywell Corporation, was guaranteed to be
accurate to 0.1°K and reproducible to 0.01°K.

APPARATUS FOR RESISTIVITY MEASUREMENTS
ABOVE 4.2 °K
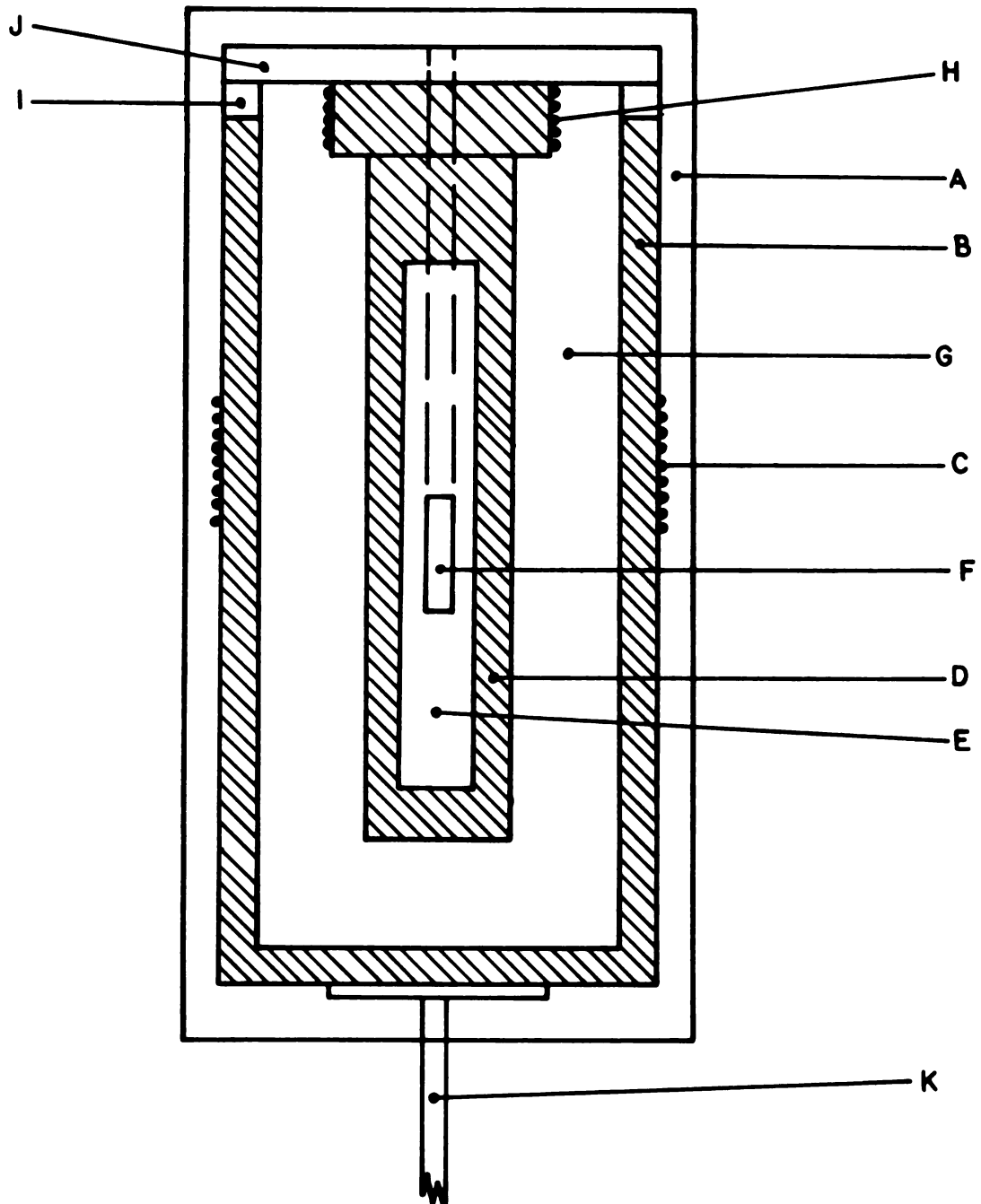
Figure 18   Apparatus for resistivity measurements above 4.2°K

The apparatus used for measurements of electrical resistivity below 4.2°K was that previously employed for measuring transverse magnetoresistance, and is described on page 20.

Results and Discussion

We have measured the resistivity of thin aluminum foils in the temperature range 1.5°K to 50°K. The thickness of the foil samples varied from 0.14×10^{-3}" to 8×10^{-3}". The temperature variation of the total sample resistivity of these foils is shown in Figure 19 for the temperature range 4.2°K to 30°K, and in Figure 20 for 1.5°K to 4.2°K. It can be seen (in the range 4.2°K to 30°K) that the thinner foils show a stronger temperature dependence than the thicker foils. This stronger dependence is made clearer if we look at the difference $\rho(T) - \rho(4.2°K)$ for each foil (see Figure 21). Here we see that the temperature dependence of the electrical resistivity increases systematically with decreasing foil thickness.

It will be noted that Figure 19 contains data on two 0.5×10^{-3}" thick samples. One sample was purposely annealed in air for a particularly long time at high temperature to introduce large amounts of surface oxides and to allow surface impurities to diffuse into the sample. The resistance ratio of this foil was about 18% lower than that of the other 0.5×10^{-3}" thick foil. Yet we note in Figure 21

that, to within our experimental error, the two 0.5×10^{-3}" thick foils have the same temperature dependence. This suggests that the effect we observe cannot, at least in this temperature range, be due to temperature dependent deviations from Matthiessen's Rule because of sample impurities.

We first take into account the size-temperature dependence inherent in Fuch's result: for a 0.14 mil diameter foil the prediction for $\rho(T,t)$ is shown as a solid line in Figure 23. This is very nearly consistant with our data without requiring any size dependent enhancement of the resistivity due to small angle electron-phonon scattering.

We now attempt a comparison of our data with the theory of Azbel' and Gurzhi.[42] To make a comparison to theory possible, the following assumptions are made. Electron-electron scattering may be considered negligible in thin plates,[42] allowing us to set $\ell_{ee} = \infty$ (see theory section for the meaning of the symbols). To obtain an estimate of ℓ_{ei}, we fit our experimental $\rho(t)$ to Fuch's theory at 4.2°K and find $\ell_\infty \simeq 6 \times 10^{-2}$ cm. Since the temperature dependent resistivity at 4.2°K constitutes less than 1% of the total resistivity in any foil, we associate ℓ_{ei} with ℓ_∞ at 4.2°K ($\ell_{ei} \simeq 6 \times 10^{-2}$ cm). We can obtain ℓ_{ep}^∞ from a knowledge of ρ_{ep}^∞ and the condition that $\rho_\infty \ell_\infty = $ constant. We therefore test the product $\rho_\infty \ell_\infty$ at four temperatures by fitting our data to Fuch's theoretical curve. The result is shown in Figure 22. In the temperature range from 4.2°K to 30°K, $\rho_\infty \ell_\infty$ is nearly a constant. Since ρ_{ep}^∞ dominates the resistivity over a large part of this

interval, we interpret this to imply that we may assume $\rho_{ep}^{\infty} \ell_{ep}^{\infty}$ = constant as well, and choose that constant to be $\rho_{\infty} \ell_{\infty} = 11.3 \times 10^{-12} \, \Omega - cm^2$--the average value over the temperatures shown.

To obtain ρ_{ep}^{∞} we use two separate methods. First we assume that the temperature dependence of the 8 mil foil is characteristic of the bulk material and can therefore be identified with ρ_{ep}^{∞}. As an alternate method we associate ρ_{ep}^{∞} with the temperature dependence of the ρ_{∞} obtained by fitting $\rho(t,T)$ to Fuch's curve at various temperatures. The two methods give the same predicted temperature dependence within our measuring error. In practice then, we take

$$\rho_{ep}^{\infty} = [\rho(T) - \rho(4.2°K)] \Big|_{8 \text{ mil foil}}$$

and

$$\ell_{ep}^{\infty} = \frac{\rho_{\infty} \ell_{\infty}}{\rho_{ep}^{\infty}} = \frac{11.3 \times 10^{-12} \, \Omega - cm^2}{\rho_{ep}^{\infty}}$$

We finally assume the Debye temperature of aluminum to be 410°K.[48] The resulting predicted and experimental results are shown in Figure 23 for a 0.14 mil thick foil. The temperature dependence of the bulk material is also shown. We note a large discrepancy between the Azbel'--Gurzhi predicted $\rho(T)$ and our experimental $\rho(T)$, particularly below 15°K, where the predicted rapid rise is not visible. The results for our 0.6×10^{-3}" foil, analyzed in the same way as the data for the 0.14 mil foil, are in general agreement with the above and

with results obtained by Holwech and Jeppeson[47] for a slightly larger foil. Small differences between our results and theirs will be discussed below.

We recall at this time that the Azbel'-Gurzhi theory, considering the effect of small angle phonon-electron scattering, describes only the Normal electron-phonon scattering. Pytte[49] in a recent calculation of the electrical resistivity for aluminum, predicts that the resistivity due to Normal electron-phonon scattering is less than 1% below 60°K. If the electrical resistivity is largely dominated at low temperatures by Umklapp scattering, we would not expect to see the effect predicted by Azbel' and Gurzhi. At very low temperatures (eg. below 4.2°K) Umklapp scattering depends very sensitively on the shape of the Fermi surface near the Brillouin Zone boundaries. Since the shape of the Fermi surface of aluminum is not well known in these regions, no reliable theoretical prediction of the electron-phonon Umklapp contribution to the very-low-temperature electrical resistivity can be made at present.

Holwech and Jeppesen[47] have also noted large discrepencies between the thin foil resistivity predicted by Azbel' and Gurzhi and the resistivity they (H & J) find experimentally in thin aluminum foils. This they have also interpreted to imply that the electrical resistivity below

50°K is dominated by electron-phonon Umklapp scattering. They also note a small additional effect which we do not appear to see. They obtain a small peak in $(\rho - \rho_\infty)(T)$ at about T = 30°K. We suggest one possible explanation for this discrepancy between our results and theirs. Our bulk material is somewhat less pure than that which they used (resistance ratios $(R_{300°K}/R_{4.2°K})$ ~ 6500 and ~ 25,000 respectively), and shows a somewhat stronger temperature dependence (see Figure 21). It is possible that this additional impurity could yield a temperature dependent deviation from Matthiessen's rule.

Since the electrical resistivity appears to be dominated by electron-phonon Umklapp scattering in the temperature range below 50°K, we thought it of interest to obtain an experimental estimate of the Umklapp resistivity by applying the theory of Blatt and Satz to data taken on fine aluminum wires.

We have measured the resistivities of fine aluminum wires (0.53×10^{-3}" $\leq$ d $\leq$ 16 $\times 10^{-3}$") over the same temperature range as the foils. The resulting resistivities are shown in Figures 24 and 25. The total resistivity change from 1.5°K to 4.2°K was in all cases less than 0.5%. Since the quantities required for comparison to the B & S theory are differences between these values, the measurements were

taken with extreme care. These data were then smoothed be-
fore they were compared to theory. An estimate of the
measuring error can be seen in Figure 24. Plotting, as
before, $\rho(T) - \rho(1.5°K)$ for $1.5°K \le T \le 4.2°K$ and
$\rho(T) - \rho(4.2°K)$ for $T \ge 4.2°K$, we again see a systematic
increase in temperature dependence with decreasing wire
diameter (Figures 26 and 27). It should be noted that the
data shown here are still unsmoothed.

We now attempt to fit our data to the $\rho(d,T)$ pre-
dicted by Dingle for $T \ge 4.2°K$. We obtain an estimate of
$\rho_\infty \ell_\infty$ for the wires from a comparison of our data to the
Nordheim relation at $4.2°K$ (Figure 28), and find $\rho_\infty \ell_\infty =$
5.61×10^{-12} Ω -cm^2. If we again assume

$$\rho_{ep}^\infty(T) = [\rho(T) - \rho(4.2°K)]\Big|_{8 \text{ mil foil}},$$

we obtain the fit shown in Figure 29. It is apparent that
the predicted behavior of Dingle does not explain the data
for the 0.56×10^{-3}" diameter wire, in contrast to Fuch's
reasonable prediction of the temperature-size variation for
the foils.

If instead of assuming that $\rho_{ep}^\infty(T)$ has the tempera-
ture dependence of

$$\rho(T)\Big|_{8 \text{ mil foil}},$$

we obtain $\rho_{ep}^\infty(T)$ from a Nordheim plot of our wire data for
$T \ge 4.2°K$, the resulting $\rho_{ep}^\infty(T)$ has a somewhat stronger tem-
perature dependence than that of the 8 mil foil. Dingle's

predicted $\rho(T)$ for this $\rho_{ep}^{\infty}(T)$ applied to the 0.56×10^{-3}" diameter wire can be seen in Figures 25 and 29. Although this lies closer to the experimental curve, the difference is still large.

If we apply the B & S theory to the wire data, using $\rho_{ep}^{\infty}(T)\Big|_{8 \text{ mil foil}}$ taking into account the deviation predicted by Dingle, we find the dependence of $\rho_{ps}(r,T)$ on $r^{-2/3}$ shown in Figure 30. In view of the experimental uncertainties, the agreement may be considered satisfactory.

To compare our data below 4.2°K to theory we must obtain $\rho_{ep}^{\infty}(T)$ by applying the Nordheim Relation to our wires at 2°K, 3°K, and 4°K (cf. Figure 31), and assuming Matthiessen's Rule to hold. The error in the measurement of $\rho(T)$ for the 8 mil foil below 4.2°K is too great to permit quantitative use of this data. The resulting $\rho_{ps}(r,T) \sim r^{-2/3}$ are shown in Figure 32. Again, considering the experimental error, the agreement is satisfactory.

To test the temperature dependence of $\rho_{ps}(r,T)$, we plot the slopes of the lines (Figures 30, 32) as a function of T on a log-log graph (see Figure 33). We obtain an estimate of $\rho_i^{\infty}(T)$ for $T \leq 4.2$°K, by noting that $\rho_i^{\infty}(T) \sim T^n$ yields n varying from 2.96 to 4.14, the variation not being correlated with sample size. We therefore take the average n = 3.55 to be characteristics of $\rho_{ep}^{\infty}(T)$ below 4.2°K. We then expect (from B & S) the temperature dependence of $\rho_{ps}(r,T)$ to be $(T^{3.55})^{1/3} T^{2/3} \simeq T^{1.85}$.

For $T \geq 4.2°K$ we find $\rho \sim T^n$ with $n \simeq 4.5$ for $T \geq 20°K$ and n decreasing to about 3.5 for $T \leq 10°K$. Assuming that the average value $n \simeq 4$ is reasonable for the temperature range $T \geq 4.2°K$ we obtain a prediction $\rho_{ps}(r,T) \sim (T^4)^{1/3} T^{2/3} = T^{2.0}$. However, since this higher temperature value of n is temperature dependent, we do not expect a good fit to theory over the entire temperature range.

Using the value of $\rho_{ep}^{\infty}(T)$ calculated from $\rho \sim 1/d$ and proceeding as before, we obtain the predicted temperature dependence (cf. Figure 33):

$$\rho_{ps}(r,T) \sim T^{2.52}.$$

If we now compare these predicted and experimental temperature dependences, (Figure 33) we see that the experimental slopes are consistently too high. However, when compared to previous attempts[40] to interpret the temperature dependence of fine wires of other materials (mercury and indium) interms of B & S theory, the discrepancies between theory and experiment for aluminum cannot be considered unreasonable.

If we carry our parallel analyses further, we obtain the predicted values of $f^N(T)$ and $\rho_{\infty}^{U}(T)$:

TABLE 3

Experimental estimates of $f^N(T)$ and $\rho_\infty^U(T)$

T(°K)	$f^N(T)^a$	$f^N(T)^b$	$\rho_\infty^U(T)\times10^{10}(\Omega\text{-cm})^a$	$\rho_\infty^U(T)\times10^{10}(\Omega\text{-cm})^b$
2		7.7×10^{-4}		9.99×10^{-4}
3		1.7×10^{-4}		2.40×10^{-2}
4		1.6×10^{-4}		7.8×10^{-2}
10	5.32×10^{-2}	1.42×10^{-2}	1.57	1.68
15	2.39×10^{-1}	2.33×10^{-1}	3.65	4.20
20	1.03	6.25×10^{-1}	-2.85×10^{-1}	7.82
25	1.12	3.63×10^{-2}	-2.47	24.5

where a implies that $\rho_{ep}^\infty(T)$ was obtained from $\rho(T)\big|_{8\text{ mil foil}}$ and b implies that $\rho_{ep}^\infty(T)$ was obtained from the Nordheim Relation.

We note immediately the large values of $f^N(T)$ for $T \geq 15°K$. This implies that a large portion of the wire resistivity at these temperatures is indeed due to Normal electron-phonon processes, in contrast to both Pytte's[49] calculation and our tentative explanation of the foil data. This could have been seen immediately from the large temperature-dependent resistivity remaining for the wires even after the dependence predicted by Dingle had been removed.

We must now attempt to explain why we see this additional temperature dependence in the resistivity of the wires, but not of the foils.

The data reported up to this point were taken on various samples studied during a series of measuring runs. One set of four samples, ranging in diameter from 0.8 mil to 32 mil, all measured on the same run, and all having relatively low resistance ratios (high impurity or detect content) yielded resistivities above 4.2°K all of which increased more rapidly with temperature than those shown in Figure 25. (The resistivities of two of these samples (at 4.2°K) appear as squares in Figure 28.) Since the data for these samples deviated systematically from the data for all the other samples measured in this temperature range, we have omitted the data for these samples from the above analysis. This discrepancy could have occurred either because the measuring system was somehow different for this one run than for all the other runs, or because these samples were less pure than the other samples. It is possible that we have observed a correlation between additional impurity content and enhanced temperature dependence of the resistivity.

The only unusually rapid increase with temperature of wire resistivity seen below 4.2°K, was observed on a single wire with an extremely low resistance ratio (the additional impurity introduced into this wire was about 25 times that introduced into the 0.5 mil foil used to test impurity-temperature effects as described above). The measurements of resistivity made on this wire were also omitted from our analysis.

If this apparent correlation between impurity content and enhanced temperature dependence of resistivity in our wires is real, it suggests that we are seeing temperature-dependent deviations from Matthiessen's Rule, perhaps of the type suggested by Wyder[33] or by Dugdale and Basinski.[44] We now consider whether such effects are also sufficient to explain various differences between our wire data and our foil data.

In the first place, the resistivity of our 16 mil diameter wires increases more rapidly with temperature than the resistivity of our 8 mil foils. Since the impurity content of the 16 mil wires is about three times greater than that of the 8 mil foils, this more rapid increase with temperature could be produced by temperature-dependent deviations from Matthiessen's Rule due to the excess impurity content.

Secondly, while we obtain agreement between our foil data and Fuch's theory, our wire data shows a size-temperature enhancement of resistivity beyond that given by the equivalent Dingle theory for wires. Although this extra enhancement was shown above to be consistent with forms predicted by Blatt and Satz,[40] its excessive magnitude, along with the absence of a similar effect in our foils, suggests that this theory is not the correct explanation for its existance. This extra enhancement could be an impurity effect. One would expect fine wires, basically more difficult to prepare than fine foils, to show an impurity content which

increases with decreasing wire diameter. If increased im-
purity content implies increased temperature dependence of
the resistivity, we would expect the resistivity of fine
wires to show a stronger temperature dependence than that
of the larger (more pure) wires.

It is important that we remember, in view of our
emphasis on impurity content of the wires to explain our
experimental data, that our wires, carefully prepared and
carefully handled, are really of quite high purity (the
resistance ratios of our 0.5×10^{-3}" diameter wires still
exceed 500). The point we wish to make is that small amounts
of impurity, only a few parts per million, may be sufficient
to cause enhancement of the temperature dependence of elec-
trical resistivity. Similar conclusions were previously
reached for tin by Reich and Försvoll[50] and for copper
and silver by Dugdale and Basinski.[44]

On the other hand, we cannot interpret our excess
temperature dependent size effect as due to higher impurity
content without reservations. In all their copper and sil-
ver alloys, Dugdale and Basinski never found a deviation
from Mattheissen's Rule larger than 10% below 25°K. At even
lower temperatures, we see a deviation as large as 70% be-
tween actual and predicted (ignoring the B & S mechanism)
temperature dependences.

It is somewhat disturbing to note, in view of the
fact that we are very likely not seeing the effect of an
Olsen (B & S) mechanism on our wires about 10°K, that we are

able to fit our data to predictions of the theory of B & S in a satisfactory way. This suggests that the B & S theory may be too insensitive to differentiate between various mechanisms which could cause enhanced temperature dependence, unless the experimental data is extremely accurate. It is therefore important that one either somehow identify the presence of an Olsen mechanism in an independent manner before applying the B & S theory or that one apply the theory only to very accurate data. We take this to mean that, even though our data below 4.2°K show temperature and size dependencies consistent with predictions of the B & S theory; in view of the uncertainties in this data and the lack of reliable, independent estimates of $f^N(T)$ (see page 69), this should not be considered definite proof of the applicability of the theory to aluminum.

Figure 19. The electrical resistivity of thin aluminum foils
at temperatures above 4.2°K

Figure 20. The electrical resistivity of aluminum foils at temperatures below 4.2°K
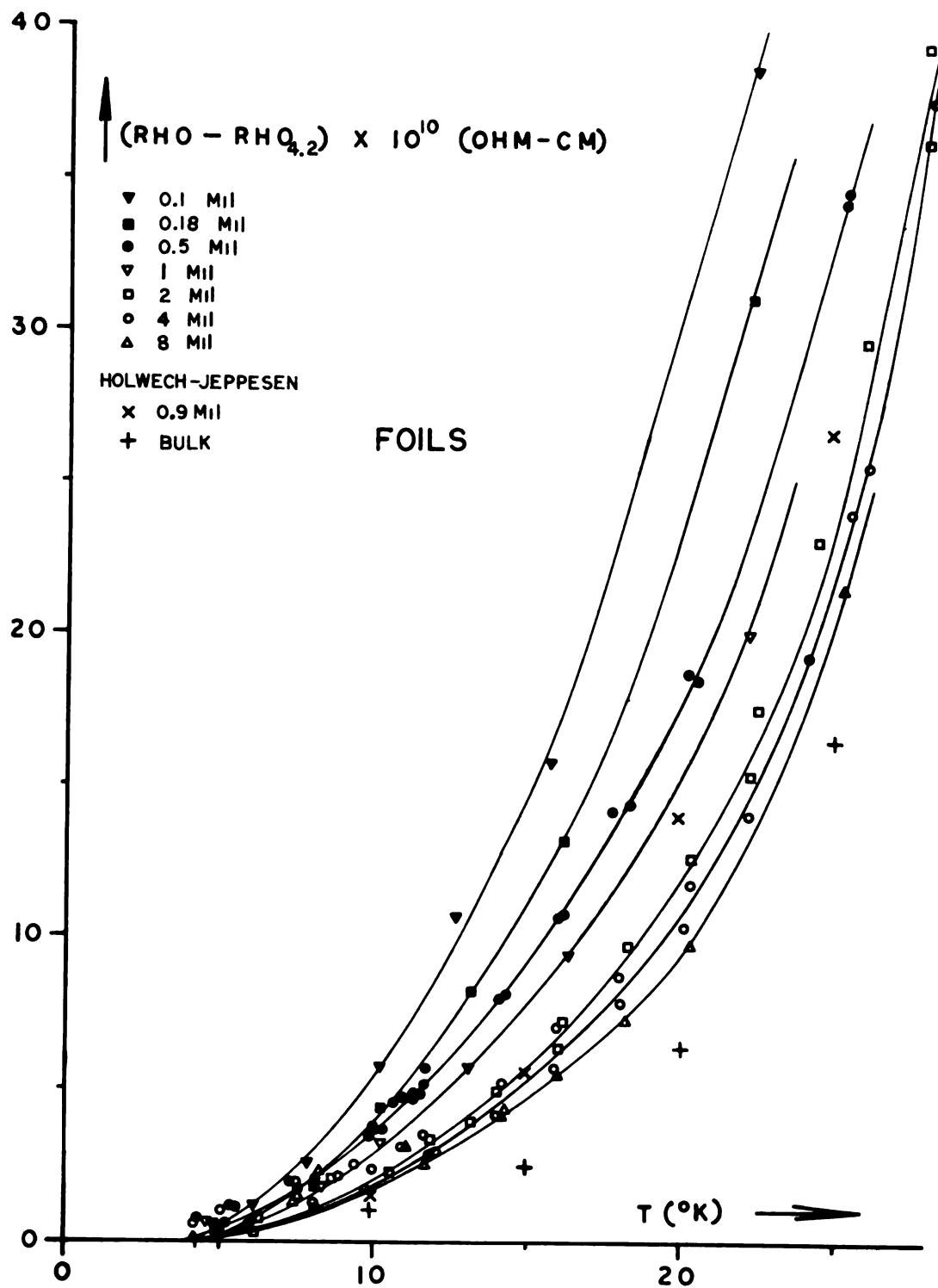
Figure 21. The data of Figure 19 plotted as RHO(T)-RHO(4.2°K)
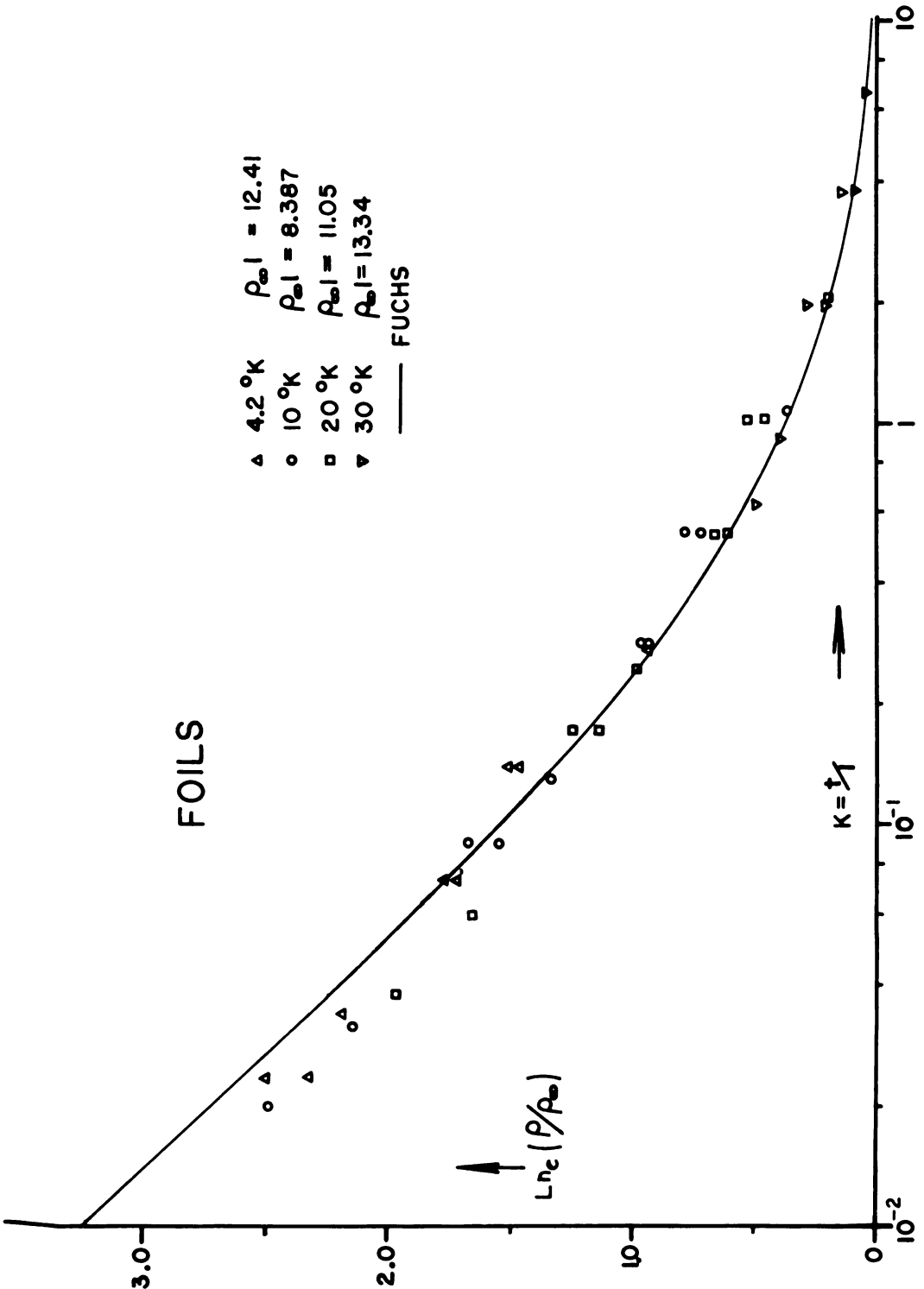
Figure 22. Comparison of the size-dependence of the electrical
resistivity of aluminum foils at various temperatures, with Fuch's
prediction
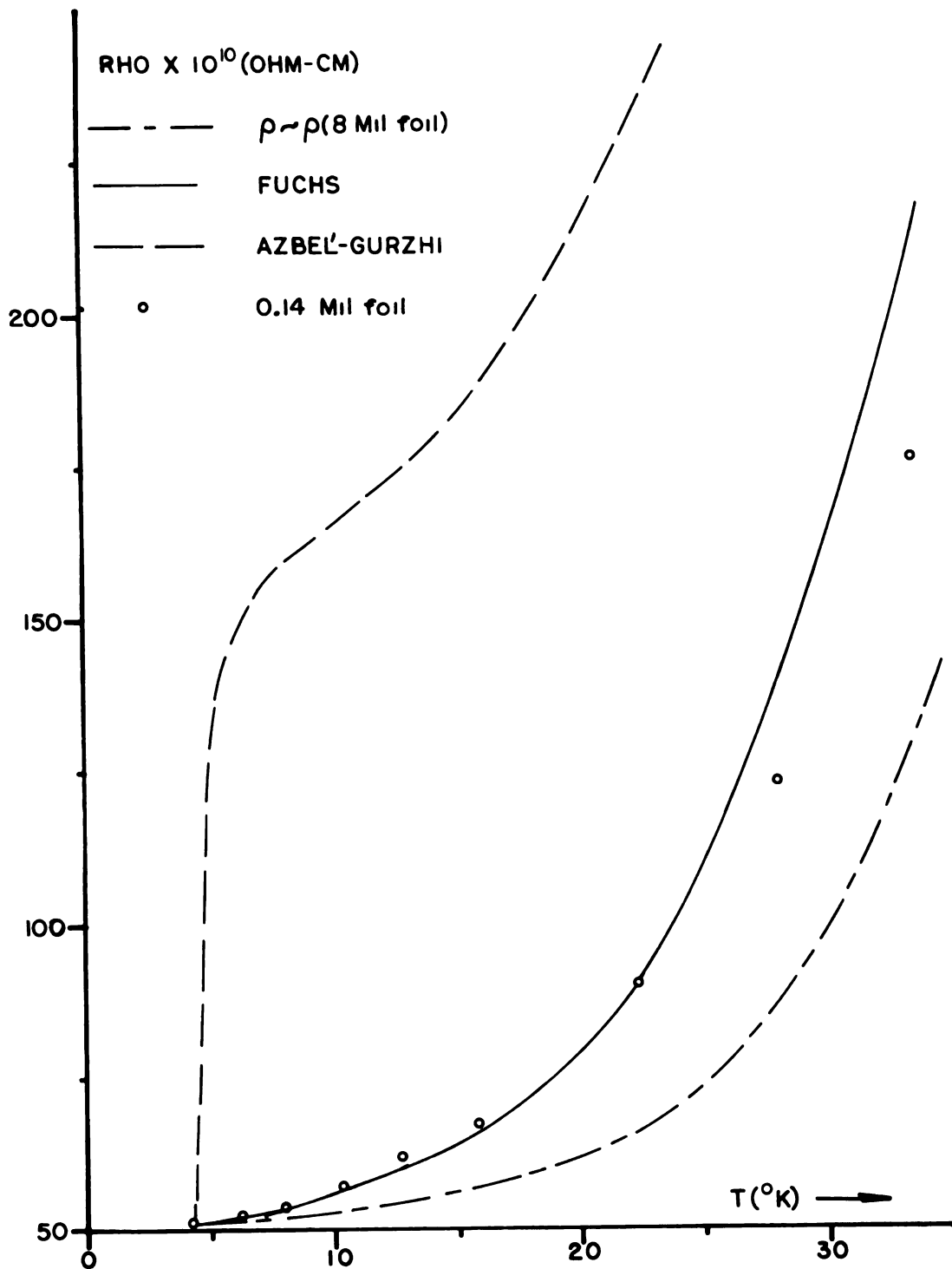
Figure 23. The temperature dependence of the electrical resistivity of an 0.14 mil thick foil compared to Fuch's prediction, to Azbel' and Gurzhi's prediction, and to the temperature dependence of the electrical resistivity of an 8 mil foil
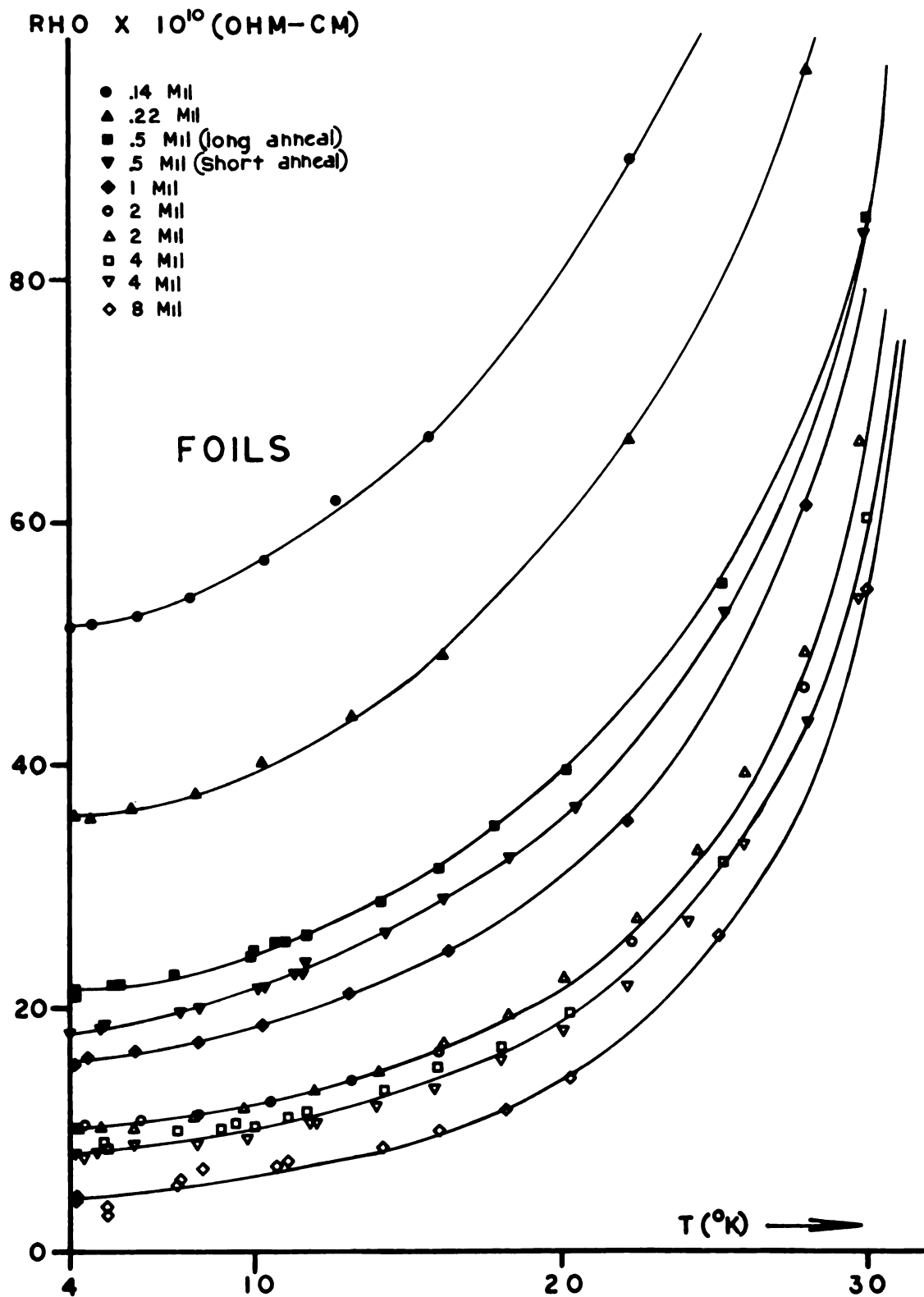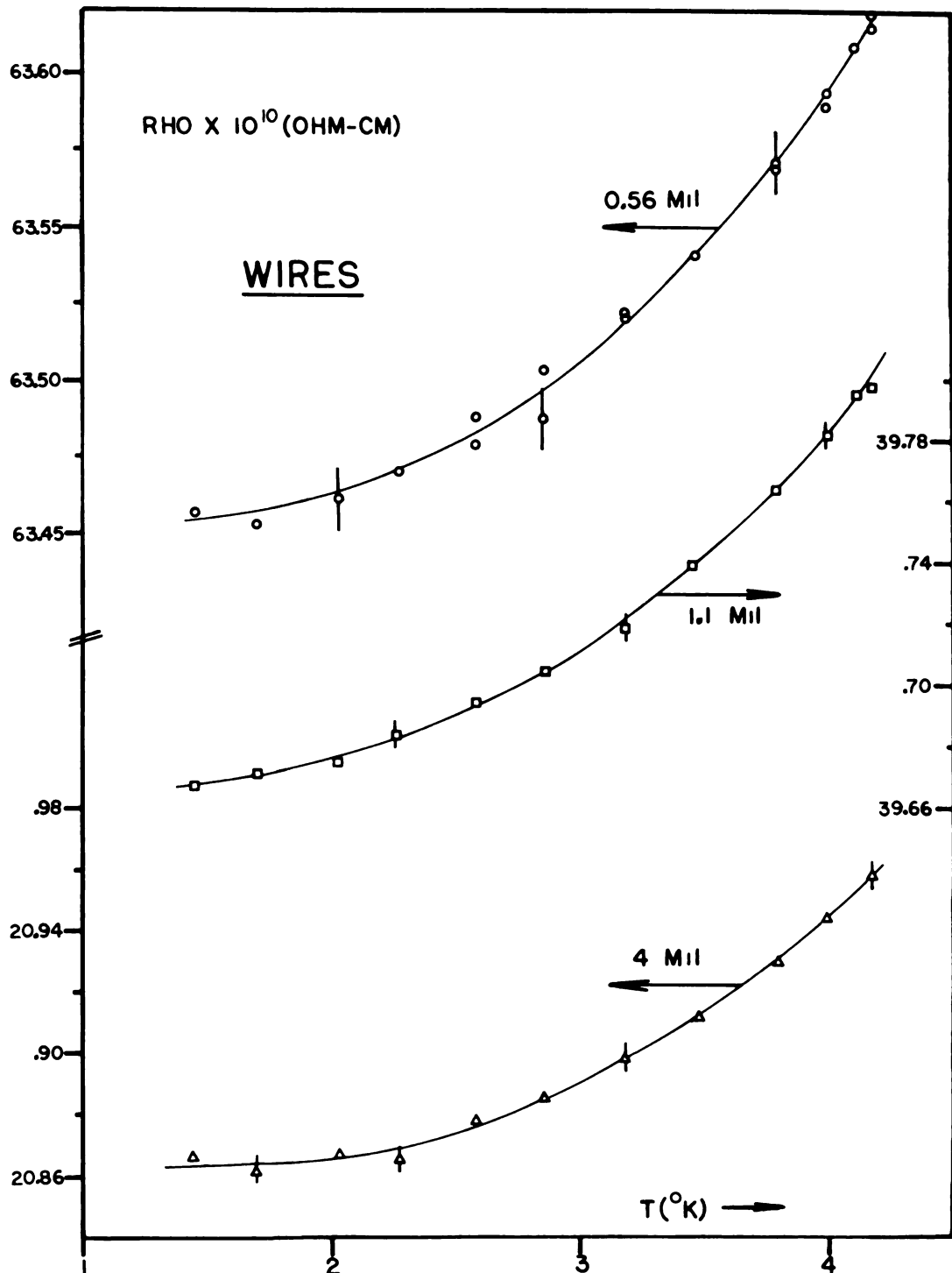
Figure 24. The electrical resistivity of aluminum wires at temperatures below 4.2°K
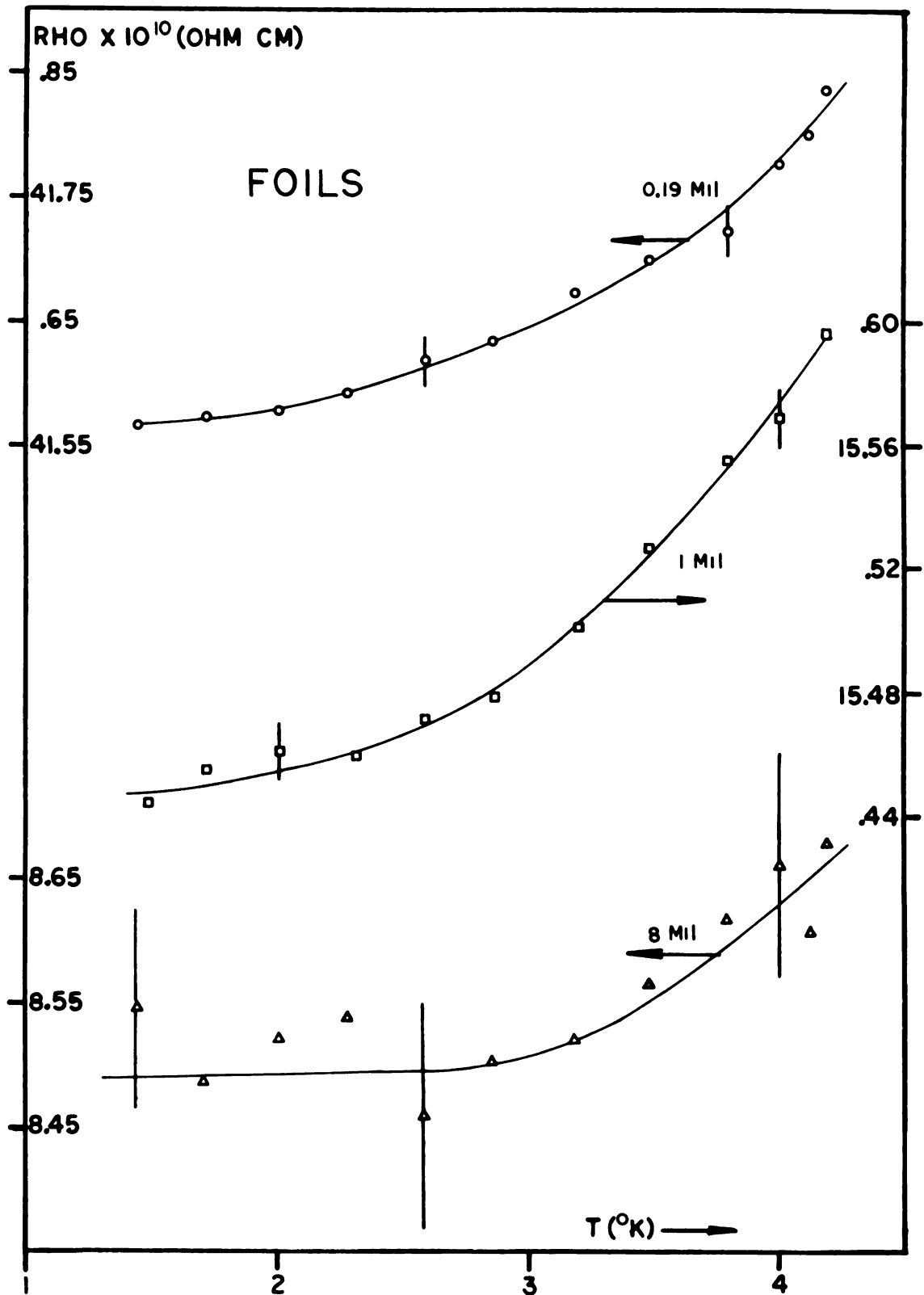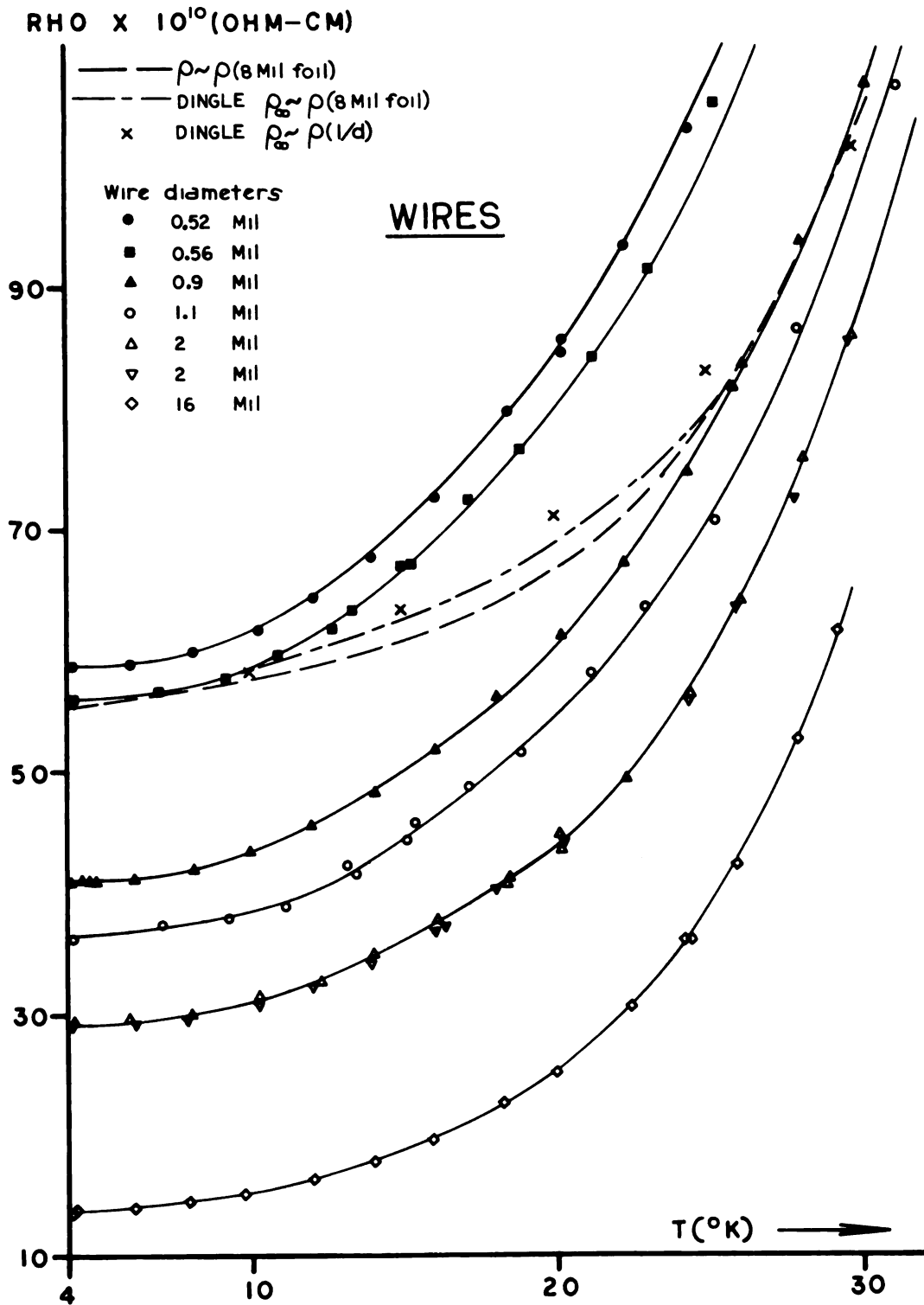
Figure 25. The electrical resistivity of aluminum wires at temperatures above 4.2°K
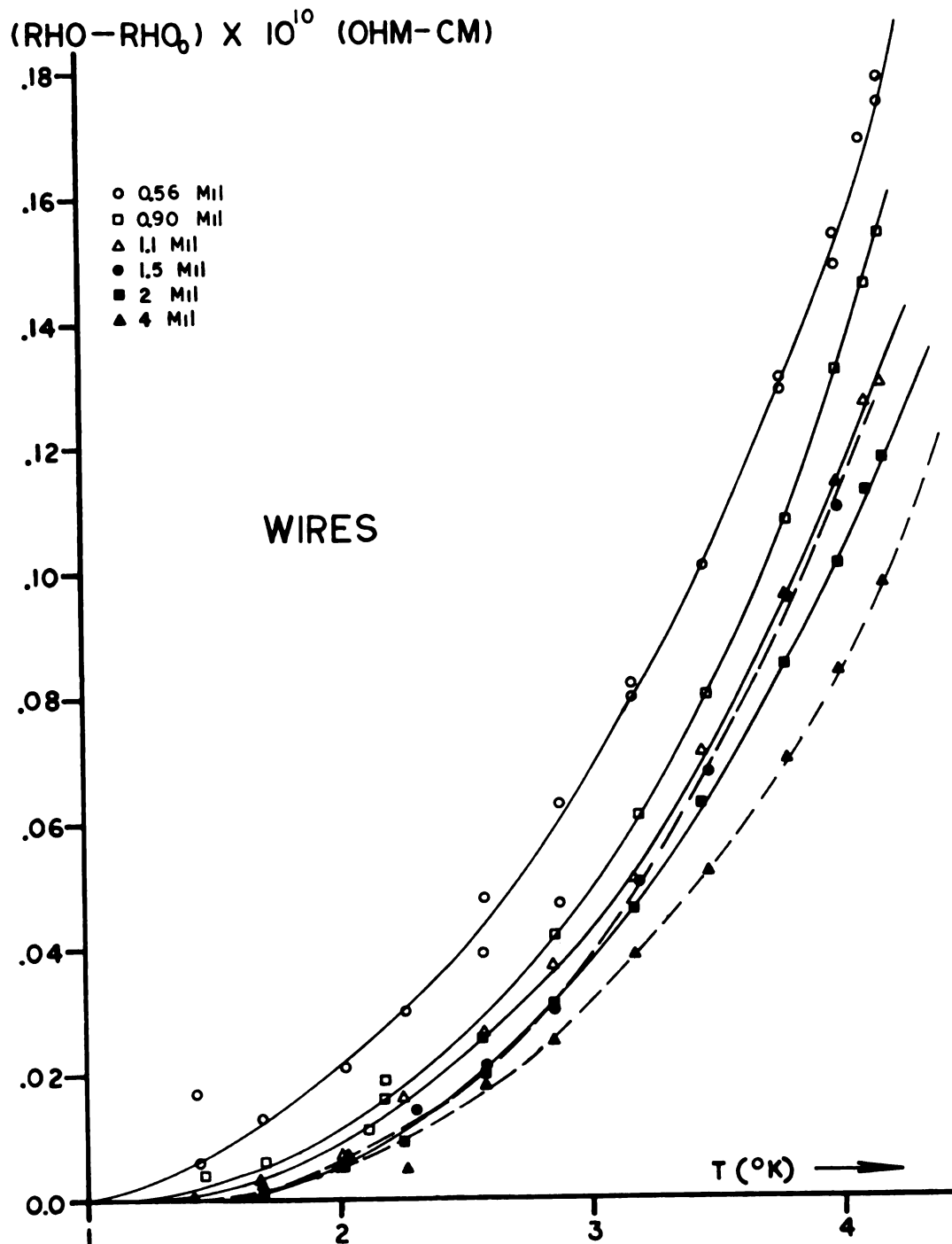
Figure 2b. The data of Figure 24 plotted as RHO(T)-RHO(1.4°K)
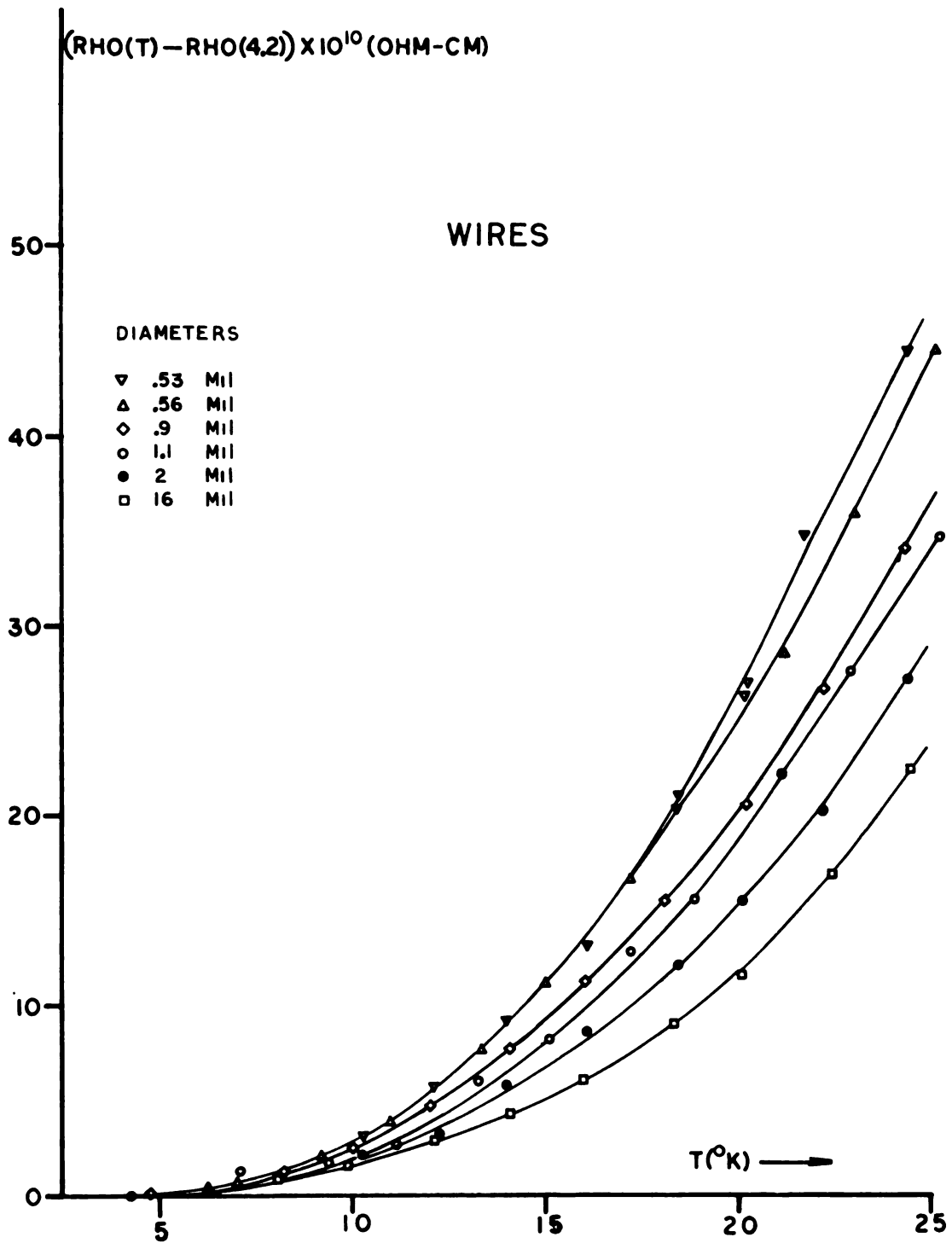
Figure 27. The data of Figure 25 plotted as RHO(T)-RHO(4.2°K)
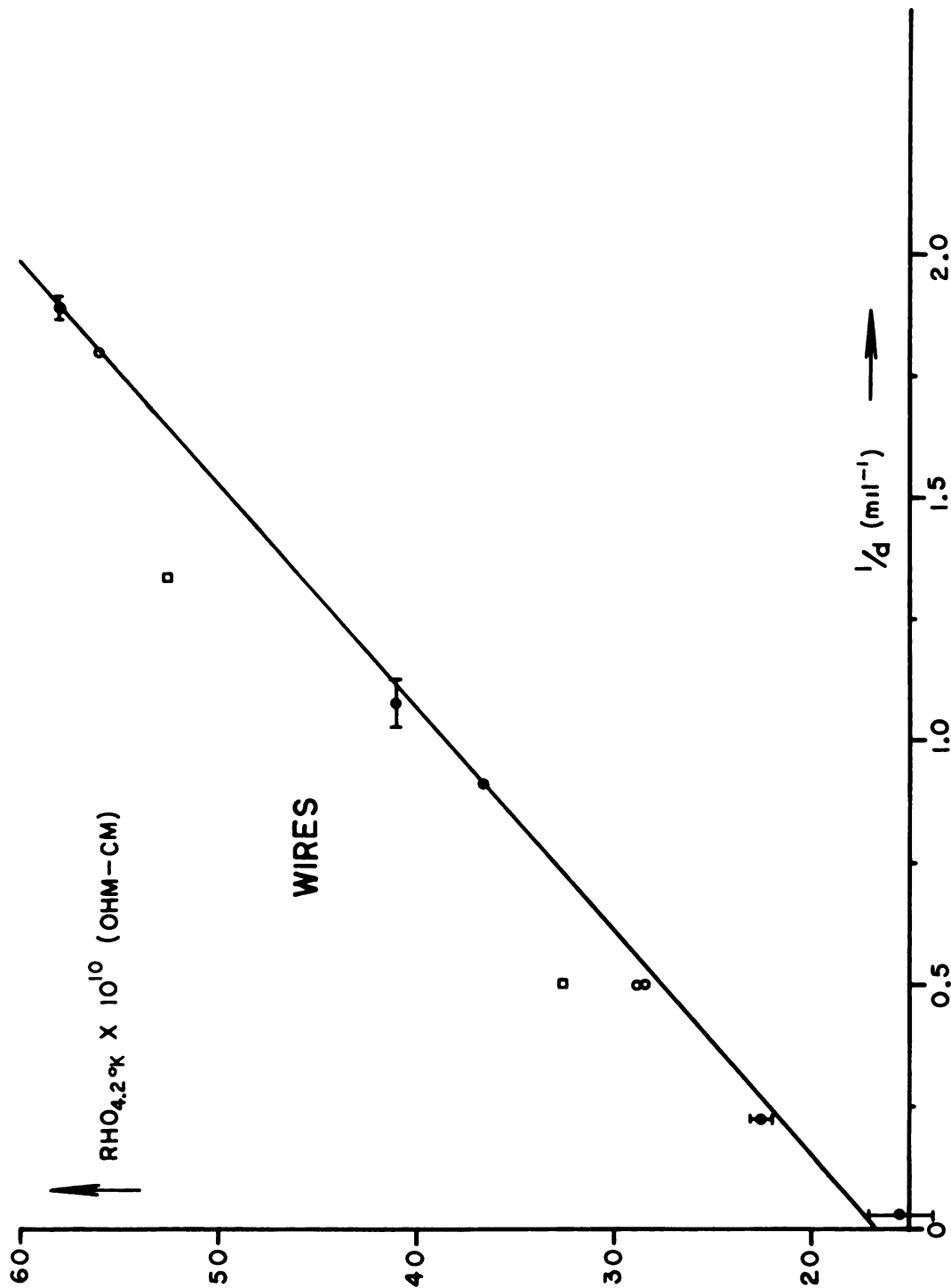
Figure 28. Comparison of the resistivity of aluminum wires
at 4.2°K with the Nordheim relation
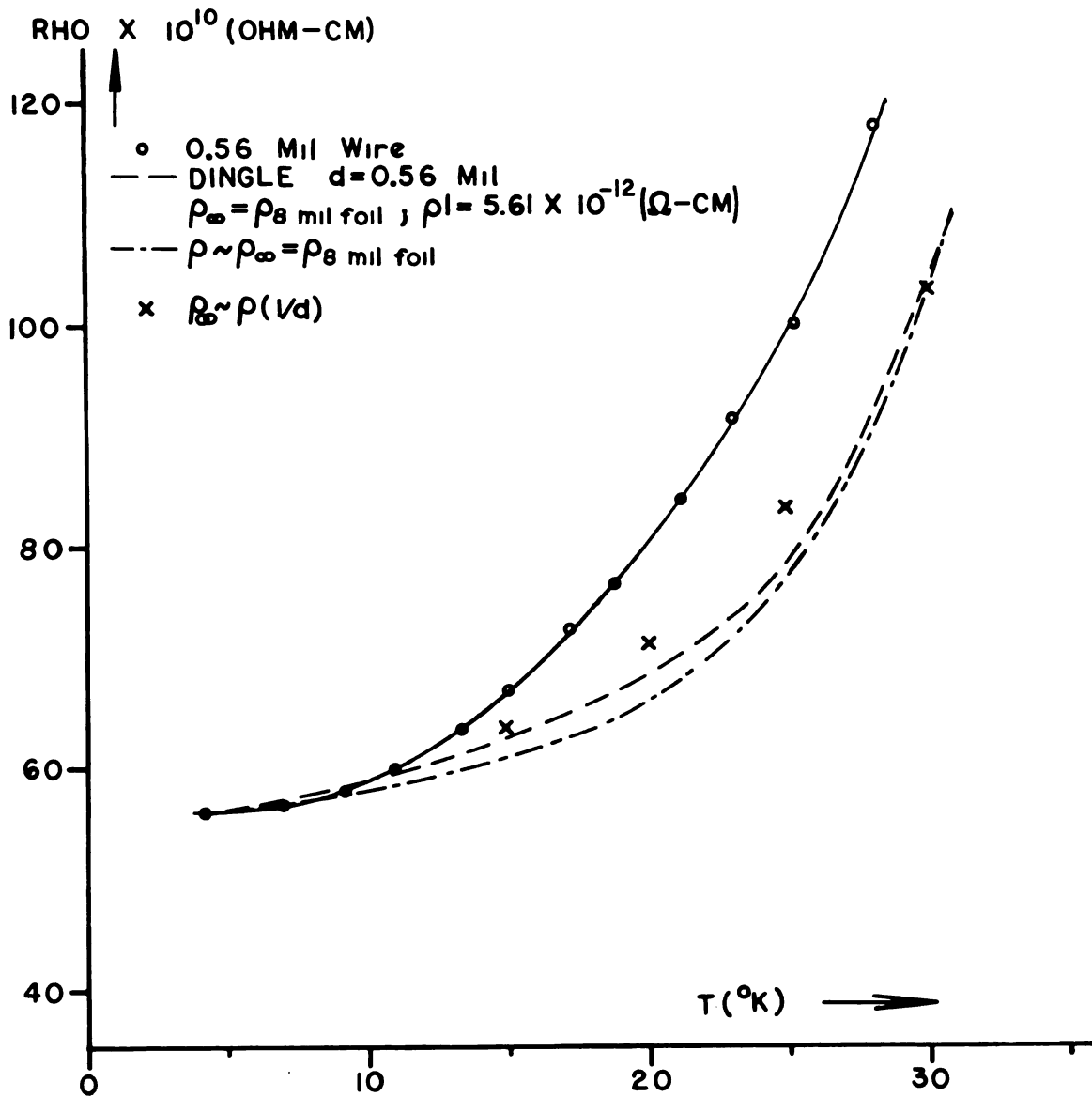
Figure 29. Comparison of the electrical resistivity of the 0.56 mil wire with the predicted resistivity of Dingle for two values of ρ_φ^∞ , and with the electrical resistivity of the 8 mil foil
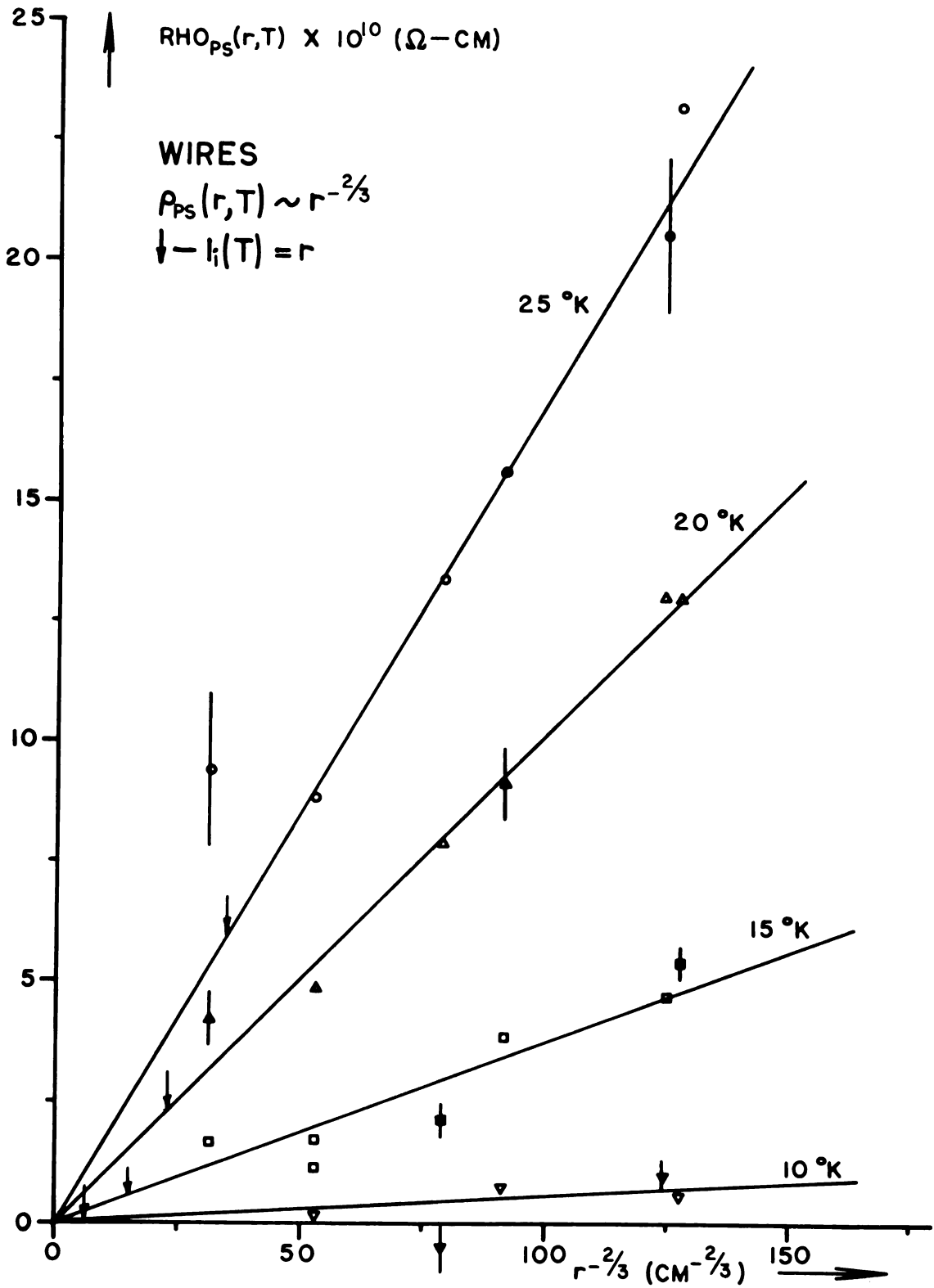
Figure 30. Comparison of the size dependence of the excess
resistivity in aluminum wires above 4.2°K with the predictions
of Blatt and Satz. An arrow indicates the point on each line
at which $I_i(T) = r$
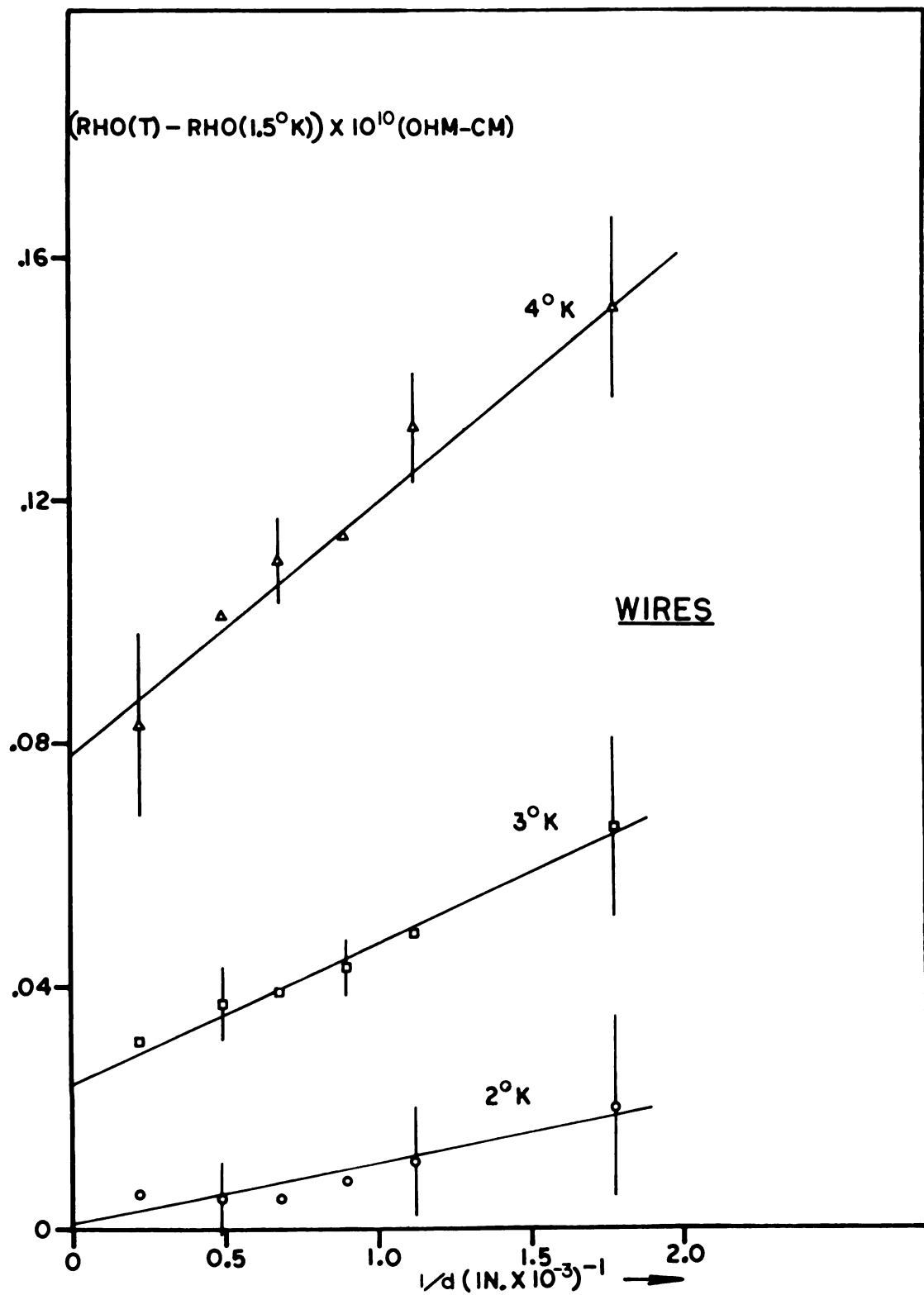
Figure 31. Determination of the bulk resistivity of aluminum
wires below 4.2°K using the Nordheim relation
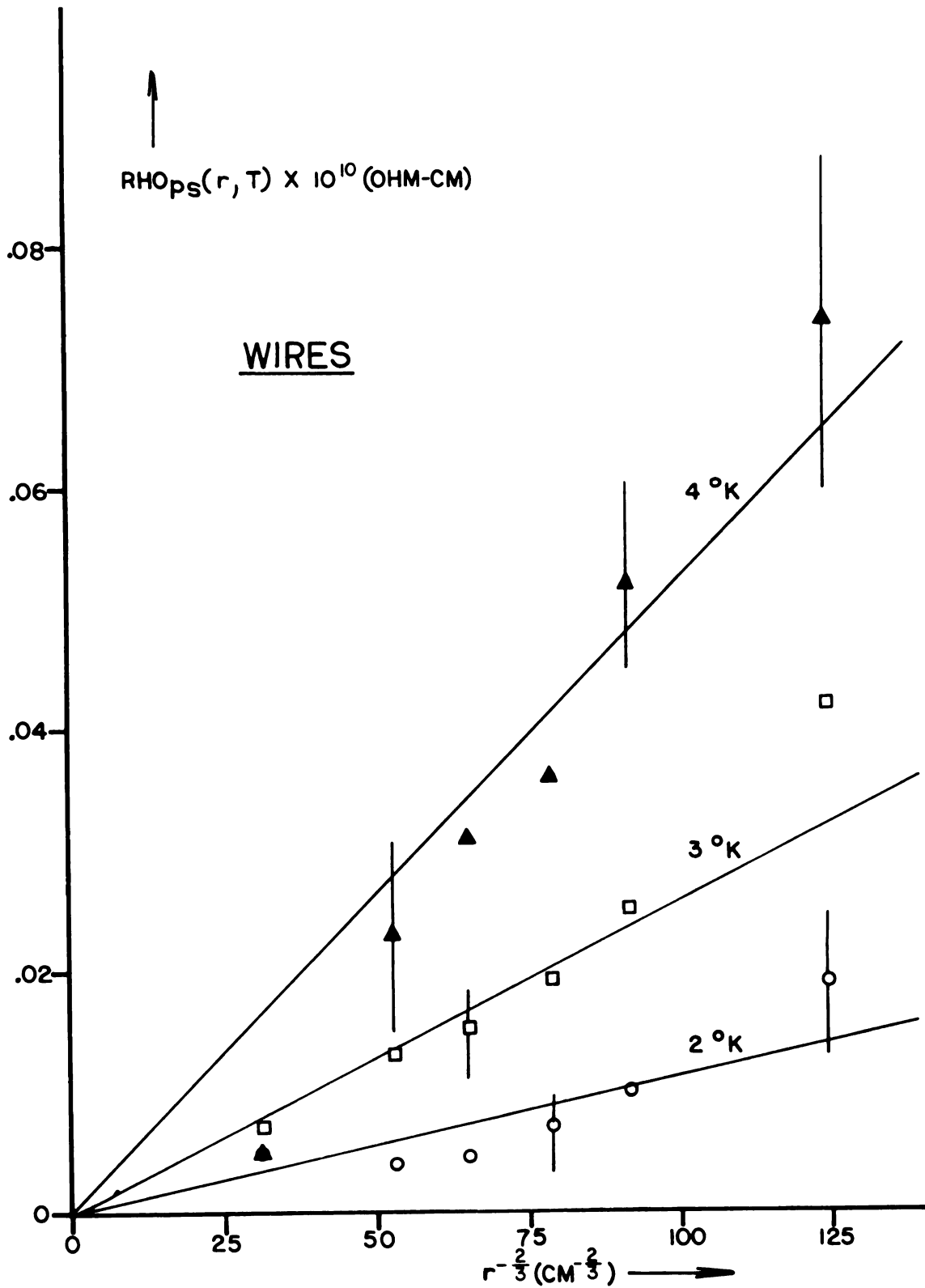
Figure 32. Comparison of the size dependence of the electrical resistivity in aluminum wires below 4.2°K with the predictions of Blatt and Satz
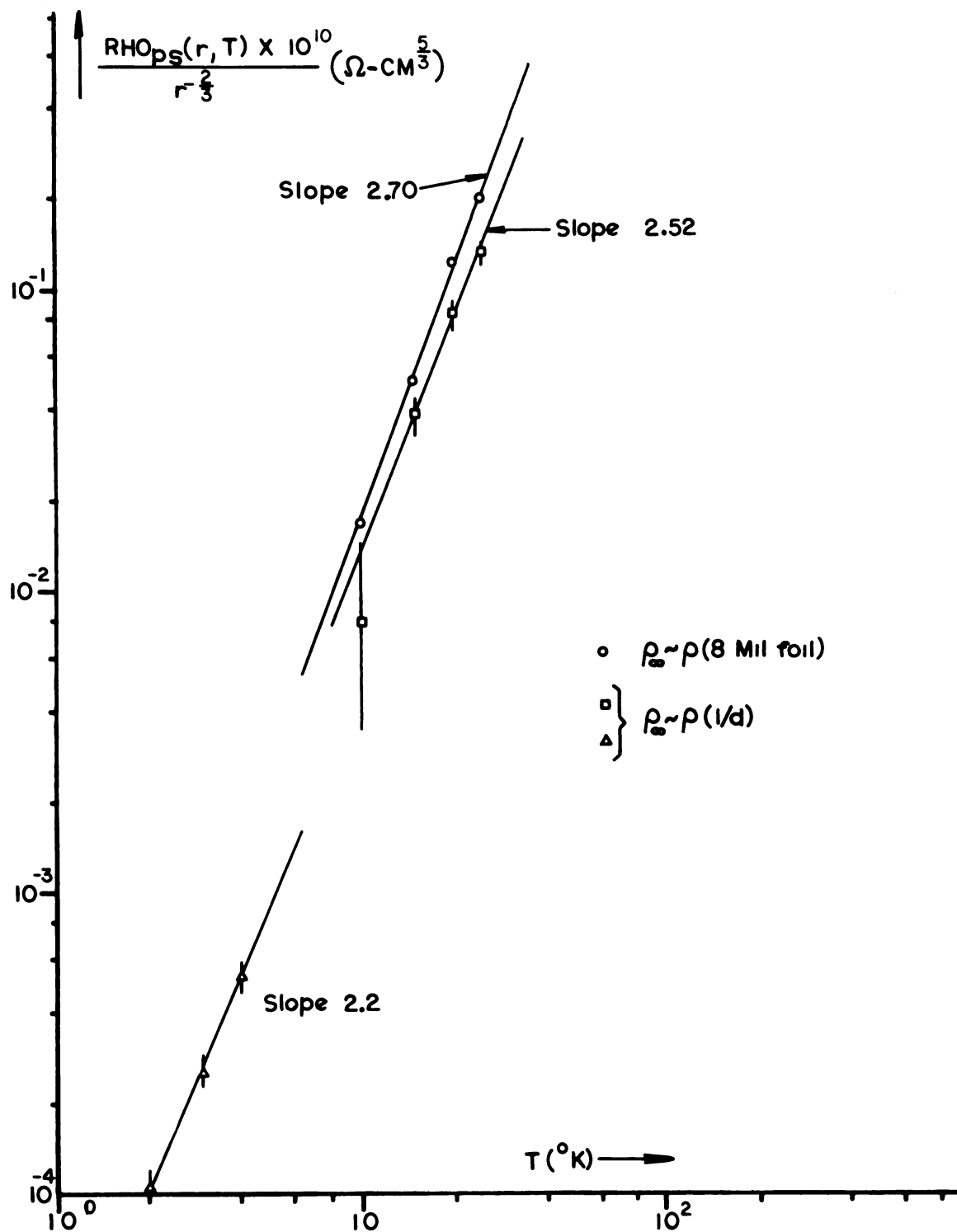
Figure 33. The slopes of the lines on Figures 30 and 32 shown as a function of temperature

V. THERMOPOWER OF ALUMINUM

Theory

General

The absolute thermopower of a nonmagnetic material can be described (to a first approximation) as the sum of two independent contributions: a diffusion thermopower, S_e, and a phonon-drag thermopower, S_{ph}. The diffusion thermopower results from the redistribution of the conduction electrons in the necessary temperature gradient; the phonon-drag thermopower results from electrons which are "swept along" by the phonon current induced by the temperature gradient. In the free electron approximation the diffusion thermopower can be expressed[51] in terms of the electronic specific heat per unit volume C_e

$$S_e \simeq \frac{C_e}{ne} \tag{39}$$

where n is the electronic density and e is the electronic charge. Since $C_e \sim T$, S_e should vary linearly with temperature. A more general form for S_e[52] based on the Boltzmann Equation is

$$S_e = -\frac{\pi^2 k^2 T}{3|e|} \left[\frac{\partial \ln \sigma}{\partial \varepsilon} \right]_{\varepsilon_f} \tag{40}$$

94

where σ = the electrical conductivity, k = Boltzmann's constant, T = absolute temperature, e = electronic charge, and ε and ε_f are the electron energy and Fermi energy respectively.

The diffusion thermopower S_{ph} has drawn considerable theoretical and experimental interest in recent years. Mac Donald[53] used a simple model to obtain a theoretical prediction of the temperature dependence of S_{ph}. Assuming that the effect of the phonon current on the electron distribution can be approximated by an effective radiation pressure on the electrons, he found that

$$S_{ph} \simeq \frac{C_p}{ne}\left(\frac{\tau_2}{\tau_1 + \tau_2}\right) \tag{41}$$

where C_p is the lattice specific heat per unit volume, n and e are the electronic density and charge respectively. τ_1 is the time constant characteristic of the electron-phonon interaction and τ_2 is the time constant for all other phonon interactions. At high temperatures $\tau_1 >> \tau_2$, $\tau_2 = \frac{1}{AT}\,\alpha\frac{1}{T}$ and $C_p \simeq 3n_o k$ = a constant (where n_o = atomic density), and we have

$$S_{ph} \simeq \frac{k}{ne\tau_1}\left(\frac{1}{AT}\right) \sim \frac{1}{T} \qquad (T \gtrsim \Theta_D) \tag{42}$$

where n = the number of free electrons per atom. At low temperatures

$$C_p \simeq 200 n_o k (T/\Theta_D)^3, \quad \tau_1 << \tau_2$$

and we find

$$S_{ph} \simeq \frac{200k}{ne}(T/\Theta_D)^3 \qquad (T/\Theta_D << 1) \tag{43}$$

Recently S_{ph} has been examined more rigorously by other workers (eg. Bailyn,[54] Blatt,[55] and McDonald and Pearson[56]),

but Equations (42) and (43) remain the only descriptions of the temperature dependence of S_{ph} which can easily be compared with experiment.

If we now write the total thermopower of a metal as the sum of the diffusion and phonon-drag contributions

$$S = S_e + S_{ph}, \tag{44}$$

we obtain in the two limiting cases of high and low temperature,

$$S \sim AT + B/T \qquad (T \gtrsim \Theta_D) \tag{45}$$

$$S \sim AT + CT^3 \qquad (T/\Theta_D \ll 1). \tag{46}$$

The absolute thermopower S_1 of a metal 1 cannot in general be measured directly. S_1 is however related to the Thomson coefficient σ_1 of the metal by the relation

$$S_1 = \int_0^T \frac{\sigma_1}{T} \, dT, \tag{47}$$

where $\sigma_1(T)$ can be determined experimentally. Alternatively, S_1 can be obtained from measurements of the relative thermopower S_{12} of a thermocouple composed of metals 1 and 2:

$$S_1 - S_2 \equiv S_{12} \tag{48}$$

where $S_{12} = \frac{dV_{12}}{dT}$ is the temperature derivative of the thermoelectric voltage V_{12} of the couple. To obtain S_1 from equation (48), metal 2 must be a standard reference material for which S_2 is known either from measurements of its Thomson coefficient, or because $S_2 = 0$ (as for a superconductor). We shall use this second method to measure the thermopower of aluminum.

Effects of Sample Size

Justi, Kohler, and Lautz[57] have developed a theory, based on the Boltzmann equation, of the effects of sample size on the <u>diffusion</u> thermopower. Their results can be summarized as follows. They define t = foil thickness, ℓ_∞ = bulk electronic mean free path, E_f = Fermi energy, k = Boltzmann's constant, and ΔS_e = absolute diffusion size effect thermopower ($\Delta S_e \equiv S(foil) - S(bulk)$).

For thick foils they find

$$\Delta S_e^{\substack{\text{thick} \\ \text{foils}}} = \frac{\pi^2}{3e} \frac{k^2 T}{E_f} \frac{3}{8x} \left(\frac{d \ln \ell_\infty}{d \ln E} \right)_{E_f} \qquad (x \gg 1) \qquad (49)$$

where $x \equiv \frac{t}{\ell_\infty}$. For the limiting case of thin foils ($x \ll 1$) they find that ΔS_e becomes independent of the thickness of the foil and equal to:

$$\Delta S_e^{\substack{\text{thin} \\ \text{foils}}} = \frac{\pi^2}{3e} \frac{k^2 T}{E_f} \left. \left(\frac{d \ln \ell_\infty}{d \ln E} \right) \right|_{E=E_f} \qquad (x \ll 1) \qquad (50)$$

For thick wires they find, for $y \equiv d/\ell_\infty$ where d = the wire diameter,

$$\Delta S_e^{\substack{\text{thick} \\ \text{wires}}} = \frac{\pi^2}{3e} \frac{k^2 T}{E_f} \frac{3}{4y} \left. \left(\frac{d \ln \ell_\infty}{d \ln E} \right) \right|_{E=E_f} \qquad (y \gg 1) \qquad (51)$$

and

$$\Delta S_e^{\substack{\text{thin} \\ \text{wires}}} \rightarrow \Delta S_e^{\substack{\text{thin} \\ \text{foils}}}$$

in the limit $d \rightarrow 0$. These results imply that the diffusion

thermopower measured for a thermo-couple composed of a bulk sample and a small sample of the same material should be linear with temperature, and in the limit of small samples, should become independent of sample size. The slopes of the curves $\Delta S_e \sim \frac{1}{x}, \frac{1}{y}$ at constant T should then be a measure of the quantity

$$\left. \frac{d \ln \ell_\infty}{d \ln E} \right|_{E=E_f}.$$

Huebner,[58] assuming that the surface scattering of phonons is analogous to the surface scattering of electrons, and also assuming that the phonon frequency spectrum can be replaced by an average frequency, has shown that the change ΔS_{ph} in the phonon-drag thermopower due to reduction of sample size can be described by

$$\Delta S_{ph} = - \frac{S_{ph}^o}{(\lambda_s / \lambda_o) + 1}, \tag{52}$$

where S_{ph}^o is the bulk phonon-drag thermopower and λ_s and λ_o are the phonon mean free path due to boundary scattering alone and the phonon mean free path in the bulk material respectively. In the limit of large samples or high temperatures $(\lambda_s >> \lambda_o)$, λ_s can be written

$$\lambda_s \simeq \begin{cases} 8t/3 \text{ (foils)} \\ 4d/3 \text{ (wires)} \end{cases} \tag{53}$$

In addition, if phonon-phonon Umklapp scattering dominates the lattice thermal resistivity, λ_o can be written[58]

$$\lambda_o = A \, e^{T^*/T} \tag{54}$$

where T* is estimated to be about one-half the Debye temperature. This yields:

$$- \frac{\Delta S_{ph}}{S_{ph}^o} = \begin{cases} \frac{3A}{4d} e^{T*/T} & \text{(wires)} \\ \\ \frac{3A}{8t} e^{T*/T} & \text{(foils)} \end{cases} \tag{55}$$

Thus, subject to the simplifying assumptions, and in the limiting case of $\lambda_s >> \lambda_o$, $- \frac{\Delta S_{ph}}{S_{ph}^o}$ should vary linearly as $1/d$ (for wires) and linearly as $1/t$ (for foils) and have the temperature dependence $e^{1/T}$ in both cases. We see that the slope of

$$- \frac{\Delta S_{ph}}{S_{ph}^o} \sim \frac{3}{4d} \text{ (for wires) and } \quad - \frac{\Delta S_{ph}}{S_{ph}^o} \sim \frac{3}{8t} \text{ (for foils)}$$

gives a measure of the phonon mean free path in the bulk material.

Effects of Magnetic Field

MacDonald and Pearson[59] simplify an expression due to Sondheimer[60] to obtain an estimate of the change in __diffusion__ thermopower expected in the limit of infinite magnetic field for quasi-free electrons. They find, for $\frac{\ell_\infty}{r_c} >> 1$ where ℓ_∞ is the bulk electronic mean free path and r_c is the cyclotron radius, that

$$S_\infty - S_o \simeq - \frac{2\pi^2 k^2 T}{3e \ E_f} \left(\frac{\rho_{iT}}{\rho_{iT} + \rho_r} \right) \tag{56}$$

where S_∞ and S_o are the diffusion thermopower in magnetic field $H = \infty$ and zero, respectively. Here $\rho_i(T)$ is the phonon

contribution to the resistivity at temperature T and ρ_r is the residual resistivity. For our sample, $\rho_{iT}(T \simeq 10°K) \simeq 2.5 \times 10^{-10}$ Ω - cm, $\rho_r \equiv 10 \times 10^{-10}$ Ω - cm, and $E_f \simeq 15_{ev}$, implying that

$$S_\infty - S_o \simeq +0.007 \text{ μv/°K.} \tag{57}$$

We now consider a second means for obtaining a dependence of the diffusion thermopower of aluminum upon magnetic field, suggested by F. J. Blatt.[61]

Feder and Lothe[62] have recently published a solution of the Boltzmann equation for aluminum which takes into account Bragg reflections at the Brillouin Zone surfaces of otherwise free electrons. They argue that a bodily translation of the Fermi surface, commonly assumed to be the result of the application of spatially constant electric and magnetic fields, violates the boundary condition that the solution of the Boltzmann equation must be continuous in a reduced zone scheme. Using their solution, which satisfies this boundary condition, they find that the Hall coefficient A_H changes sign with increasing magnetic field H:

$$\frac{A_H}{|A_{H,o}|} \simeq \begin{cases} -1 & \omega_c \tau \ll 1 \\ +3 & \omega_c \tau \gg 1 \end{cases} \tag{58}$$

where $A_{H,o} = \frac{1}{nec}$ is the Hall coefficient from free-electron theory, ω_c is the cyclotron frequency $\left(\omega_c = \frac{eH}{m*c}\right)$, τ is the effective relaxation time of the charge carriers. This change of sign can be explained qualitatively on the basis of the shape of the Fermi surface of aluminum in the reduced zone scheme.

Such a change in sign of the Hall coefficient has been observed experimentally by several workers (cf.[63,64]). They find that the charge carriers in aluminum change from effectively three electrons per atom for H = 0 to one "hole" per atom at H = ∞, just as predicted by Feder and Lothe.[62] Blatt[61] suggested that since the diffusion thermopower depends directly upon the sign of the charge carriers, measurements of the magnetic field dependence of the bulk thermopower of aluminum might show a change of sign in the diffusion component. This can be seen mathematically (in the free electron approximation) if we express S_e in terms of Equation (39):

$$S_e = \frac{C_e}{ne} \tag{39}$$

Since $A_H = \frac{1}{nec}$, we have

$$S_e = cC_eA_H. \tag{59}$$

Review of Previous Experiments and Purpose of the Present Study

Previous measurements of the thermopower of aluminum have been made below 10°K and above 78°K. DeVroomen et al.[65] have been able to fit the thermopower below 10°K, measured relative to superconducting niobium, to the form

$$S = AT + CT^3 \tag{46}$$

but find that whereas the constant C appears to be well specified by their data, the constant A varies greatly from one sample to another. Dewar and Fleming[66] have measured the thermopower of aluminum relative to Pb in the temperature

range 78°K to 373°K. No previous measurements had been made of the thermopower of aluminum in the range from 10°K to 78°K. Also, above 10°K no satisfactory separation of the thermopower into its diffusion and phonon-drag components had been demonstrated.

There have been few attempts to study the effect of magnetic field on the thermopower of pure metals. MacDonald and Pearson[59] measured the effect of magnetic field on the thermopower of pure copper and pure sodium, finding qualitative disagreement between their experimental results and Equation (56). They find, in both cases, that the change in thermopower predicted by Equation (56) is larger and of the opposite sign to that observed experimentally. Grüneisen and Erfling[67] and Steel and Babiskin[68] have measured the effects of magnetic field on the thermopower of single crystals of beryllium and bismuth respectively.

Huebner[58,69] investigated the effect of sample size on the thermopower of thin _foils_ of Au and Pt for temperatures below 300°K. He found that the size effect on the electronic component of the thermopower can be explained theoretically, yielding the energy dependence of the electronic mean free path and the energy dependence of the total area of the Fermi surface, evaluated at the Fermi energy. Huebner also found a size effect on the high temperature phonon-drag thermopower in Pt which, when compared with theory, yielded an estimate of the phonon mean free path in the bulk material. The effect of sample size on the diffusion

thermopower in Pt again provided estimates of

$$\left.\frac{d\ell_\infty}{dE}\right|_{E_f} \quad \text{and} \quad \left.\frac{dA_s}{dE}\right|_{E_f},$$

where A_s is the area of the Fermi surface.

Measurements of the effect of sample size on the thermopower of thin evaporated metal _films_ have been published by several authors.[70-74] Most of these results, obtained at and above room temperature, have largely only qualitative value, since in thin films the nature of the film and the substrate upon which it is deposited can greatly affect the electronic properties of the film (cf. Reimer[70]).

However, Worobey _et al._[74] made some interesting measurements on Au foils at cryogenic temperatures, finding a

$$\left.\frac{d\ell_\infty}{dE}\right|_{E_f}$$

for thin films of Au which differs in sign from the value found by Huebner[69] from high temperature studies of Au foils.

In our present set of experiments on the thermopower of aluminum, the following purposes were projected. We hoped to measure the absolute thermopower of bulk aluminum over the entire temperature range from 4.2°K to 300°K, looking for a phonon-drag peak at about $T = \Theta_D/5$. We would attempt to separate the diffusion and phonon-drag contributions to the thermopower at high and low temperatures by

their respective dependences on temperature. A knowledge

of these quantities for the bulk material is essential to

a study of the effects of sample size on these quantities.

We hoped to be able to determine the effects of

specimen size on the diffusion and phonon-drag components

of the thermopower for both fine wires and thin foils of

aluminum. These would give measures, as shown in the theory

section, of

$$\frac{d\ell_\infty}{dE}\Bigg|_{E_f}$$

and λ_0 for aluminum. We also hoped to be able to compare

the electron-phonon relaxation time τ_1, obtained as a func-

tion of temperature and size from the temperature dependence

of the resistivity of the small samples, to that obtained

from the size dependent phonon-drag thermopower for the

same small samples.

We planned to make a preliminary study of the effect

of a magnetic field on the bulk thermopower of aluminum,

first of all to see if an effect could be found, and

secondly to see whether such an effect, if observed, could

be described either by the theory of MacDonald and Pearson[59]

or by the suggestion of Blatt.[61]

Description of Apparatus

For measuring the bulk thermopower of aluminum from

4.2°K to 300°K, we used the apparatus described previously

by Henry and Schroeder.[75] The thermopower, obtained using a lead (Pb) standard, was measured relative to a helium bath in the range $4.2°K \leq T \leq 90°K$ and relative to a nitrogen bath for $78°K \leq T \leq 300°K$.

Measurements of thermopower relative to superconducting niobium-zirconium (with and without a magnetic field) and measurements of differential thermopower were made using the apparatus described below.

The following description refers to Figures 34 and 35. Samples (E) were mounted in an evacuated chamber (A) immersed in a liquid helium bath. The bath was held at 4.2°K or at 1.5°K. The thermopower was obtained experimentally from the voltage measured in a thermocouple circuit containing the sample and a suitable standard metal. For measurements on bulk aluminum, superconducting niobium-zirconium was used as a standard; measurements of differential thermopower were made relative to "bulk" aluminum (0.016" diameter wire) (D).

One junction of the thermoelectric circuit was held at the temperature of the bath, while the temperature of the other junction was varied by means of an electrical heater (G). The heater, wound non-inductively of manganin wire (L), was supported in the evacuated chamber by a small rod (I) of glass-impregnated plastic. This rod provided electrical and thermal insulation between the heater and the chamber. The temperature of the heater was measured by an

Au + 0.02 at . % Fe--chromel thermocouple (C) relative to the bath temperature.

The reference materials (Au - Fe, chromel, bulk Al) were passed through epoxy plugs (J) directly into the bath to ensure that the proper base temperature was maintained. These plugs were made from Epibond 100-A epoxy as described by Roach et al.[76] We noted no failure of any of these plugs, even though they were often cycled between 1.5°K and 300°K.

The Au + 0.02 at . % Fe--chromel thermocouple was calibrated against a helium bath (1958 Helium Temperature Scale) in the range 1.5°K to 4.2°K, and against a platinum resistance thermometer in the range 4.2°K to 300°K. The calibration is believed accurate to 0.2°K and reproducible to 0.01°K.

Samples were mounted entirely inside the evacuated chamber. This removed the necessity for constantly changing epoxy plugs. One end of the sample material was pressed onto a high purity copper disc (nominally 99.999$^+$% Cu, from the Asarco Co., South Plainfield, N.J.) which was soldered into the top of the vacuum chamber and was in contact with the helium bath. The large size (0.5" diameter) and high thermal conductivity of the copper plug kept estimated thermal gradients across the plug below 0.1°K for a 0.040" thick foil and a total temperature difference of 40°K across the sample. Gradients across the copper were proportionately less for thinner samples. This arrangement, however, required the

the entire vacuum chamber to be in electrical contact with
the sample. The chamber was electrically insulated from
the rest of the apparatus by a copper-to-glass graded seal
(K) in the supporting vacuum line (F). The electrical con-
nection was provided by a copper wire pressed beneath the
head of a high-purity copper screw which was threaded into
the copper plug. A thin styrofoam cylinder (B) was placed
on the inside wall of the vacuum chamber to reduce radiation
loss to the walls from the heater and the sample. This was
designed to reduce thermal gradients across the heater and
to permit formation of a more homogeneous thermal gradient
along the sample.

The thermal voltages in the external system were
measured or zeroed out (depending on the measuring instru-
ment) by means of a pressure activated shorting switch located
below the bath level (for the basic design of the switch see
Haen and Weil[77]). The switch, having platinum and gold
contacts, introduced less than 0.01 microvolts of spurious
voltage into the measurements.

The thermometer thermocouple voltage was measured on
the Minneapolis-Honeywell Rubicon Instruments six-dial poten-
tiometer to an accuracy of 0.1 microvolts (0.01°K). The
sample-reference thermoelectric voltage was read on a Kiethley
Nanovoltmeter to an accuracy of 0.5%. The instrument was
capable of measuring 1×10^{-8} volts full scale (2×10^{-10} volts
per scale division). The Kiethley was equipped with a zero-
suppress which was used with the shorting switch to "buck out"

the thermals in the external circuit, permitting direct measurement of sample voltages free of slowly varying thermal voltages. In this manner, voltages could often be measured reproducibly to an accuracy of $0.001\mu v$. The thermal voltages in the thermometer circuit were measured directly on the six-dial and subtracted later.

The heater (see Figure 35) was designed to place the sample-reference junction and the thermometer thermocouple (X) junction in as close physical and thermal contact as possible, while remaining electrically insulated from each other. The heater (Z), wound about a threaded sleeve, provided a source of heat located symmetrically about the thermometer and samples. Cigarette paper (Y), covered with Apiezon N grease to provide thermal contact, electrically insulated the conductors from the heater. Due to the relatively large thermal current in the samples, the bulk-foil couple was placed in electrical contact with the heater at the point at which the bulk sample (W) and the foil (V) contacted each other. All parts of the heater assembly (including the screws) were made from the same block of aluminum to keep inhomogeneities in the heater to a minimum.
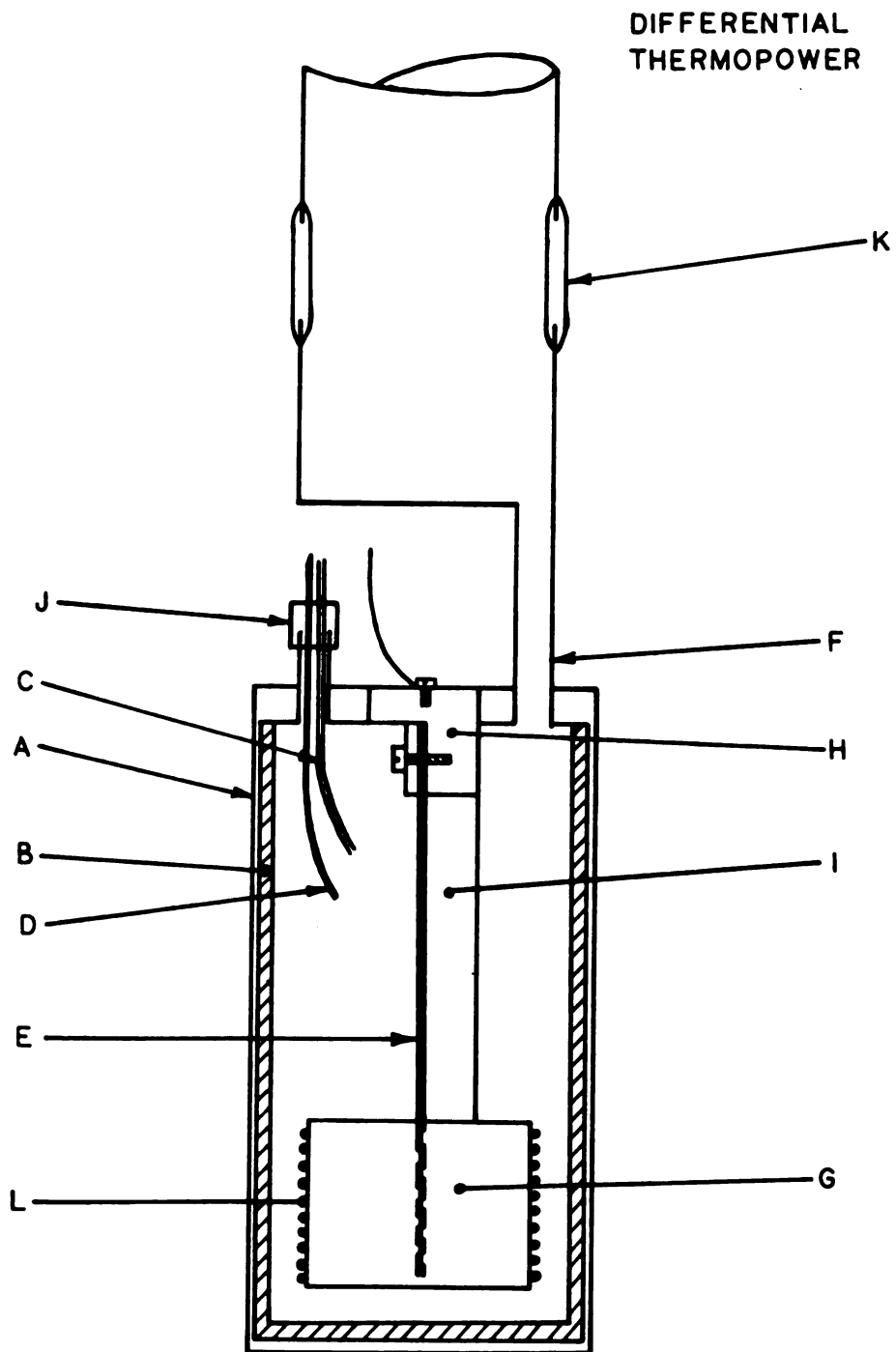
**DIFFERENTIAL
THERMOPOWER**

Figure 34. Apparatus for measuring thermopower at low temperatures
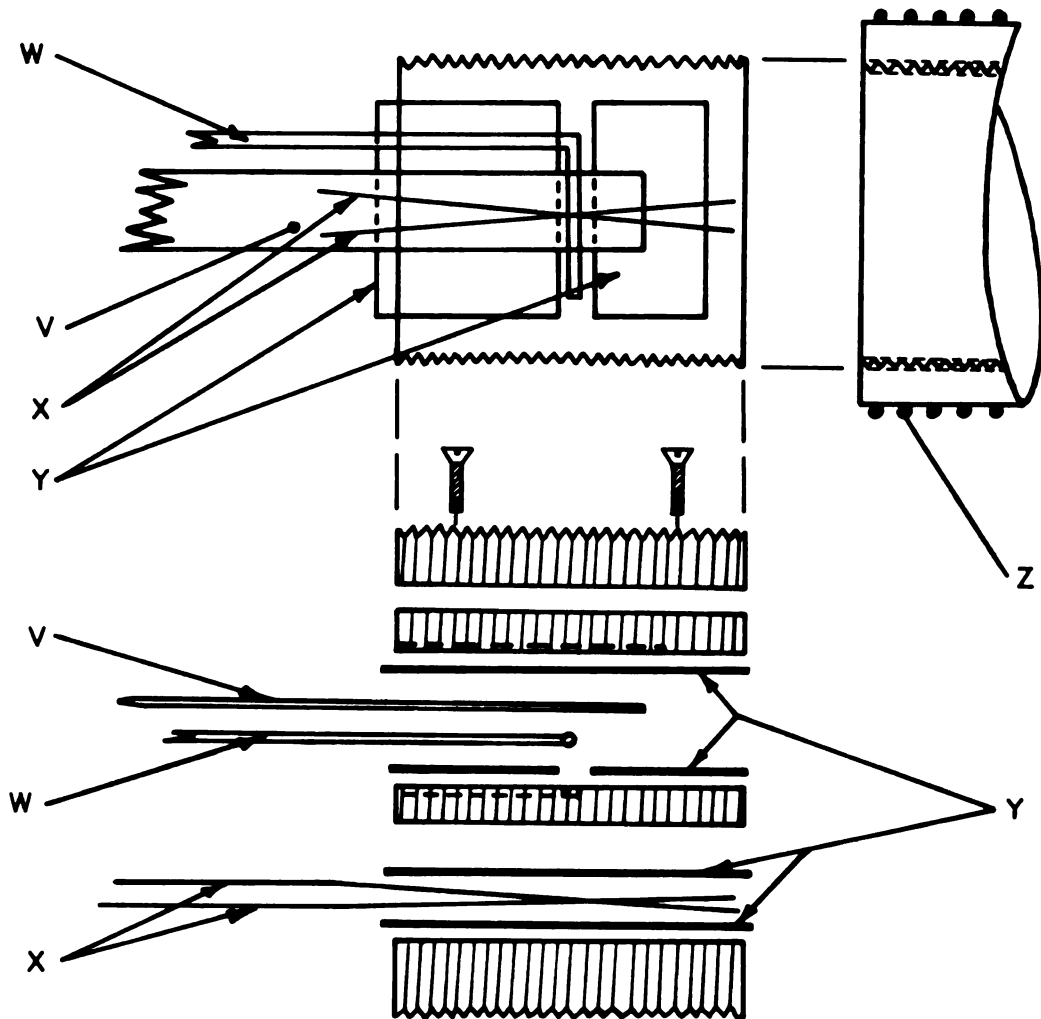
HEATER ASSEMBLY
DIFFERENTIAL THERMOPOWER

Figure 35. Heater assembly for thermopower apparatus

Results and Discussion

Thermopower of Bulk Aluminum

We have measured the thermoelectric voltage of bulk aluminum from 4.2°K to 300°K relative to a lead (Pb) standard. The data of Christian et al.[78] were used for the thermopower of lead.

Our data was computer analyzed in the following way. The raw data consisted of an experimentally determined thermoelectric voltage E_i at a temperature T_i. Linear interpolation of this data provided $E_i(T_i)$ at equally spaced intervals of T. This data was then smoothed by fitting a cubic equation to each set of nine equi-spaced points, the smoothed points being taken from the cubic. The integrated thermopower (thermoelectric voltage) of the lead was then subtracted out and the remaining thermoelectric voltage differentiated numerically to give the absolute thermopower of aluminum.[79]

The absolute thermopower of aluminum obtained in the above way is shown in Figure 36. Nine independent samples were measured, five annealed and four unannealed, from three different manufacturers. These measurements were made relative to two independent lead (Pb) reference samples.

The deviation between samples was largest in the temperature range between 20°K and 50°K, where the thermopower is varying most rapidly with temperature. The thermopower may vary from sample to sample by as much as 0.1μv/°K

in this temperature range. It should be noted that aluminum samples supplied by three different manufacturers also showed their greatest relative differences in this same temperature range. Annealed samples generally yielded thermopowers slightly lower in magnitude than unannealed samples in this region. The accuracy in the thermopower above 150°K is probably limited by knowledge of the thermopower of the reference lead (Pb), since our experimental variations do not exceed ±0.02μv/°K.

We see that we do indeed observe a phonon-drag peak in the thermopower of aluminum at T ≈ $\Theta_D/5$ (see Figure 36). To compare our high temperature thermopower to the relation

$$S = AT + B/T, \tag{45}$$

we plot $\frac{S}{(T/100)}$ vs. $\frac{1}{(T/100)^2}$ (cf. Figure 37). We see that, for high temperatures, such a plot does yield a straight line, with

$$S = \left[-.238 \left(\frac{T}{100} \right) - 2.80 / \left(\frac{T}{100} \right) \right] \mu v/°K.$$

We note two things here: both the diffusion and phonon-drag thermopowers are negative at these temperatures as predicted by simple theory (cf. Equation (45)); and the phonon-drag thermopower is not negligible with respect to diffusion thermopower at 300°K. We see, in fact, that the thermopower of aluminum is negative over its _entire_ range up to 300°K. Thus we may expect on this basis as well, that aluminum approximates a free electron metal. That the phonon-drag thermopower is not negligible with respect to the diffusion
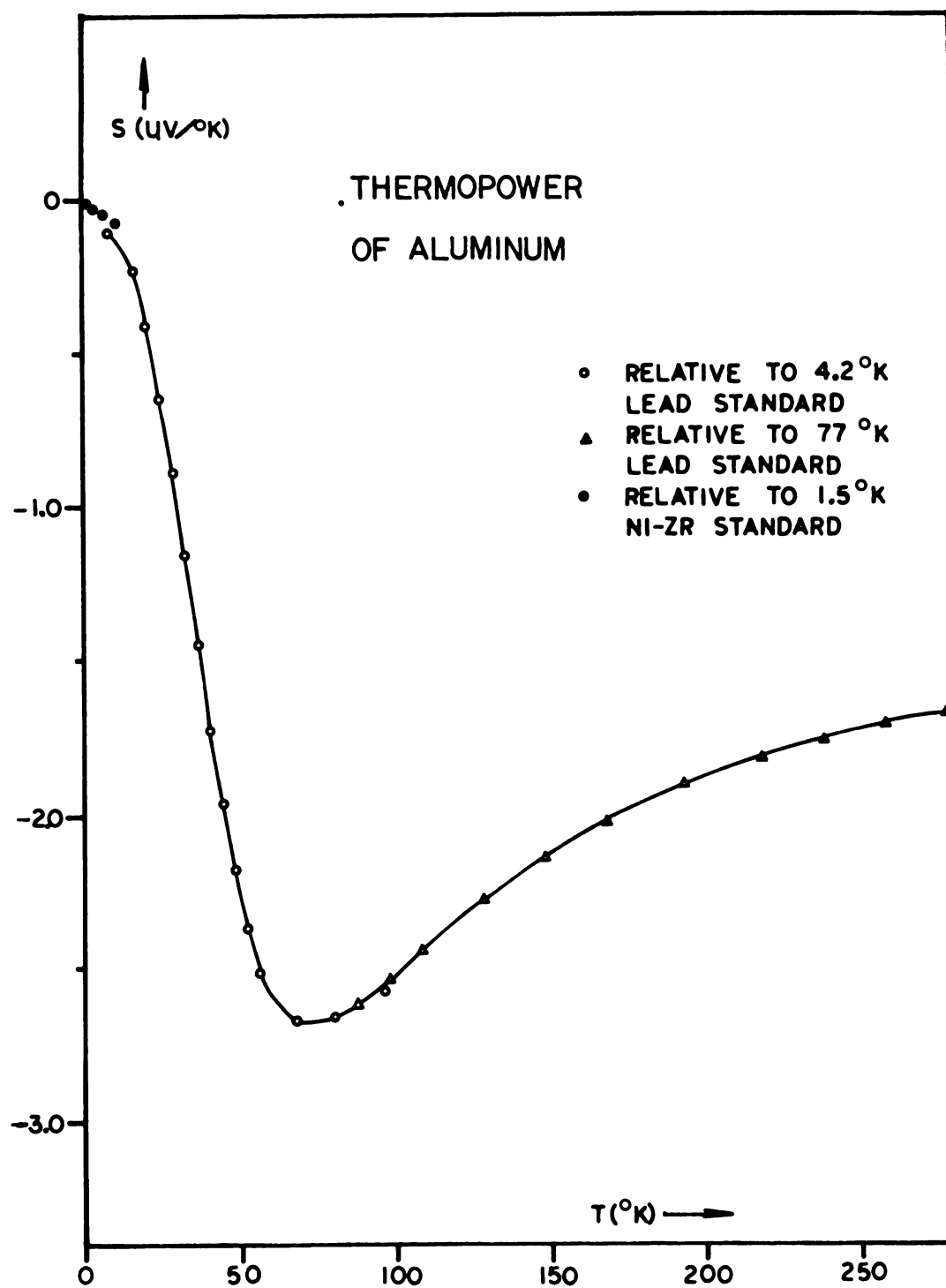
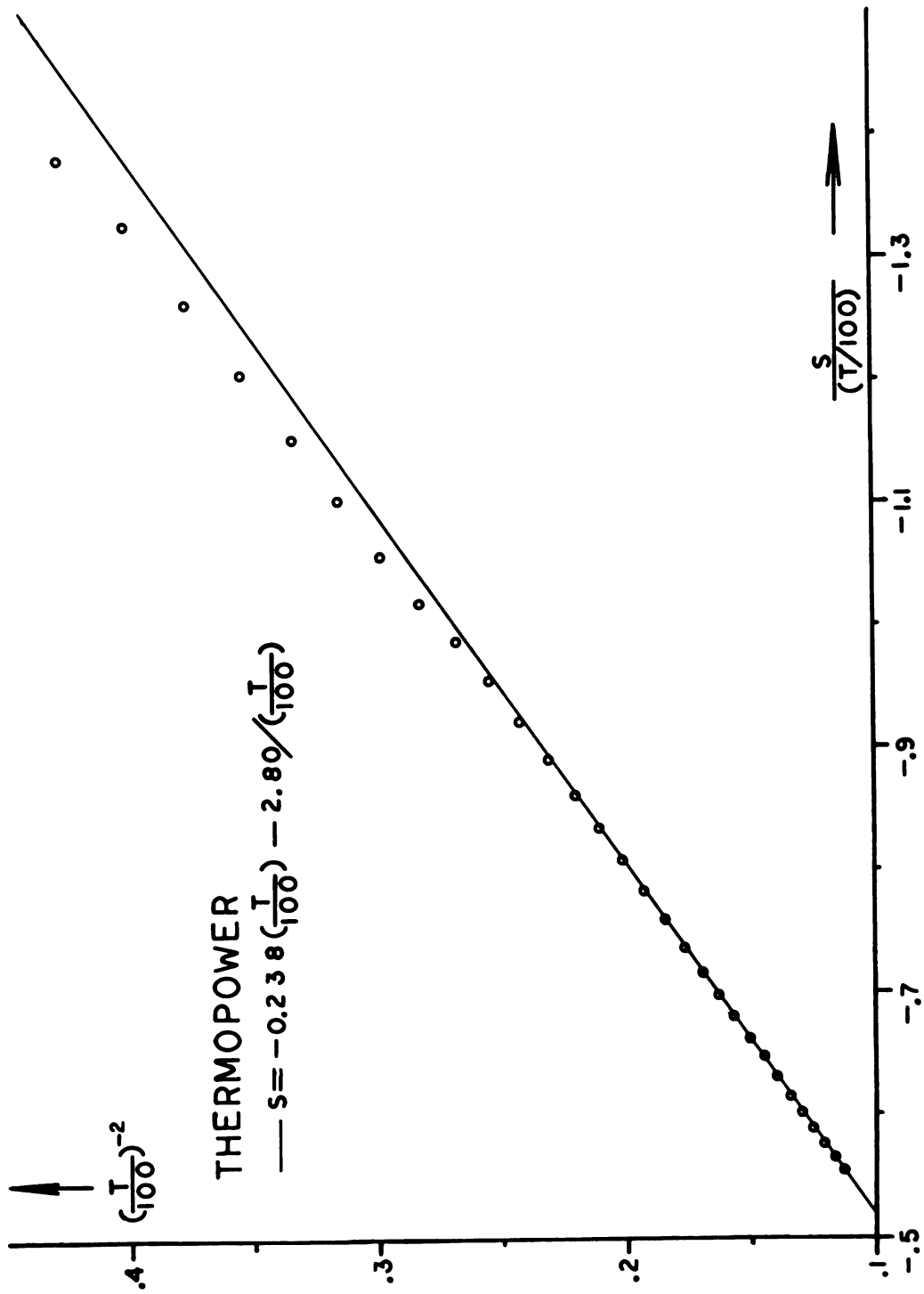Figure 36. The absolute thermopower of 99.999% pure, polycrystalline aluminum

Figure 37. Comparison of the high temperature data of
Figure 36 with the equation $S = AT + B/T$

thermopower at 300°K is somewhat surprising. In nearly all other metals tested to date, S_{ph} has become unimportant by this temperature; S is found experimentally to vary nearly linearly with T. This observation spurred an experiment to measure the thermopower of aluminum above 300°K to see if indeed S_{ph} does persist to higher temperatures.[80]

We have measured the thermopower of bulk aluminum against superconducting niobium-zirconium up to 13°K. Typical points are shown on Figure 36. We attempted to fit the data to an $S = AT + CT^3$ curve, but with ill success. While the low temperature data (T $\leq$ 8°K) plotted as S/T vs. T^2 yielded straight lines for both cases attempted, the slopes of the lines actually differed in sign. The constant A was found to be $A \simeq -5 \times 10^{-3} \frac{\mu v}{(°K)^2}$ in both cases. Since S_e dominates the thermopower at low temperatures, the measurements did not differ as much as the change in slope might imply.

Effect of Sample Size on Thermopower

We have attempted to measure the differential thermopower of a bulk Al/small foil Al thermocouple over the temperature range 4.2°K to ~120°K. Typical results are shown in Figure 38. These were measured relative to a 16 mil diameter Al wire which was slightly less pure than the foils. There seems to be a general tendency for the thicker foils to show an initial negative peak not seen in the thinner foils and a larger negative differential thermopower above

$60°K$. No consistant size correlated changes can be identified in the area of the peak at $40°K$. This peak (at $40°K$) appears to be correlated with defect and impurity content in the 16 mil diameter reference wire. We note also that the experimental apparatus was designed to operate well only below about $25°K$. Above this temperature, gradients across the copper plug (the cold junction) and lack of thermal equilibrium at the heater (high temperature) junction can be expected to introduce significant errors into the thermopower of the larger samples. The possibility of effects on the thermopower due to surface oxides must also not be neglected. While the data shown in Figure 38 was obtained from samples annealed in a vacuum of about 1×10^{-4} Torr, the surface of these samples cannot be assumed free of a very thin layer of oxide[81] and its possible effects on the thermopower.[65,70]

Since all of our differential thermopowers appear to approach zero at high temperatures we cannot compare our data to the theories of Justi et al.[71] and Huebner.[69] As was mentioned above, even if our data had not tended to zero, limitations on the design of the system might have prevented quantitative analysis of the high temperature data.

To add to the difficulty of analysis, we noted in every case a discontinuous jump in the thermoelectric voltage of the bulk/small couple at approximately $30°K$. The origin of this jump ($\sim.3\mu v$) is yet unknown, but it does appear to be associated with the cold junction of one or the

other of the sample thermocouple legs. It is hoped that replacing the copper plug at the cold junction with a piece of high purity aluminum set in epoxy may eliminate this problem. For the data shown in Figure 38, the discontinuity was removed by subtracting the step voltage from the thermoelectric voltage for each experimental point of temperature higher than the "step." In support of this approach, we found that by performing the experiment in a superfluid helium bath, the "step" did not appear and the resulting thermopower agreed satisfactorily with that obtained by subtracting out the "step." In view of all the problems encountered, we will merely state that we see a variation of thermopower below 25°K which appears to be correlated with sample size. (We show the differential thermopowers below 25°K relative to the 4 mil foil in the inset to Figure 38.) More detailed experiments are necessary before further analysis is warranted.

Effect of Magnetic Field on Thermopower

We have measured the thermoelectric voltage of bulk aluminum (0.016" diameter) wire relative to superconducting Ni-Zr in magnetic fields from 0-20 Kilogauss.

The temperature of the hot junction of the couple was measured, as before, with a Au + .02 at . % Fe--chromel thermocouple. It was therefore necessary to consider the effect of the magnetic field on the thermoelectric voltage of our thermometer. On the basis of our work, and studies by Berman et al.[82,83] on Au + .03 at . % Fe thermoelements,

we estimate that the change in the thermoelectric voltage of the thermometer due to the application of a 20 Kilogauss magnetic field does not exceed 10%. This means that since the thermometer calibration is approximately linear above $3°K$, the error we introduce into our measurement of the absolute temperature, by assuming no magnetic field effect on our thermometer, should be about $1K°$ at $10°K$ and a 20 Kilogauss magnetic field. Since we will be looking at temperature differences in the thermopower we will ignore the magnetic field dependence of the thermometer in the first approximation, estimating the error introduced in the results later.

The measurements were taken in the following way. A temperature gradient (~$10°K$) was imposed on the sample couple, and the thermometer thermocouple voltage was held constant while the magnetic field was varied. This was done with the cold junction at $1.5°K$ and the hot junction at various temperatures between $4°K$ and $12°K$. At $9.2°K$ and at $11.7°K$ sufficiently detailed data was obtained to allow further analysis. The resulting thermoelectric voltages are shown as a function of magnetic field in Figure 39. The two curves are seen to cross, implying a change in sign of the thermopower. We obtain an estimate of the absolute thermopower by assuming that the thermopower is constant over the temperature interval $\Delta T = (11.7 - 9.2)°K$ and equal to the value at the mean temperature of the interval (~$10.5°K$). In this way we obtain

for the zero magnetic field thermopower at 10.5°K:

$$S \simeq \frac{(.3 - .48)\mu v}{2.5°K} \simeq -.072\mu v/°K$$

in good agreement with the value from the computer analyzed data:

$$S(10.5°K) \simeq -.07\frac{\mu v}{°K}$$

(see Figure 36). We obtain in this same way

$$S = \frac{\Delta E}{\Delta T}$$

at each value of magnetic field, obtaining the thermopower S(10.5°K) as a function of magnetic field shown in Figure 39. We see that S(10.5°K) does change sign with increasing magnetic field, crossing the S = 0 axis at about 10 Kilogauss. The fairly large error bars in Figure 39 are the result of fluctuations in the sample thermocouple voltage, possibly due to time dependent fluctuations in the magnetic field cutting the sample thermocouple loop. We estimate from Berman et al.[82] the error introduced into the thermopower by the assumption of no magnetic field effect on the thermometer to vary from $0.00\frac{\mu v}{°K}$ at H = 0 and $0.01\frac{\mu v}{°K}$ at 20 Kilogauss. If we correct our values of S(10.5°K) for the estimated magnetic field dependence of our thermometer, we obtain the values shown also on Figure 39.

If we now compare our experimental thermopower in a magnetic field with the prediction of MacDonald et al.[59] for our aluminum sample,

$$S_\infty - S_0 \simeq +0.007\mu v/°K, \tag{57}$$

we see that they predict the correct sign but far too small a magnitude for the change of thermopower in a magnetic field from H = 0 to H = ∞. They found just the opposite-- an incorrect prediction of sign, and too large a predicted magnitude--in their studies of the thermopower of copper and sodium. On the other hand, we appear to see a change in sign in the thermopower, in qualitative agreement with the suggestion of F. J. Blatt.

We conclude, therefore, that the study of the magnetic field dependence of the bulk thermopower of aluminum shows considerable interest. At least in this very preliminary study, the experimental evidence seems to favor the mechanism suggested by Blatt.
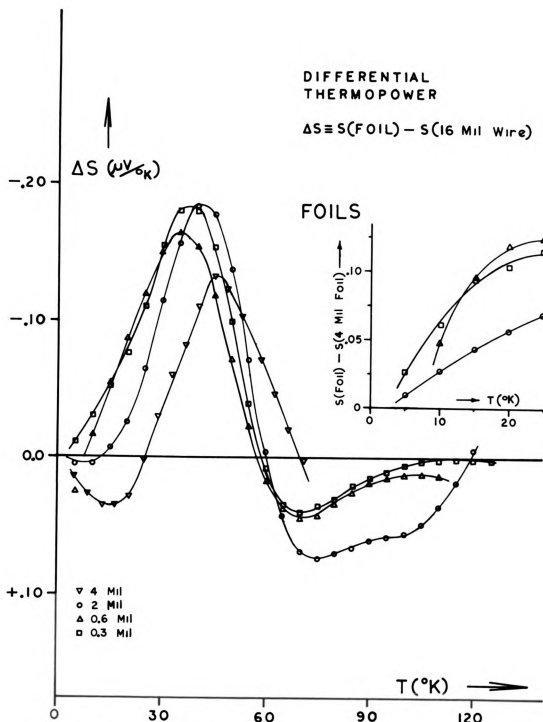
Figure 38. Thermopower of aluminum foils measured relative to less pure, 16 mil diameter wire. Insert: Thermopower of the small aluminum foils relative to the 4 mil foil

$S(10.5°K)$ $(\mu V/°K)$

H (KILO-GAUSS)

△ CORRECTED FOR
THERMOMETER H DEPENDENCE

Figure 40. Thermopower of aluminum
at 10.5°K as a function of magnetic
field

$V(\mu V)$

□ $\Delta T = 11.7°K - 1.5°K$
○ $\Delta T = 9.2°K - 1.5°K$

H (KILO-GAUSS)

Figure 39. The thermoelectric voltage
of an aluminum-superconducting Ni-Zr
couple in a magnetic field

VI. GENERAL CONCLUSION

We have measured some effects of sample size, mag-
netic field, and temperature on the electrical resistivity
and thermopower of aluminum.

We have measured the transverse magnetoresistance
of thin aluminum foils, reproducing the results of Försvoll
and Holwech:[24] we observed Sondheimer oscillations for
$\vec{H}\perp$(the plane of the foil) and a MacDonald-Sarginson peak
for $\vec{H}||$(the plane of the foil). The Sondheimer oscillations
provided an estimate of the Fermi momentum of aluminum:
$P_f \simeq 1.35 \times 10^{-19}$gm cm/sec. Our zero-field resistivities
yielded $\rho_\infty \ell_\infty \simeq 11.5 \times 10^{-12}$ Ω - cm^2 and n $\simeq$ .63, where n
is the effective number of electrons per atom. We have mea-
sured the transverse magnetoresistance of fine aluminum
wires, and have been able to isolate a peak which is con-
sistant with the MacDonald-Sarginson theory. No Sondheimer
oscillations were observed in the fine wires.

We have measured the longitudinal magnetoresistance
of both thin foils and fine wires of aluminum, and found
substantial discrepancy with theory. We discuss several
possible explanations for this discrepancy.

We have measured the temperature dependence of the
electrical resistivity of thin aluminum foils, and found it

to be nearly consistent with Fuch's theory. We were not able to reproduce the systematic variations from Fuch's theory reported by Holwech and Jeppeson.[47] No substantial effect attributable to the Azbel'-Gurzhi theory was found. This we interpreted to mean that electron-phonon umklapp scattering dominates the electrical resistivity of aluminum at low and intermediate temperatures.

Measurements of the temperature dependence of the electrical resistivity of fine wires did show an anomalous enhancement which had a temperature- and size-dependence consistent with the theory of Blatt and Satz. However, at temperatures above 4.2°K the magnitude of this effect was too large to reconcile with independent estimates of the contribution of Normal electron-phonon scattering to the electrical resistance of aluminum. We have suggested that the observed behavior at these temperatures may be due to impurity induced deviations from Matthiessen's Rule. The theory of Blatt and Satz is satisfactorily consistent with data obtained at temperatures below 4.2°K.

We have determined the absolute thermopower of bulk aluminum over the temperature range 1.5°K to 300°K, finding a negative phonon-drag peak in the thermopower in the vicinity of 75°K. We have also observed that the thermopower of aluminum fits at AT + B/T law above 200°K, and that the phonon-drag portion of the thermopower estimated from this relation appears to constitute nearly 50% of the total thermopower at 300°K; for all previously reported metals, the

phonon-drag thermopower, analyzed in the same way, was negligible by this temperature.

Preliminary measurements of size effects on thermopower revealed changes in the thermopower of thin foils of aluminum, below 25°K, which could be correlated to the sample size. The high temperature variations were neither sufficiently reproducible, nor of the right form to allow comparison with the theories of Justi et al.[57] or Huebner.[58]

Preliminary measurements of the magnetic field dependence of the thermopower of bulk aluminum at ~10°K, yielded a thermopower which appears to change sign with increasing magnetic field. This is qualitatively consistant with the change in sign of the Hall coefficient of aluminum with increasing magnetic field.

REFERENCES

1. Thomson, J. J. Proc. Cambridge Phil Soc. $\underline{11}$, 120 (1901).

2. Patterson, J. A. Proc. Cambridge Phil Soc. $\underline{11}$, 118 (1901).

3. Appleyard, E. T. S. and A. C. B. Lovell. Proc. Roy. Soc. $\underline{A158}$, 718 (1937).

4. Matthiessen, A. Ann. Physik $\underline{122}$, 19 (1864).

5. Harrison, W. A. Phys. Rev. $\underline{118}$, 1182 (1960).

6. Segall, B. Phys. Rev. $\underline{131}$, 121 (1963).

7. Wilson, A. H. The Theory of Metals, Cambridge University Press, New York (1965), pp. 4-12.

8. Fuchs, K. Proc. Cambridge Phil. Soc. $\underline{34}$, 100 (1938)

9. Dingle, R. B. Proc. Roy. Soc. $\underline{A201}$, 545 (1950).

10. Nordheim, L. Act. Sci. Et Ind., No. 131 (Paris: Hermann) (1934).

11. MacDonald, D. K. C. and K. Sarginson. Proc. Roy. Soc. $\underline{A\ 202}$, 223 (1950).

12. Ditlefsen, E. and J. Lothe, Phil. Mag. $\underline{14}$, 759 (1966).

13. Sondheimer, E. H. Phys. Rev. $\underline{80}$, 401 (1950).

14. Kao, Y. H. Phys. Rev. $\underline{138}$, A1412 (1965).

15. Koenigsberg, E. Phys. Rev. $\underline{91}$, 8(1953).

16. Chambers, R. G. Proc. Roy. Soc. $\underline{A202}$, 378 (1950).

17. Azbel', M. Y. Sov. Phys. JETP $\underline{17}$, 851 (1963).

18. Kohler, M. Annalen Der Physik $\underline{32}$, 211 (1938).

19. Justi, E. Phys. Z. $\underline{41}$, 563 (1940).

20. Olsen, J. L. Helv. Phys. Acta $\underline{31}$, 713 (1958).

21. Blatt, F. J., A. Burmester and B. Laroy. Phys. Rev. 155, 611 (1967).

22. Babiskin, J. and P. G. Siebenmann. Phys. Rev. 107, 1249 (1957).

23. Zebouni, N. H., R. E. Hampurg and H. J. Mackey. Phys. Rev. Letters 11, 260 (1963).

24. Försvoll, K. and I. Holwech. Phil. Mag. 9, 435 (1964).

25. Steel, M. C. Phys. Rev. 97, 1720 (1955).

26. Aleksandrov, B. N. Sov. Phys. JETP 16, 871 (1963).

27. Chopra, K. L. Phys. Rev. 155, 660 (1967).

28. Sondheimer, E. H. and A. H. Wilson. Proc. Roy. Soc. A190, 435 (1947).

29. Lüthi, B. Helv. Phys. Acta 33, 161 (1960).

30. Borovik, E. S. JETP 23, 83, 91 (1952).

31. Pippard, A. B. Proc. Roy. Soc. A191, 385 (1947).

32. Chambers, R. G. Proc. Roy. Soc. A215, 481 (1952).

33. Wyder, P. Phys. D. Kond. Mat. 3, 263 (1965).

34. Parrot, J. E. Proc. Phys. Soc. 85, 1143 (1965).

35. Montariol, F. and R. Reich. C. R. Acad. Sci. (France) 254, 3357 (1962).

36. Försvoll, K. and I. Holwech. J. Appl. Phys. 34, 2230 (1963).

37. Sondheimer, E. H. Adv. In Phys. 1, 1 (1952).

38. Mott, N. F. and H. Jones, The Theory of the Properties of Metals and Alloys, Dover Publications, Inc., New York (1958), pp. 249-258.

39. Andrew, E. R. Proc. Phys. Soc. (London) A62, 77 (1949).

40. Blatt, F. J. and H. G. Satz. Helv. Phys. Acta 33, 1007 (1960).

41. Lüthi, B. and P. Wyder. Helv. Phys. Acta 33, 669 (1960).

42. Azbel', M. Y. and R. N. Gurzhi, Sov. Phys. JETP 15, 1133 (1962).

43. Pippard, A. B. Phil. Mag. 46, 1104 (1955).

44. Dugdale, J. S. and Z. S. Basinski. Phys. Rev. 157, 552 (1967).

45. Yaqub, M. and J. F. Cochran. Phys. Rev. 137, A1182 (1965).

46. Aleksandrov, B. N. Sov. Phys. JETP 16, 286 (1963).

47. Holwech, I. and J. Jeppesen. Phil. Mag. 15, 217 (1967).

48. Gschneidner, K. A. Jr. In Solid State Physics, edited by F. Seitz and D. Turnbull (Academic Press, Inc., New York, 1964). Vol. 16, p. 384.

49. Pytte, E. J. Phys. Chem. Solids, 28, 93 (1966).

50. Reich, R. and K. Försvoll. C. R. Acad. Sc. (France) 261, 124 (1965).

51. Pearson, W. B. Sov. Phys. Sol. State 3, 1024 (1961).

52. Wilson, A. H. The Theory of Metals, Cambridge University Press, New York (1965), pp. 202-208.

53. MacDonald, D. K. C. Physica 10, 996 (1954).

54. Bailyn, M. Phil. Mag. 5, 1059 (1960).

55. Blatt, F. J., Proc. Phys. Soc. 83, 1065 (1964).

56. MacDonald, D. K. C. and W. B. Pearson. Proc. Phys. Soc. 78, 306 (1961).

57. Justi, E. M. Kohler and G. Lautz. Z. Naturforschg. 6A, 544 (1951).

58. Huebner, R. P. Phys. Rev. 140, A1834 (1965).

59. MacDonald, D. K. C. and W. B. Pearson, Proc. Roy. Soc. A241, 257 (1957).

60. Sondheimer, E. H. Proc. Roy. Soc. A193, 484 (1948).

61. Blatt, F. J. Private communication.

62. Feder, J. and J. Lothe. Phil. Mag. 12, 107 (1965).

63. Lück, R. Phys. Stat. Sol. 18, 49 (1966).

64. Försvoll, K. and I. Holwech. Phil. Mag. 10, 921 (1964).

65. DeVroomen, A. R., C. Van Baarle, and A. J. Cuelenaere, Physica 26, 19 (1960).

66. Dewar, J. and J. A. Fleming. Phil. Mag. 40, 95 (1895).

67. Grüneisen, E. and H. D. Erfling. Ann. Phys. Lpz., 36, 357 (1939).

68. Steel, M. C. and J. Babiskin. Phys. Rev. 94, 1394 (1954).

69. Huebner, R. P. Phys. Rev. 136, A1740 (1964).

70. Reimer, L. Z. Naturforschg. 12A, 525 (1957).

71. Justi, E., M. Kohler, G. Lautz. D. Naturwissenschaften 20, 475 (1951).

72. Savornin, J. and G. Couchet. Acad. D. Sciences, Paris, Com. Ren. 234, 1609 (1952).

73. Savornin, F., J. Savornin and A. Donnadieu. C. R. Acad. Sci. (France) 254, 3348 (1962).

74. Worobey, W., P. Lindenfeld and B. Serin. Physics Letters 16, 15 (1965).

75. Henry, W. G. and P. A. Schroeder. Canad. J. Phys. 41, 1076 (1963).

76. Roach, W. R., J. C. Wheatley and A. C. Mota De Victoria. Rev. Sci. Instr. 35, 634 (1963).

77. Haen, P. and L. Weil. Cryogenics 5, 46 (1965).

78. Christian, J. W., J. P. Jan, W. B. Pearson, and I. M. Templeton. Proc. Roy. Soc. A245, 213 (1957).

79. We are indebted to V. Rowe for providing the basic computer program used here.

80. Gripshover, R. J., J. B. Van Zytveld, and J. Bass. To be published.

81. Ramsey, J. A. and G. F. J. Garlick. Brit. J. Appl. Phys. 15, 1353 (1964).

82. Berman, R., J. C. F. Brock and D. J. Huntley. Cryogenics 4, 233 (1964).

83. Berman, R., D. J. Huntley. Cryogenics 3, 70 (1963).

84. Simmons, R. O. and R. W. Balluffi. Phys. Rev. 117, 62 (1960).

APPENDIX I

METHOD OF CALCULATION OF LOW TEMPERATURE
ELECTRICAL RESISTIVITIES

The following method was used to obtain the low-temperature electrical resistivities for all samples measured. The resistance of the sample in question was measured, in air, at room temperature, using at least two different measuring currents to ensure that no measurable joule heating occurred in the sample. The air temperature, t, was measured to ±0.1C° at the same time on a mercury thermometer. The resistance of the sample was then measured at the desired experimental temperature T; the resistivity $\rho(T)$ was calculated from the relation

$$\rho(T) = \frac{\rho(t)}{R(t)} R(T).$$

$\rho(t)$ was taken to be (cf.[84])

$$\rho(t°C) = [2.70 + 0.01(t°C - 20°C)] \times 10^{-6} \ \Omega - cm.$$